RESPONSES IN *E. COLI* TO COMBINATORIAL STRESS TREATMENTS (HCL,EDTA, H_2O_2, AND $CUSO_4$)

By

STEVEN MIDDLER

A thesis submitted to the Graduate School-Camden

Rutgers, The State University of New Jersey

in partial fulfillment of the requirements

for the degree of Masters in Science

Graduate Program in Chemistry

written under the direction of

Dr. Peter Palenchar

and approved by

_____

Dr. Alex Roche, Associate Professor, Chemistry

_____

Dr. Joseph Martin, Professor, Biology

_____

Dr. Peter Palenchar, Assistant Professor, Biochemistry

January, 2010

Abstract of the Thesis

Responses in *E. coli* to Combinatorial Stress Treatments

(HCl, EDTA, H_2O_2, and $CuSO_4$)

By

Steven Middler

Thesis Director:

Dr. Peter Palenchar

All living organisms adapt to their environment through a series of biochemical responses. *Escherichia coli* (*E. coli*) have a plethora of different enzymes, sigma factors, and other biomolecules that assist in stress relief. These experiments showed that *E. coli* have stress responses for individual stresses. These stress responses are not always additive when exposed to multiple stress factors.

Many times an individual stress response is triggered to counteract a single environmental change. Sometimes this same stress response will aid the cells with a different, unrelated stress. When both stresses are present, more of this stress response will materialize as a response to both stresses and will help prevent too much damage to the cell. This is called "cross-protection" of stress. After seeing the results of these experiments, it is believed that *E. coli* has some global stress responses and many

of the biomolecules used to fight stress are involved in cross-protection of multiple stresses.

These results were generated using a method where *E. coli* were grown onto control agar plates as well as plates treated with small concentrations of lethal substances. Using a technique called "Blue/White Screening" and colony counting software, the amount of colonies grown overnight on these plates could be counted. The area of the colonies and the relative amount of β-galactosidase transcribed and translated could also be measured. The control plates and treated plates were compared using these three criteria. The different individual stresses were also compared.

Plates were also treated with combinations of the same stresses and compared to the single treatment plates. Much of the data collected indicated a difference in *E. coli's* responses to an individual stress and how *E. coli* would be expected to react if the stress responses were additive. This proves that there was some cross-protection taking place in some instances.

Changes in distributions were also examined for each set of plates in order to examine the effect of the stresses on the stochastic nature of *E. coli* growth and functional protein production. Differences were noticed when comparing the distributions of control plates and stress plates. Differences were seen in different types and combinatorial stressors as well.

The second half of the experiments done here focused on using high performance liquid chromatography to find differences in concentration of molecules in

E. coli extracts that were treated with hydrogen peroxide for a brief amount of time and control *E. coli* extracts not put under any stress. This experiment proved to be too inconsistent to learn any facts. There was an issue with the chemistry involved in the *E. coli* extracts reactions with the indicator molecules used to find free thiols and free amines in the extracts.

Acknowledgements

Thank you to Dr. Peter Palenchar,
Sal Gomez, Chris Parker,
Dr. Alex Roche, Dr. Joseph Martin,
Dr. Georgia Arbuckle,
And the Chemistry Department at Rutgers University

Table of Contents

List of Figures

List of Tables

Chapter 1

INTRODUCTION

Section 1A: Bacterial Responses to Stress

This chapter includes information about the stresses studied in these experiments, including how the stresses are known to damage *E. coli*, how *E. coli* are known to respond to the individual stresses, how the stresses are known to interact, and how *E. coli* are known to respond to combinations of these stresses. In order to survive, bacteria must respond and adapt to their surrounding environment. Bacteria thrive almost everywhere on Earth and must deal with many different stresses to do so (1). These stresses can be any environmental change, from pressure or heat changes, to a presence of toxic agents (heavy metals, oxidants, acids, etc.), to high population density caused stress (2) (Table 1). Different bacteria react to stresses differently and some are more adapt at dealing with potentially lethal circumstances. For example, *Escherichia coli* are particularly adapt at handling diverse situations (3). *E. coli* can survive almost everything in moderation, from drops in pH to oxidative stress to the presence of metal cations, as these experiments have shown.

E. coli is an excellent organism to use to study stress on bacteria. *E. coli* is the best biologically characterized organism due to it being the most thoroughly biochemically and genetically studied (4). The idea has always been that the more scientists know about *E. coli* and its mechanisms to handle stress on a molecular level, the more they will be able to theorize about larger organism's mechanisms for their own stress responses.

Many stresses and responses have previously been studied using a variety of methods on different prokaryotes. For example, stationary-phase *Listeria monocytogenes* cells were exposed to heat, ethanol, and acid in order to study the contribution of sigma B as a response to these stresses (5). Sigma B also contributes to the transcription of more than 100 genes involved in heat, acid, ethanol, salt, and oxidative stress resistance by regulating the expression of a large general stress operon in *Bacillus subtilis*. Using a 10403S strain and a null sigma B mutant strain, the bacteria was exposed to these stresses, plated on agar plates, counted, and data was presented as a percentage of cell survival (5). This, like several other experiments (e.g. 6; 7), was conducted to show whether or not a bacteria's particular biomolecule is merely involved in stress relief of certain stresses. The majority of the mechanisms on how exactly these biomolecules react to stress are currently unknown. In this example, heat and ethanol stress were found to be partly dependant on sigma B, as the bacteria with sigma B intact had a greater survival percentage than the mutants with a null sigma B (5). Our project was not designed to test an individual biomolecule's response to stress, but the bacteria as a whole.

E. coli has the opportune ability to undergo transformation with ease (8). It is commonplace when growing *E. coli* to add antibiotic resistance in the plasmid, usually ampicillin resistance, and then to add ampicillin to the original plate (or test tube) of the second generation, so only pure *E. coli* with the recombinant DNA survives (9). For this experiment, *E. coli* was transformed and contained a plasmid including ampicillin resistance. *E. coli* was plated onto agar based plates to show the ability of the bacteria

to grow and the relative health of the bacteria when grown under stress. Stress responses to oxidative stress caused by hydrogen peroxide, response to acid stress caused by hydrochloric acid, response to the presence of a metal cation caused by copper sulfate, and response to the presence of a chelating agent caused by ethylenediaminetetraacetic acid (EDTA) were all studied.

Almost all of the studies done on bacteria under stress in the past have been done so using bacteria cultures, either while growing or in the stationary phase (e.g. 10; 11). The stationary phase is when bacteria in a culture no longer multiply. Very few experiments have used colonies grown on agar based plates because data is more difficult to ascertain, as no spectrometry can help give growth or survival levels. However, using "Blue-white screening" (see Section 2B) and the Kodak Molecular Imaging software, the ability to collect data on not only how many colonies are growing but how large they grow and the amount of "blueness" the colonies reflect is available. From here, these tools can be used to show differences in how *E. coli* respond to the four different stresses studied, degrees of affect that these stresses have compared to each other, and interactions between these stresses and the response of the bacteria to these interactions. There is very little known about combination of stresses on the biological level (3; 12).

Studies have been performed about the difference between the growth of colonies in liquid culture compared to on a solid plate (13). Bacteria have an additional lag time once introduced to a solid agar plate that is not dependent on the bacteria's physiological state (whether its in stationary or log phase), the number of cells added to

the plate, or the solid medium composition. The bacteria's genotype does affect the lag time however. It is believed that the transfer of bacteria from a liquid medium to a solid medium is a form of stress itself (13).

Section 1B: Oxidative Stress – Addition of Hydrogen Peroxide

Inside most living cells is a reduced environment preserved by enzymes that maintain the reduced state by a constant input of metabolic energy (14). Oxidative stress (OS) is the result of redox-sensitive biomolecules overexposure to oxidizing agents and becoming oxidized. Disturbances in this normal redox state can cause toxic effects through the production of peroxides and free radicals that damage many components of the cell (14).

Oxidative stress has been found to be involved in causing the diseases atherosclerosis (15) and Alzheimer's disease (16), as well as in the chemistry of an organism's aging experience (17). Human beings have macrophages that use oxidative stress as a component of their defense systems against bacteria (18). On a molecular level, many different molecules undergo oxidative stress. These include, but are not limited to, short chain sugars, iron-sulfur clusters, aromatic amino acids such as phenylalanine, and free thiols, such as a cysteine (Figure 1). These smaller molecules can affect entire biological systems, including metabolic systems.

Since cells are exposed to oxygen repeatedly, organisms have developed many responses to oxidative stress. Two main stress responses are invoked in *E. coli*, the peroxide stimulon and the superoxide stimulon, named after which oxidant is causing the stress. Both stimulons contain a set of over thirty genes (19). The SoxR and SoxS

proteins positively control the expression of the genes *soxR* and *soxS.* These genes in turn regulate the expression of at least six of the superoxide stimulon proteins. SoxR includes iron-sulfur clusters in its protein structure, which undergo a 1-electron oxidation when exposed to superoxide. This oxidation state binds DNA and activates transcription of SoxS. Increased levels of SoxS result in greater expression of several other genes, including enzymes responsible for DNA repair due to OS, as well as genes involved in detoxification (20). For example, the protein endonuclease IV, which is a DNA-repair enzyme, is regulated by SoxS and is elevated in cells treated with superoxide - producing compounds (21). An example of a protein that is a part of the superoxide stimulon but not regulated by the SoxRS genes are the two superoxide dismutases (SODs), Mn-containing SOD (Mn-SOD, encoded by sodA) and Fe-containing SOD (Fe-SOD, encoded by sodB), found in aerobically grown *E. coli*. SODs convert superoxide into hydrogen peroxide (22).

It is difficult to study how H_2O_2 reacts with all organics because many possible reactions occur with H_2O_2 and biomolecules. It reacts quickly with metals to form more reactive species for further redox reactions. It can also act as a weak oxidizing agent that attacks thiol groups of proteins or reduced glutathione. In addition, it can react directly with some keto acids (23).

The responses to hydrogen peroxide include a regulatory gene, *oxyR,* which controls the expression of eight proteins in *E. coli.* The active protein OxyR acts as a positive repressor of the gene (24). The protein is activated by the reaction of two of OxyR's cysteines, Cys199 and Cys208, coming in contact with hydrogen peroxide,

oxidizing Cys199 ‘s free thiol side chains, most likely forming a sulfenic acid, which in turn reacts to form a disulfide bond, activating the protein (25). The oxidized form of OxyR activates the expression of *katG* (a hydroperoxidase I enzyme), *gorZ* (a glutathione reductase), and *oxyS*. OxyS is a small untranslated RNA that regulates roughly forty other genes, including *rpoS* (26).

Expression of *gorZ* reduces glutathione because the oxidized state of glutathione in excess will inactivate OxyR. When oxidized, glutathione acts as a non-enzymatic reducing agent tripeptide, made up of γ-glutamic acid, cysteine, and glycine. Glutathione keeps cysteine thiol side chains in a reduced state on the surface of proteins. Glutathione has also been found to prevent oxidative stress in most cells by trapping free radicals (27).

Another example of enzymes that activate in OS response to H_2O_2 are catalases, hydroperoxidase catalase I (HPI) encoded by *katG* and HPII encoded by *katE*, which catalyze disproportionate reactions of H_2O_2 into water and elemental oxygen (28). It has been found that when cells from log phase cultures are plated on agar based plates, oxidative-stress regulons, like SoxRS, OxyR, and Fur are immediately induced (13).

Section 1C: Stress Caused by Lowering of pH – Addition of Hydrochloric Acid

E. coli has developed acid resistances to very low pH (as low as 2.0) over years of evolution (29). Stationary-phase *E. coli* in particular have the ability to survive in highly acidic conditions, since *E. coli* survives in gastric acidity and volatile fatty acids produced by fermentation in the intestine. However, growth of *E. coli* needs much more moderate conditions (pH 4.4- 9) (30). Compared to other bacteria, the minimum growth

pH of *Salmonella typhimurium* was shown to be significantly lower (pH 4.0) than that of either *E. coli* (pH 4.4) or *Shigella flexneri* (pH 4.8), yet *E. coli* and *S. flexneri* both survive exposure to lower pH levels (2 to 2.5) than *S. typhimurium* (pH 3.0) in complex medium (29). Studies have shown that acid tolerance resistance systems (ATRs) made up of regulatory networks of genes in *E. coli* that are expressed in low pHs during stationary-phases protect colonies to pH of 2.0 (29-31). It is believed that the same ATRs protect log-phase colonies as well, except to more mild pHs of 3.0-6.0 (29).

There are four acid resistance systems existing in *E. coli,* each using multiple genes and various other organics to protect stationary-phase cells under acidic conditions (31). They are very specific and only will be effective if they exist in clearly defined environments. The first is a glucose-repressed system (called the "oxidative system") induced in Luria-Bertani (LB) broth that is dependent of the alternative sigma factor σ^S, encoded by the gene *rpoS* (31). The method of acid stress protection by this system is unknown. In many situations, this system proved to be dependent on the cyclic AMP receptor protein, most likely due to the lack of glucose available and the need for cellular metabolism of other sugars (31). The glucose/cAMP system is presumably detecting general unhealthiness of the cells when glucose concentration drops. The gene *rpoS* and its sigma factor are regulated by OxyS (31).

The second ATR is activated following growth in LB broth containing 0.4% glucose (LBG) or brain heart infusion broth containing 0.4% glucose (BHIG) and requires the amino acid arginine to protect colonies under extreme pH conditions (to pH 2.5) (31). The structural gene for arginine decarboxylase, *adiA*, and the regulator *cysB* have

been identified as the crucial genes for this ATR. It is believed that this system consumes excess protons in the cell during the decarboxylation of arginine catalyzed by AdiA (31). An end product agmatine is then exported from the cell in exchange for new arginine catalyzed by an antiporter system, a membrane-bound protein encoded by the gene *adiC,* with the whole system being driven by the free energy of decarboxylation (32). Control of AdiA synthesis is dependent on DNA supercoiling and bending using DNA gyrase and integration host factor to put the DNA in position for transcription by allowing activators to be in juxtaposition with RNA polymerase. The presence of H-NS, a nucleoid-associated protein, and CysB is also needed for activation (33).

The third ATR system has recently been added and is a bit controversial in the belief of its existence. It is similar to the arginine system, except requires lysine and is less effective. Lin et al. (29) reported lysine to be ineffective in protecting *E. coli* cells from low or even mild pH stress. Lyer et al. (34) reported *E. coli* uses a lysine decarboxylase and its accompanying lysine-cadaverine exchanger, the *cadBA* system, to protect against mild acid shock (about pH 5.5) in a similar fashion to how the arginine ATR system works. CadA is regulated by the CadC activator and interaction of lysine with lysine permease (35).

The final ATR system is the most effective at the lowest pH of the four (Table 2) (31). This ATR system also uses an amino acid, glutamate, its corresponding decarboxylase, and an antiporter to reduce internal pH of *E. coli*. The end product γ-aminobutyric acid (GABA), formed from the reaction of glutamate with excess protons using the enzyme glumatate decarboxylase (GAD) as a catalyst, is transported out of the

cytoplasm by GadC, the putative glutamate:GABA antiporter (36) in the same fashion as in the arginine system. The GAD system includes three genes. The genes *gadA* and *gadB* encode two highly homologous glutamate decarboxylase isoforms (37). The loss of either one of these genes reduces the ability of the system to survive low pH. The gene *gadC* encodes for the antiporter protein. Even though both isoforms are found while in the log-phase of *E. coli* growth at pH 5.5, the cells fail to survive at pH 2.5 while still multiplying. This shows that more genes are induced when stationary-phase is reached to assist in lower pH survival (31). The GAD system is regulated by a much more complex system of regulators than the other two amino acid decarboxylase systems, including at least 10 genes involved in regulation. Of these ten known, a two component system made of EvgA and EvgS as well as an associated protein YdeO are well characterized. This system regulates *gadE*, the essential activator of *gadAB* and *gadC* by an unknown mechanism (38).

Section 1D: Stress Caused by the Presence of a Metal Cation – The Addition of Copper Sulfate

Copper (II) sulfate is a common metal salt that is naturally occurring. It has many uses, including as a fungicide used to control bacterial and fungal diseases of fruit, vegetable, nut, and field crops. It is also used as an algaecide, an herbicide in irrigation and municipal water treatment systems, and as a molluscicide, a material used to repel and kill slugs and snails (39). Copper ions in prokaryotic cells are useful but can also be lethal. Copper is required in the active sites of many enzymes, including terminal oxidases, monooxygenases, and dioxygenases and is essential for the transport of

electrons in several respiratory pathways (40). Copper ions can also catalyze harmful redox reactions resulting in oxidation of lipid membranes, damage to nucleic acids, and generation of free radicals from hydrogen peroxide (41). Cells therefore have responses specific to copper ions (42).

Although copper is considered to be a heavy metal, it is more clearly defined as a soft metal ion (43). Soft metal ions are those with high polarizing power (a large ratio of ionic charge to the radius of the ion) in comparison to hard metal ions such as Na^{+} and Ca^{2+} found in Groups I and II of the periodic table. Hard metals bind to biomolecules, such as proteins, mostly using weak ionic interactions, commonly to carboxylates of glutamate or aspartate residues. Soft metals usually make much stronger, nearly covalent bonds with such side groups as thiolates of cysteine residues and the imidazolium nitrogen of histidine residues. Other soft metals include nickel, zinc, mercury, lead, arsenic, and others (43). All metal ions are toxic in excess and over time bacteria have developed resistance genes to inorganic salts of soft metals found in the chromosomes and extrachromosomal plasmids. The copper resistance determinant of *E. coli* appears to need proteins that are in the normal homeostasis system of *E. coli* and are therefore found on the chromosome (43).

Bacteria have a family of enzymes that transport cations either into or out of a cell (and sometimes do cation exchange) called P-type ATPases. These ATPases are split up into soft and hard metal ATPases and then further divided into divalent or monovalent cation pumps. These metal pumps are also found in a variety of eukaryotes, including human beings (44).

E. coli has an 834-residue protein P-type ATPase called CopA (45). CopA acts as an efflux pump, discarding any interior surplus of copper (I) ions, as well as gold (I) and silver (I) ions. CopA's metal binding domains are two N-terminal CXXC sequences. Copper (II) is believed to not be able to be transferred using CopA. During an uptake assay of copper sulfate, only when Cleland's reagent (dithiothreitol), a strong reductant, was added, did copper ions leave *E. coli* cells. These copper ions were all copper (I) (45). The transcription of *copA* is regulated solely by CueR, which is a copper, silver, and gold responsive member of the MerR family of transcriptional activators (46). CueR, once bounded to the metal, acts as a dimer on the promoter of CopA, recruiting RNA polymerase to the promoter in the process. It is activated by Cu (I) (or Ag(I) or Au(I)) binding to 3 cysteine residues in a trigonal planar fashion (47).

E. coli also has two chromosomal genes, *cusRS* (*ylcA ybcZ*), from *Escherichia coli* K-12 that encode a two-component, signal transduction system that is responsive to copper ions (48). These genes are required for the copper-inducible expression of *pcoE* and a chromosomal gene called *cusC* (*ybcZ*). PcoE is a periplasmic protein that reduces the time required for *E. coli* strains to recover from copper ion stress but is not strictly required for copper resistance in standard growth assays (48). *CusC* is found within a locus, *cus*, which is theorized to contain a copper efflux system (due to homology to other metal efflux systems). Less is known of CusC itself but it is believed to be on the outer membrane and possibly a membrane lipoprotein (48).

Section 1E: Stress Caused by the Presence of a Chelating Agent – The Addition of EDTA

Of the four stresses chosen to study, the addition of the chelating agent EDTA has the least amount of information available about any stress responses caused by its addition to bacteria, specifically *E. coli*. Chelating agents like EDTA are used to bind di- and tricationic metal ions such as Cu^{2+} and Fe^{3+} (Figure 2), which remain in solution but become much less reactive (49). It is commonplace for EDTA to be used to suppress damage to DNA and proteins by deactivating metal-binding enzymes, in particular nucleases (4). Many times EDTA is used as a scavenger to pick up traces of unwanted metal ions, mostly using displacements. For example, Ca-EDTA is used as a treatment of lead poisoning. When Ca-EDTA is injected to a lead containing cell, the Ca^{2+} is replaced with the more stable Pb-EDTA complex (50).

EDTA has demonstrated the ability to cause an increase in permeability of *E. coli* (51). *E. coli* was observed to have a high permeability barrier, not allowing molecules such as actinomycin and o-nitrophenylgalactoside entrance (52). However, the addition of EDTA allows higher percentages of molecules into the cell walls. It is not known whether any molecules leave the cell with the addition of EDTA but it can be assumed that no essential metabolites are dismissed, as growth rates do not change (51). It is also unclear how EDTA reacts with the cell wall to allow this added permeability but it has been observed that chelation of Ca^{2+} or Mg^{2+} by EDTA in the outer membrane causes a loss of lipopolysaccharides. EDTA has been used to introduce antibiotics, detergents, substrates, and proteins into bacteria that were unable to enter prior to EDTA addition. For example, ovotransferrin, an iron-binding molecule found in egg

albumen, can not control *E. coli* activity alone. With the addition of EDTA, however, the ovotransferrin activity inside the bacteria increases, the ovotransferrin acts as an antibiotic, and *E. coli's* iron source is cut off (53). Others have used EDTA treated *E. coli* to test molecules for genotoxicity (54). EDTA induced permeability does have a limit due to the size of molecules trying to enter at molecular weights of 1,000 or more (55).

Section 1F: Reactions of One Stress with Another in *E. coli*

Plates in this project were set up to judge not only how each component itself affects the growth of the colonies, the size of the colonies, and the health of the colonies (described by the ability to make functional β-galactosidase) but how multiple components react with each other and their combined affects on *E. coli*. This information should help give insight to the relative strengths of each parameter or any indication of a combination that works together to either harm or assist in the cell's ability to grow or produce functional protein. Some previous experiments have provided data and some conclusions about certain responses to combinations of these and other stresses (e.g. 5; 56) but the amount of research dedicated toward these or any combinations are scarce. This is the first project to study the affects of these combinations on *E. coli* while adhered to an agar plate and the first to study the affects of the higher combinations (three or four combined) on *E. coli* in any state (liquid culture or adhered to a plate).

H_2O_2 & HCl.

There are a few stress response genes and proteins that both acid stress and oxidative stress share. It has been theorized that acidic conditions accelerate the creation of oxygen radicals, inducing a partial oxidative stress response (57).

The ferric uptake regulator (fur) is a global bacterial regulator that uses iron as a cofactor to bind to specific DNA sequences. Some of these sequences control the expression of various acid tolerance genes and oxidative stress regulation (58). Fur itself is regulated by two oxidative stress regulators. Under oxidative-stress conditions with the influence of OxyR and SoxRS, the number of Fur proteins per cell increases from 5,000 to about 10,000. The oxidative stress genes *nrdH* and *nrdI,* which code for small redox proteins, were both found to be activated by Fur (58). *SodB* is an iron dependent superoxide dismutase activated by Fur. The link between Fur and oxidative stress is believed to exist to hinder any sort of creation of dangerous iron or iron-sulfur cluster radicals in the cell (58).

As for acidic stress, fifty genes are induced when *E. coli* goes under acidic shock. Acidic shock takes place when colonies are grown under acidic conditions (~pH 4.5) and then are introduced to even lower pH (pH 2-3) for a period of time (59). Five of the genes activated during this process are done so by Fur, in what is believed to be done with a mechanism independent of iron. As of 2001, these genes have not been characterized and no further research regarding these genes has taken place (60).

The DNA-protecting protein Dps makes a significant contribution to acid tolerance and oxidative stress in *E. coli* (61). Like Fur, Dps is an iron-binding molecule that repairs and protects DNA. It has been theorized that Dps protects DNA by forming

instant Dps-DNA crystals, inside which DNA is sequestered and effectively protected against varied assaults, including radicals (61). Dps most likely protects DNA from the deleterious effects of low pH in a similar fashion, however, it is possible that Dps influences expression of other genes that protect or repair DNA or provide acid tolerance by another mechanism (62). Two nucleoid-associated proteins, FIS and H-NS, control regulation of Dps (63).

Very recent studies have shown that the glutamate- and arginine- dependent acid-resistance systems (as discussed in Section 1C) of *E. coli* O157 : H7 have been determined to protect against oxidative stress during extreme acid challenge (64). The first ATR system (oxidative system) was proven to not defend the cells against OS and the third (lysine) was not tested. Presence of either glutamate or arginine offered significant protection against hydrogen peroxide induced oxidative stress during pH 2.5 acid challenge. OS defense at low pH required *gadC* and *adiA* for the glutamate and arginine dependent acid-resistance systems, respectively (64).

Another gene involved in both oxidative and acid stress is *rpoS* (see Section 1C), the gene in the glucose-dependent ATR system that encodes for the sigma factor σ^S. It also encodes a separate stationary-phase only sigma factor, RpoS, which controls a regulon of over 30 genes required for survival in the stationary phase, including several genes providing protection against oxidative stress and resistance to low pH (65). As noted in Section 1B, OxyS is induced when *E. coli* is under oxidative stress and regulates *rpoS* (24).

H_2O_2 & $CuSO_4$.

Studies have shown that adding low-valent transition metal ions, like Cu^+ salts, clearly increase the amount of H_2O_2 caused oxidative degradation of various biological compounds, including nucleotide bases, sugars, proteins, and membrane lipids (66). Experiments have shown that with *E. coli* in metal ion-depleted media, relatively high concentrations of H_2O_2 alone were toxic (67). The H_20_2 dose level required for killing was sharply reduced if copper (II) salts and reductants were added (giving slightly stronger effects than only Cu (I)) (67). This information has been formulated into a model for disinfection known as the "site-specific" hypothesis, wherein H_2O_2-inflicted cellular damage is determined by the intracellular location of the catalytic metal ions (68). These studies were done using CuCl and in the absence of added oxidants, cuprous ion has been shown to be more toxic than cupric ion to *E. coli.* However, both cuprous and cupric ion-mediated bactericidal mechanisms involve inhibition of cellular energy-transducing capabilities and $CuSO_4$ is still toxic but at higher concentrations. The toxicity of both ions is increased in the presence of H_2O_2, though as stated above, Cu (II) is more lethal with a reductant (66).

H_2O_2 will react with reduced iron (II) or copper (II) ions to generate hydroxyl radicals ($^{\cdot}OH$) in the Fenton reaction (69). These hydroxyl radicals are extremely reactive, oxidizing almost anything but ozone (70). For example, the oxidation of NADH by H_2O_2 has been shown to be catalyzed by Cu^{2+}, giving an oxidation product identified as enzymatically active NAD^+ and Cu^+. EDTA actually inhibits this reaction, most likely chelating the Cu^{2+} (71).

The creation of protein carbonyls by metal-catalyzed oxidations are likely mediated by hydroxyl radicals (43). In particular, cuprous ions can be oxidized by peroxide to generate hydroxyl ions and radicals, which can attack and damage phospholipids in biological membranes and inactivate membrane bound enzymes. This type of damage is characteristic in people with copper toxicosis (Wilson's disease) due to a defect in the WND copper transport protein (47).

Superoxide dismutase (SOD) has been widely found to contain manganese or iron ions in bacteria. Recently, it has been discovered that a few species of bacteria, including *E. coli*, actually contain a copper and zinc containing SOD as well (72). The Cu,Zn- SOD is periplasmic and is inducible by dioxygen. This enzyme is inactivated by H_2O_2 and diethyldithiocarbamate. Moreover, the diethyldithiocarbamate- inactivated enzyme can be reactivated with Cu (II) (72). This SOD has the same basic function as other metal containing SODs (see Section 1B), which is to protect the cell from superoxide and other free radicals (22).

H_2O_2 & EDTA.

EDTA has been found to be partially effective in protecting *E. coli* cells from the effects of hydrogen peroxide (73). Studies have shown that other metal chelating agents, such as *o*-phenanthrolie and dipryidyl were very successful protecting *E. coli* from hydrogen peroxide caused oxidative stress (56). However, while these molecules do assist in OS protection, once OS does take place, especially when causing DNA damage, these same agents have been demonstrated to slow the repair process. It is believed that DNA repair uses not only DNA polymerase I but a metal ion that the

chelating agents bind, ending its activity and slowing DNA repair (56). EDTA specifically was not tested in these experiments but would be hypothesized to have similar affects against OS.

EDTA & $CuSO_4$.

Obviously, EDTA can form a complex with Cu^{2+} ions independent of *E. coli.* These compounds are formed very easily, as the association constant (K_a) for Cu^{2+} ion with EDTA is $6.3x10^{18}$. Compare that to K^+, the cation with the lowest association constant with EDTA at 6.31 and you can see the EDTA-Cu^{2+} complex is extremely stable. Most importantly for this research, the K_a for Mg^{2+} is 4.9×10^8, so a EDTA-Cu^{2+} complex will not dissociate for the formation of an EDTA-Mg^{2+} complex unless the Mg^{2+} concentration far outweighs the Cu^{2+} concentration (74) (see Table 3 for concentrations in experiment). The significance of this particular metal ion, Mg^{2+}, will be discussed in Section 2A.

EDTA (200 µM) was found to decrease the activation of the *copA* promoter in *E. coli* in the presence of copper (47).

Permeability of copper ions into *E. coli* is likely to be increased in the presence of EDTA (51). It is unclear if this is due to an EDTA-Cu^{2+} complex being easier to enter a cell or because EDTA increases the permeability of the *E. coli* membrane for entrance of ions.

HCl & EDTA.

Though rare, at very low pH and low metal ion concentration, EDTA will take on extra protons and form an $EDTA^{+2}$ compound (75). HCl has a lower permeability than

EDTA, so EDTA would increase the ability of the dissociated H^+ and Cl^- ions to enter cells (76).

HCl & $CuSO_4$.

HCl and $CuSO_4$ do not react in solution but rather only dissociate into ions. Cu,Zn- superoxide dismutase has been found to help survival rates of *E. coli* when introduced to low pH (65). Also, it has been shown that under acidic anaerobic conditions copper becomes much more toxic (77).

Figure 1. Example reactions of biomolecules undergoing oxidative stress.

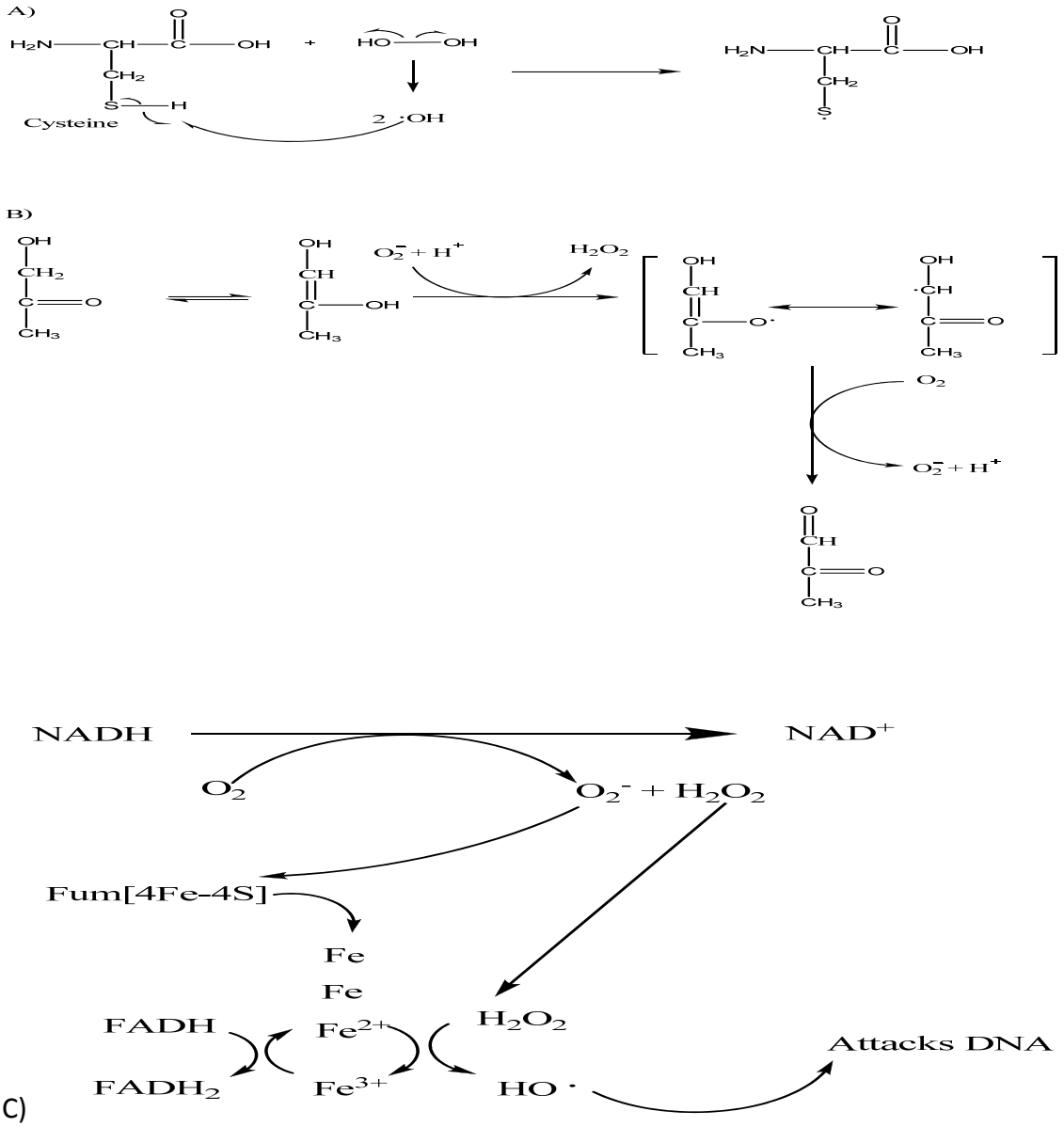

(A) cysteine reacting with hydrogen peroxide to form a cysteine radical; (B) a short-chained sugar reacting with superoxide forming methyl glyoxal, and regenerating another superoxide; (C) Iron-sulfur cluster interacting with oxygen to create DNA damage). Adapted from Imlay (14).

Figure 2. EDTA's structure (fully protonated) and metal chelating abilities.

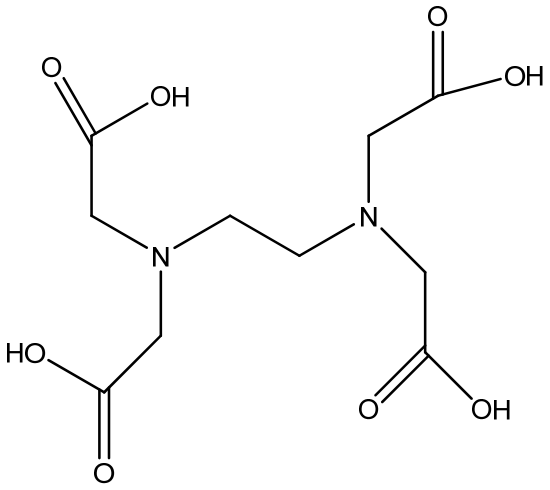

EDTA

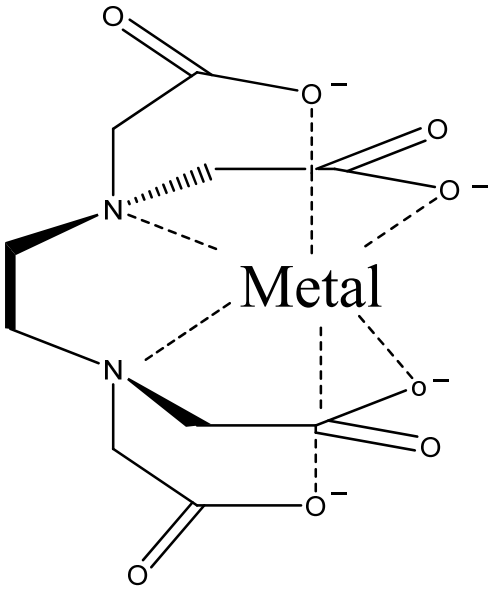

Metal-EDTA chelate

After EDTA fully chelates a metal, the metal's reactivity is lessened significantly. All six of the possible coordinate covalent bonds are full with ligands from the free electrons available on the EDTA's nitrogens and oxygens.

Table 1. A list of stresses not studied in these experiments.

Type of Stress	Biological Reaction of *E. coli* to Response*	*E. coli*'s Known Primary Response Genes**	Other Known Factors, if any, in Response***
Hydrostatic Pressure	Depression of *lac* operon. Extended lag and slower growth of cells (78). Ceased DNA, RNA, protein synthesis (79).	*fruK, fruB, aceA, ptfB, phoR, prfA, pstS*	Adaptation for pressure responses are all combinations of other stress responses (79).
Heat Shock	Unfolded proteins (12).	*uspA, yecG, yiiT, ydaA, ybdQ, rseA, degP, rpoH, clpB, clpP, dnaJ, dnaK, htpX*	σ^E, an extracytoplasmic function sigma factor (3). CpxAR system (12). Trehalose (80).
Starvation (lack of glucose/phosphate)	Degradation of ribosomes (81).	*uspA, yecG, yiiT, ydaA, ybdQ, dinB, rpoS*	
Low Temperature Shock	Solidifies cellular membrane lipids. Decrease in polysomes.	*aceF, aceE, hscB, gyrA, hns, rbfA, csp operon*	σ^E. Increase of branched-fatty acids.
Osmotic Stress	Increases the thermotolerance and oxidative-stress resistance of *E. coli*.	*katF, rpoS, otsA, otsB, treA, osmE*	Trehalose (80). Calcium. Upregulated genes on SoxRS and OxyR regulons (82).
UV-Light Radiation	Cross-linking between adjacent cytosine and thymine bases, creating pyrimidine dimers, resulting in distorted DNA structures (83).	*lexA, hns, dnaA, yeiE, cspC, fur, flhD, hcaR, phoB*	SOS response.

Table 2. Comparison of 4 known acid tolerance systems (ATRs).

ATR	Gene	Activation needs	pH range
Oxidative system	σ^S encoded by *rpoS.* (31)	LB broth, cAMP +CRP (31), actually does not need low pH to activate, but activates at entry into stationary phase, glutamate of glutamine during adaptation – but neither form of the a. a. has a function during acid resistance (31).	2-3, 5-6, 9.5-10
Arginine decarboxylase system	*adi* locus, *adiA* (agr decarboxylase), *adiC* (antiporter) (31;32;33)	Glucose, LB broth, arginine (31), regulator *cysB* (32), low pH.	2.5
Lysine decarboxylase system	*cadA* (lys decarboxylase), *cadB* (antiporter) (31;33;35)	Glucose, LB broth, lysine (31), lower than neutral pH, regulator *cadC* (34).	~5.5
Glutamate decarboxylase system	*gadA + gadB* (glu decarboxylase), *gadC (antiporter)* (31;36;37;38)	Glutamate (glu's carboxylate anion), σ^S, *rpoS* (31), low pH for gadA, entry into stationary phase for gadB (38).	2-3, also *E. coli* grown at neutral pH before acidification

CHAPTER 2

β-Galactosidase and The Lac Operon

Section 2A: β-Galactosidase's Function and Structure.

This chapter discusses *E. coli's* protein β-galactosidase and its ability to undergo α-complementation, allowing for *E. coli* to be assayed with blue/white screening. *E. coli's* β-galactosidase is a symmetrical homotetramer. Four identical subunits, each consisting of 1,023 amino acid residues, fold into five sequential domains (84). Each monomer (subunit) has a molecular weight of 465,000 Daltons. The monomers each have active sites, with the majority of the sites found on the third (or center) domain. The protein structures third monomer consists of an eight-stranded "TIM" barrel, also known as an α/β barrel (85). Domains 1, 2, 4, and 5 mainly include β-sheets (Figure 3). All domains include a section of the active site and all contribute when binding substrates (84).

β-galactosidase is a well conserved enzyme, found in species from *lactobacilli* to humans (86; 87). The catalytic purpose of the enzyme is to catalyze lactose to glucose and galactose by a three activity mechanism. The first activity carried out by the enzyme is a general acid-catalyzed (probably using Tyr503 as a proton donor) hydrolysis of lactose to form glucose and galactose, which in turn enters glycolysis (84). The second activity substrate is the transglycosylation of lactose to give allolactose. The enzyme lastly hydrolyzes allolactose into glucose and galactose. Any leftover allolactose is an inducer of β-galactosidase, so eventually all lactose introduced to *E. coli* will be converted to glucose and galactose. Glu537 is thought to be the catalytic nucleophile,

forming a covalent bond with the lactose. It is oriented by hydrogen bonds to Tyr-503 and Arg-388 (84).

Two Mg^{2+} metal cations are found in each monomer. While the data supporting a catalytic purpose for these Mg^{2+} ions is inconclusive, it is known that the loss or replacement of the ions significantly lowers the rate of the reactions, though does not fully inactivate the enzyme (88; 89). Experiments done on mutants of β-galactosidase discovered that Glu-461 appeared to be very important in the binding of Mg^{2+} (90; 91). It is believed Glu-461 could function as the acid catalyst whose location is mediated by the presence of Mg^{2+}. The Mg^{2+} site is also ligated by Glu-416 and His-418 (90; 91). Binding to this site causes K_M to decrease, and k_{cat} to increase. Mg^{2+} can bind to this site via a direct bond with the main chain carbonyl of Asn-597 and indirectly (via water molecules) with Glu-797. This interaction can only occur when the loop is in the open conformation (90). When the loop is closed, Glu-797 flips into another orientation and is no longer available for binding Mg^{2+}. Na^{+} (or K^{+}) is also needed for full activity. The loss of the monovalent cation was not as significant to the rate of the reaction as the loss of the divalent cation (90).

There are two different methods of ligand binding by β-galactosidase (92). The first, called “shallow“ mode, includes substrate analogues and one product (allolactose) binding at the mouth of the active site. The ligand is situated on top of Trp999 and the galactosyl hydroxyls 2, 3, and 4 make specific contacts to the enzyme and to bound water. The 6-hydroxyl contacts the enzyme and the situated Na^{+} ion (92). The second, the “deep” binding mode, includes intermediates, transition state analogues, and

another product (galactose) penetrates 1−4 Å deeper than the “shallow” mode. In this mode as well, the galactosyl 6-hydroxyl directly ligands the active site sodium ion (92). A direct interaction is never seen between any ligand and the magnesium ion that is in the active site. Except for the galactose complex, the deeper mode of binding is accompanied by an enzyme conformational change, in which Phe601 rotates, and the 794−804 loop from domain 5 moves up to 10 Å closer to the active site. The glucose complex has no preference in either mode and will bind both ways (92).

β-galactosidase is encoded by the *lacZ* gene, the first gene in the *lac* operon. An operon is a series of structural genes that are expressed as a group and share a promoter and operator. There are two other genes included on the *lac* operon, the *lacY* gene, encoding for β-galactosidase permease, and the *lacA* gene, which encodes for β-galactosidase transacetylase (93). Without lactose or a lactose substitute, the *lac* operon is not expressed because of a *lac* repressor protein. This protein binds to the operator and prevents RNA polymerase from transcribing the genes in the operon. When lactose is introduced, it acts as an effector molecule, binding to the repressor protein and freeing up the operator to allow RNA polymerase access to the promoter and the genes of the *lac* operon (4).

However, the preferred carbohydrate source of *E. coli* is glucose. When lactose and glucose are both available to the cell, the *lac* operon is inhibited by catabolite repression (4). This takes place by a second binding site on the promoter of the *lac* operon. The first site is for RNA polymerase binding, while the second site binds a complex made up of the catabolite activator protein (CAP) and cyclic AMP (cAMP). This

binding of the CAP-cAMP complex to the promoter site is required for transcription of the *lac* operon (94). As the concentration of glucose increases inside the cell, the amount of cAMP and therefore the CAP-cAMP complex decreases. This decrease in the complex inactivates the promoter and the *lac* operon is consequently turned off, even if lactose is present to halt the repressor protein (94).

Section 2B: Blue/White Screening

α-Complementation is the property that is the chemical basis for blue/white screening (95). This phenomenon takes place because β-galactosidase is a tetramer and each monomer is made of two parts, the lacZ-α and the lacZ-ω. The two fragments come together in the cell. If the α-fragment is deleted, the ω-fragment is non-functional (95). The α-fragment functionality can be restored in-trans via certain plasmids. If the strain of *E. coli* has the deletion of the lacZ-α (in this experiment DH5-α) and a plasmid with the lacZ-α fragment (in this experiment pBluescript) (Figure 4), the resulting transformation will have a fully functional *lac* operon with the ability for transcription, translation, and expression of β-galactosidase. Without the plasmid, DH5-α cells will express the *lac* operon (with the addition of lactose, allolactose, or a lactose/allolactose substitute) including the *lacZ* fragment, however it will be non-functional. The DH5-α cells have been manipulated to produce an incomplete *lacZ* based on the sequence of their chromosome so that the complementation can be carried out (95). "Wild-type" *E. coli* contain a full gene encoding a complete *lacZ* gene (96).

Blue/white screening is the process used to indicate whether this functional β-galactosidase is expressed in a cell (97). Since β-galactosidase expression happens when

there is a functional *lacZ* gene in the *lac* operon of the cell, blue/white screening is also an assay to more specifically tell whether the *lac* operon is being expressed. When β-galactosidase is present, the addition of a compound 5-bromo-4-chloro-3-indolyl- beta-D-galactopyranoside (X-gal) yields 5,5'-dibromo-4,4'-dichloro-indigo, an insoluble blue product, coloring the cells blue. The X-gal itself is cleaved by the β-galactosidase to give galactose and 5-bromo-4-chloro-3-hydroxyindole, which is oxidized and spontaneously dimerized to give the 5,5'-dibromo-4,4'-dichloro-indigo. The dimer is the blue product (97).

There is a repressor protein promoter in front of the *lacZ* gene that prevents it from being transcribed with regular *E. coli* cells (97). However, as mentioned above, this repressor promoter can be "turned off" by it binding it to lactose or allolactose, leaving the *lac* operon and the *lacZ* gene open for transcription. Instead of using lactose, Isopropyl β-D-1-thiogalactopyranoside (IPTG), a mimic allolactose, was added as an inducer to bind to the repressor and therefore start transcription of the *lac* operon. IPTG has a sulfur-linkage that is not hydrolyzed well and unlike allolactose, does not degrade (97).

For these experiments a pBluescript plasmid was needed to assist in blue/white screening and also insert a gene to make the *E. coli* ampicillin resistant. DH5-α *E. coli* contains the allele Δ*(lacZ)*M15, the alpha acceptor allele needed for blue-white screening with the pBluescript plasmid (98). The new DH5-α pBluescript *E. coli* were streaked on LB-agar based plates with ampicillin and the resulting bacteria were able to undergo blue-white screening.

Figure 3. Three-dimensional structure of beta-galactosidase (From Juers et. al (99)).

Removed Due to Copyright

The tetramer looking down at the two-fold axis. Coloring is by domain. Domain 1 is the blue. Domain 2 is the green. Domain 3 is the yellow. Domain 4 is the cyan. Domain 5 is the red. The lighter and darker colors are used to distinguish the same domains in different sub-units. The spheres are the four metal cations used in each activation site. Green spheres are the Na^{+} ions, and the blue spheres are the Mg^{+2} ions.

Figure 4. pBluescript vector. (From Amplicon Express, 2009 (100)) .

Removed Due to Copyright.

The vector contains an ampicillin resistance gene and the lacZ-α gene.

CHAPTER 3

Experimental Design Issues

Section 3A: Goals of This Thesis.

The main purpose of this thesis is to show the interaction, if any, of H_2O_2, HCl, EDTA, and $CuSO_4$ with respect to *E. coli* and the ability of *E. coli* to develop and replicate and produce functional proteins, with the ability of translation, transcription, and activity of β-galactosidase as an indicator, while grown on an agar plate. Different stresses would also be compared to one another. Interactions of these treatments with each other and the colonies were also studied. Once this information is gained, the function of this data could serve as a stepping stone to some very useful biochemistry in the future. Hopefully these experiments will help point scientists in the right direction for discovering the pathways *E. coli* change due to its growth environment or in particular which stress responses are triggered by these stresses in these conditions and exactly what happens when multiple stresses are introduced. The roles of different stressors on *E. coli's* stochastic processes that control colony growth and protein expression by looking at the distribution data of colonies were examined as well. Most importantly, a basis for understanding how combinations of stresses are sensed and responded to in *E. coli* was attempted to be provided.

Section 3B: Determination of Backgrounds and Treatment Concentrations

The purpose of this chapter is to display the process of choosing treatment and background concentrations. The amount of colonies that were desired on each background (control) plate was a range of 400-1800. This range was so large because

the desired number of colonies was determined by the ability to use the Kodak Molecular Imaging software correctly and effectively, while still giving enough colonies that when treatments were added, at least 200 colonies would remain. In theory, the UV-Vis determination of relative concentrations in each overnight was done to keep these amounts of colonies somewhat constant. In practice, these plates varied from day to day. In some cases where more than one treatment was added, the amount of colonies was much lower than 200 colonies. In order to fix this issue, the treatment plates were plated with 100 µL of the second dilution of cells from the overnight, instead of the 50 µL of the second dilution of cells from the overnight added to control and most of the single and double treatment plates. The first time any new treatment was used, 50 µL of the second dilution was attempted first, and if less than 200 colonies remained, the first set would be ignored and triplicate plates would be produced using 100 µL of the second dilution. No plates required more than 100 µL of diluted cells from the overnight.

Another issue seen when completing this experiment on a day to day basis was the Kodak software's inability to count and measure colonies that grew too close to the edge of the plate. The 100 µL of diluted cells from the overnight were more difficult to keep within the borders, as more liquid added tended to be more difficult to keep under control when spreading.

The 1X IPTG + 1X X-gal background was determined by literature (101) and slightly tweaked to get more blue colonies. The desired amount of blue colonies for each background was about 75% blue and 25% white. Different plates with varying

concentrations of IPTG were plated with 1X X-gal, with half the original concentration of IPTG giving the closest results to 75% blue, 25% white, with the least amount of IPTG added. The same was done with varying X-gal concentrations and 1X IPTG, with 75% of the original X-gal concentration giving the best results with the lowest amount of X-gal added. If a stress response depended more on the amount of substrate available (lower X-gal, lower substrate concentration), then differences should be noticed in the 1X IPTG + 0.75X X-gal plates when compared to the 1X IPTG + 1X X-gal plates for the same stress. If a stress response depended more on the amount of enzyme available (lower IPTG, lower transcribed β-galactosidase concentration), then lowering the concentrations of IPTG should generate greater differences observed in the 0.5X IPTG + 1X X-gal plates compared to 1X IPTG + 1X X-gal plates for the same stress.

The ideal plates with a single treatment were to have about 66% of the amount of original colonies that were found on corresponding background plates. To decide the concentration used for HCl, 10 µL and 100 µL of 12.1 M HCl were added to 1X IPTG + 1X X-gal plates, plated with colonies, and growth was observed as usual. The 10 µL of 12.1 M HCl gave fewer colonies than the controls but the 100 µL of 12.1 M HCl gave no colonies at all. It was determined that the 10 µL of 12.1 M HCl would be sufficient but while this experimentation was going on, it was also determined that the dilution of colonies added needed to change. So, the next time 10 µL and 20 µL of 12.1 M HCl were added to 1X IPTG +1X X-gal plates, plated with the dilution of colonies described on page 8 that was used for every plate from then on and growth was observed. With this dilution, less colonies were observed in the 10 µL experiments but the difference

between the controls and the 10 µL of HCl treated plates were not significant enough for the experiment. The 20 µL of 12.1 M HCl gave roughly 3/7th the amount of colonies that were in the controls and this was too few for the experiment. The next time 15 µL of 12.1 M HCl was added to 1X IPTG + 1X X-gal plates, plated, and growth was observed. These plates were considered to remove a sufficient amount of colonies, while leaving enough for comparisons.

A stock solution of 0.5 M, 7.8 pH EDTA was added to plates at varying volumes to determine the acceptable level of EDTA to be used in theses experiments. First 1 mL, 0.75 mL, 0.5 mL, 0.25 mL, 0.1 mL, and 0.05 mL of EDTA were added to 1X IPTG + 1X X-gal plates. These were plated with DH5-α/pBluescript *E. coli* as described above, and growth was observed. No cells grew on any of these plates. The concentration was kept constant but even less volume was added the next try. The 0.5 M EDTA was added in 100 µL, 50 µL, 25µL, 10 µL, and 5 µL increments to 1X IPTG + 1X X-gal plates, cells were plated, and growth was observed. The 100 µL and 50 µL plates gave no colonies. The 25 µL plate gave very few colonies. The number of colonies on the 10 µL plate was slightly lower than what was desired, but the 5 µL plate was slightly higher. So 8 µL of 0.5 M EDTA was attempted on all three backgrounds and it was determined that the amount of colonies grown on each was sufficient.

The stock solution of the hydrogen peroxide was 5 M. This was much too strong and was diluted in distilled water to 0.05 M hydrogen peroxide. This dilution (5 µL and 10 µL) was added to 1X IPTG + 1X X-gal plates, cells were plated, and growth was observed. Both volumes of this dilution gave too many colonies. So the volumes were

increased to 15 µL and 20 µL of the 0.05 M hydrogen peroxide the next time, cells were plated and growth was observed. While the 15 µL was deemed alright, the 20 µL was determined to be a better dilution for these experiments as it was closer to the 60-70% survival rate that was desired.

The $CuSO_4$ concentration and volume treatment took multiple weeks to determine. $CuSO_4$ (20 mM) was attempted first, with 50 µL, 25 µL, and 12.5 µL added to 1X IPTG + 1X X-gal plates. Cells were plated and growth was observed. All plates were covered in much too many colonies. Next, 100 µL of 20 mM was attempted and still, much too many colonies were grown. So the concentration of the $CuSO_4$ was increased to 500 mM and 100 µL, 75 µL, 50 µL, 25 µL, and 10 µL were added to the 1X IPTG + 1X X-gal plates. Again, too many colonies grew on all plates. The concentration of the $CuSO_4$ was then increased to 1 M and 100 µL and 50 µL were added to 1X IPTG + 1X X-gal plates. The plate with 50 µL of 1 M $CuSO_4$ still gave too many colonies but the 100 µL plates had too few colonies. So, 60 µL, 70 µL, 80 µL, and 90 µL of the 1 M $CuSO_4$ were added to 1X IPTG + 1X X-gal plates, cells were plated, and growth was observed. It was determined that the 70 µL of the 1 M $CuSO_4$ gave the best results for the number of colonies for these experiments.

After each treatment concentration and volume added were decided, all four treatments on one plate were used to show if the combination of the four would cease all growth. It did not.

Table 3. Physical properties of each stress and reactant added.

Stress added	Concentration (M) outside of plate	Concentration (M in agar) inside plate	Preparation	Volume added to plate (µl)
HCl	12.1M	5.14 E-3	No dilution. Direct from bottle.	15
$CuSO_4$	1M	2.0E-3	Oven dried $CuSO_4$, with distilled water as solvent.	70
H_2O_2	0.05M	2.86E-5	5M H_2O_2 with a 1:100 dilution in distilled water.	20
EDTA	0.5M	1.14E-4	EDTA with distilled water as solvent. Filtered and sterilized. Adjusted to a pH of 8.0 with NaOH.	8
1X X-gal	0.122M	1.95E-4	5-bromo-4-chloro-3-indolyl-β-D-galactoside (solid) kept at -20°C. Was dissolved in 2ml N,N-dimethylformamide, then immediately covered with aluminum foil and stored at –20°C.	56
0.75X X-gal	0.122M	1.46E-4		42
1X IPTG	0.1M	5.0E-4	IPTG (solid) kept at -20°C. Distilled water used as solvent. Filtered and sterilized, and stored at -20°C.	175
0.5X IPTG	0.1M	2.5E-4		87

Table 4. Table of pH's of treatment(s) in 35ml LB broth.

Treatment	pH in 35ml of LB broth
None (Amp, X-gal, IPTG)	7.15
EDTA	7.13
HCl	5.95
H_2O_2	7.17
$CuSO_4$	6.24
EDTA, HCl	5.99
EDTA, $CuSO_4$	6.39
EDTA, H_2O_2	7.16
HCl, H_2O_2	5.97
HCl, $CuSO_4$	5.13
H_2O_2, $CuSO_4$	6.27
EDTA, HCl, H_2O_2	5.95
EDTA, H_2O_2, $CuSO_4$	6.37
EDTA, HCl, $CuSO_4$	5.14
H_2O_2, HCl, $CuSO_4$	5.15

CHAPTER 4

Data Generation for Input Interactions

Section 4A: Materials and Methods

Reagents.

DH5-α cells and the pBluescript vector were gifts from Dr. Vivian Bellofatto, UMDNJ. IPTG (0.1 M solution in distilled water, bought sterilized) was filtered using a sterile 50 mL Norm Ject syringe using a sterile Cameo 25NS nylon filter. The IPTG and filtered 25 mg/ml ampicillin (amp) were bought from Acros Organics. EDTA and $CuSO_4$ solids were bought from Sigma and were made into 0.5 M EDTA and 1 M $CuSO_4$ solutions in distilled water. The EDTA was filtered using another sterile 50 mL syringe and a sterile nylon filter. LB-agar, 12 M HCl, and 5 M H_2O_2 were bought from Fisher Scientific. LB broth was purchased from Teknova. The LB Broth, LB-agar, pipette tips, and graduated cylinder used for transfer of agar to plate were sterilized using an autoclave. Materials were sterilized to make sure no other bacteria would interfere with the experiments. IPTG, EDTA, and ampicillin were filtered to ensure the chemicals were as pure as possible. IPTG, ampicillin, EDTA, $CuSO_4$, and H_2O_2 were all diluted with distilled water.

*X-gal***.**

To make 2 mL of 0.122 M X-gal, 100 mg 5-bromo-4-chloro-3-indolyl-β-D-galactoside bought from Bioline was dissolved in 2 mL N,N-dimethylformamide (purchased from Fischer Scientific). This was immediately covered with aluminum foil (to keep out light) and stored at –20°C.

Streaking a DH5-α/pBluescript Plate for Creation of Overnights.

DH5-α/pBluescript plates for creation of overnights were produced. Cells were stored in a -80°C freezer in a 1.5 mL plastic sterilized tube. When a plate was needed, a tube was removed and placed directly on ice. A plate containing only ampicillin and LB-agar was used as the solid medium. An inoculating loop was used to spread a small amount of *E. coli* from the tube onto the plate. The tube was then returned immediately to the -80°C freezer. The plate was incubated at 37°C for 20-24 hours and then kept in a 4°C refrigerator until needed.

Pouring Plates.

Desired amounts of LB-agar were autoclaved in a 1 L Erlenmeyer flask. A 50 mL Pyrex graduated cylinder was autoclaved and used to pour all LB-agar. After autoclaving all needed reagents and equipment, including the 50 mL graduated cylinder, 25 mg/mL ampicillin was added directly to the LB-agar to a final concentration of 0.02% v/v of 0.072 M ampicillin in LB-agar. Using Fisherbrand Standard, Sterile Polystyrene (size 100x15 mm) plates, 35 mL of LB-agar (with amp) was added to each plate. Different concentrations of IPTG and X-gal were added to see how some of the stress responses in *E. coli* function. X-gal was directly pipetted into LB-agar in the graduated cylinder. IPTG, HCl, EDTA, H_2O_2, and $CuSO_4$ were added straight into the plates before LB-agar with ampicillin and X-gal were poured on top. Once poured, plates were left out at room temperature overnight. The standards used were 56 µL of 0.122 M X-gal (1X X-gal) and 175 µL of 0.1 M IPTG (1X IPTG). For lower X-gal, 42 µL of 0.122 M X-gal (0.75X X-gal) was used, along with 1X IPTG. For lower IPTG, 87 µL of 0.1 M IPTG (0.5X IPTG) was added,

along with the standard 1X X-gal. Controls of IPTG and X-gal alone featured all three of these types of plates, 1X IPTG + 1X X-gal, 1X IPTG + 0.75X X-gal, and 0.5X IPTG+1X X-gal (See Table 3 for physical properties of added chemicals).

HCl (15 µL), H_2O_2 (20 µL), EDTA (8 µL), and $CuSO_4$ (70 µL) were added alone or in combinations as necessary to cause stress conditions. Stresses were added to all three types of IPTG + X-gal plate. Each stress and every possible combination were done in triplicate.

Overnights.

Ampicillin (10 µL, 25 mg/mL) was added to a labeled test tube filled with 5 mL of LB broth. One colony taken from the saved plated DH5-α/pBluescript plate was transferred using a sterile pipette tip, and the tip was then dropped into the LB broth. The tube was covered and left in incubator at 37°C for 20 hours, shaking at 220 rpm.

Plating E. coli.

The absorbance of a 1 to 10 dilution of overnight to LB broth was taken using a Cary 50 Bio UV-Visible Spectrophotometer Simple Reads program set at the wavelength of 600 nm to determine the amount of overnight to add to the first of two serial dilutions and to keep the amount of cells plated as constant as possible. Measurements were performed in a 10.00 mm quartz cuvette with a sample size of 1 mL. It was determined experimentally to use the following equation in order to find the amount of cells needed for plating and eliminate variability in the amount of overnight growth: 0.25(100 µL)=x(Abs @ 600 nm), with x = volume in µL of overnight needed to add per 1400 µL LB broth. Of this first dilution, 4 µL was added to another 1400 µL broth to make a second

dilution. Of this second dilution, 50 µL was then plated onto all the control plates. All dilutions of overnights took place in 1.5 mL sterilized centrifuge tubes. All the single parameter plates and all but the HCl + EDTA treated double parameter plates were plated using 50 µL of this second dilution. The HCl + EDTA double parameter, all the triple parameters, and the combination of all four parameters were plated using 100 µL of the second dilution due to the fact that these parameters stunted too much cell growth, giving poor results when adding only 50 µL. A steel spatula was used to spread cells onto agar plates. The spatula was washed with ethanol and enflamed with a Bunsen burner and then cooled by touching the cool plate. Once bacteria had been added, plates were incubated at 37° C for 1 hour with their tops facing up and then flipped with the tops now facing down for the remaining 17 hours. Pictures were taken at exactly 18 hours from the entrance of plates into the incubator.

Section 4B: Determination of Data for Evaluation

The rest of this chapter discusses how data was analyzed and the discussion of the results. Pictures of each individual plate were taken using a Gel Logic 100 Imaging System camera while placed on a transilluminator. Using the Kodak Molecular Imaging Software (v. 4.5.1), colonies were counted (Figure 5) with their borders enclosed. The interior area of the colony (in pixels) and the intensity emitted by each colony were given by the software. Conditions were done in triplicate and means of area and intensity were determined of each type of stress treatment and each background (1X IPTG + 1X X-gal, etc.).

Using a basic formula of $y = C_xX_x + b$, where y = the mean of intensity, area, or the total colony count for a specific background and treatment, b = a universal constant for all treatments, C_x= a constant for designated treatment, given as the result, x = the treatment used (x=(E=EDTA, H=HCl, O=H_2O_2, C=$CuSO_4$)), X_x= 0 for a control sample, where the treatment is not there, and X_x=1 in the experimental plates where the treatment is there, data for single treatment plates was calculated and compared. Modeling of the interactions was done using R 2.8.1 with commands for linear models (e.g. summary.lm).

For two or three treatments, the equation grows a bit. For example, if a mean intensity of a certain background of a HCl and EDTA treated plate were to have $y_i \neq C_EX_E + C_HX_H + b$, then an extra constant would be created and added, giving $y_i = C_EX_E + C_HX_H + b + C_{EH}X_{EH}$. This extra combinatorial constant gave an indication on whether the terms making up the combination were additive or not. If the individual terms making up the constant were not found to be significant, then these were determined to not have any affect. If the individual terms making up the constant are non-significant, and the combinational term is significant, that is evidence of a non-additive interaction. If these individual terms were significant and the combinatorial term was significant, than the responses to the combinatorial stresses were deemed non-additive responses. If the individual terms were significant and the combinatorial term was insignificant, than it is possible that the responses to the combinatorial stresses were additive.

The total equation for all plates is:

$$y = b + C_E X_E + C_O X_O + C_H X_H + C_C X_C + C_{EO} X_{EO} + C_{EH} X_{EH} + C_{EC} X_{EC} + C_{OH} X_{OH} +$$

$$C_{OC} X_{OC} + C_{HC} X_{HC} + C_{EOH} X_{EOH} + C_{EOC} X_{EOC} + C_{EHC} X_{EHC} + C_{OCH} X_{OCH} + C_{EOCH} X_{EOCH}.$$

Section 4C: Results and Discussion Introduction

Data sets were sorted according to the output (colony count, mean size, or mean intensity), background (1X X-gal + 1X IPTG, 1X X-gal + 0.5X IPTG, or 0.75X X-gal + 1X IPTG), and then treatment (either individual or combinations of stress). Fifteen different treatments were done, all in triplicate, giving forty-five plates per background. Data from one hundred thirty-five treatment plates across all backgrounds were compared to the thirty-five control sets (some treatments were done on the same day, sharing one set of controls). So for each of the two hundred forty total plates, colony count, intensity of each individual colony, and area of each individual colony were measured.

Using the modeling equation (Section 4B), the most useful piece of information came from looking at the "C" values for each type of treatment using each background. In particular, the nature of these C values, either positive or negative, was constructive. For single treatment plates, the C values are a direct representation of whether or not the treatment causes a change when compared to the corresponding control plates. So if a C value was determined by the model to be significantly positive, it suggests that the results of the output of the treated plates were greater than the control plates (either more colonies, a larger area, or more intense coloring).

For double and triple treated plates, the C values do not suggest an actual higher or lower output when compared to the controls but do suggest a change in expected

growth when compared to the model. The linear model takes the single treatment data and computes an ideal model for additive interactions between the stresses. The C value for the combination then is used by the model to realign what was expected by the model to what the actual data gave. For example, if a C value for two separate single treatments (e.g. C_{T1} and C_{T2}) for an output and background are additive, than C_{T1T2} would be zero and $C_{T1} + C_{T2} + b = y$. No C_{T1T2} value was found to equal exactly zero and all models used a C_{T1T2} value, sometimes significant and sometimes insignificant, to adjust the model. The combinatorial C values that were insignificant could be seen as possible additive terms if the individual terms were significant, as the C_{T1T2} value is not significantly different than zero.

In order to state that the combinatorial term is not additive, than a significant p-value associated with the term must be given. All the individual treatments making up the combination must also give significant C values. This shows that the combinatorial term is significantly different than zero. Treatments that gave p-values under 0.05 were determined as significant data and not just random data, which would mean in the combinations that the terms were not additive.

The b value of the equation was also given by the R software while modeling the equation. The ideal control data would make $y_{control} = b$. The amount of variation in the data in some cases decreased the reliability of the results of the model, which results in an overall model that is not useful. One indicator of that was that b values do not appear to correspond to the actual results for single treatments. P-values were also determined for these b values.

Due to the nature of some of the stresses not being additive, in most cases a pattern was observed when a second stress and then a third stress were added, no matter the background, output, or stress. According to the data, when a second stress was introduced, the sign of the C value describing the new combination (e.g. C_{EH}) would switch. Then, when the third stress was introduced, the sign of the C value for this new combination would again switch. The most exceptions to this rule took place when using colony count as the output (Table 14). There were 33 single treatments across all backgrounds and inputs that gave the same sign for the C value. Of those, 26 switched the sign for all possible C values in all double treatments made up of any combinations of the single treatments. For example, in the colony count data for the 1X IPTG + 1X X-gal background, EDTA, HCl, and H_2O_2 were all significant negative C values. The combinations of EDTA + HCl, EDTA + H_2O_2, and HCl + H_2O_2 all gave significant positive C values. There were also 26 of the 33 possible that had the same sign on the C value as all of the single treated plates when all three of the single treatments with the same sign were combined as a triple treatment plate. Following the previous example, the combination of EDTA + H_2O_2 + HCl for the 1X IPTG + 1X X-gal background for colony count was again a significant negative C value. There were 29 combinations across all backgrounds and inputs that had all three single treatments one sign C values, then all possible two way combinations of these three the opposite sign C values, and the combination of all three treatments giving the same sign C value as each individual treatment.

Even when the C value results are not significant, this pattern is still observed. The fact that the signs are flipping so many times is good evidence that even thought the individual combinations may not be significant, the repetition observed in the pattern leads to the belief that generally the terms are not additive. The equation without the combinatorial term (e.g. C_{T1T2}) and assuming an additive nature of the individual stress responses usually over-estimates the effect compared to what actually happened in each case. The combinatorial term is frequently needed to compensate with the opposite sign across all backgrounds and outputs.

When looking at the three term level, the pattern again leads to the belief that in general without the three stress C term (e.g. C_{T1T2T3}), the equation will often underestimate the effect and need to be corrected with another opposite term C value. The fact that these terms were needed in significant cases proved that some of the resulting responses from *E. coli* were generally not additive but rather new or cross protecting when combinations of stresses were added.

Section 4D: Colony Count Data

Colony count data was not compared to a normal distribution curve because all outputs were positive, whole numbers. Instead, a Poisson curve was used in the linear model. Colony count data (and as discussed later, mean area and mean intensity data as well) for two backgrounds, the 1X IPTG + 1X X-gal and 1X IPTG + 0.75X X-gal data sets, followed very similar patterns in both magnitude and sign of the C value in respect to how each treatment reacted with *E. coli* for each background when compared to control plates. The 0.5X IPTG + 1X X-gal data set generally (with a few exceptions) had an

opposite influence than the other two backgrounds on how a treatment reacts with *E. coli* when compared to the control plates.

For single parameter treatments, the 1X IPTG + 0.75X X-gal (Table 6) and 1X IPTG + 1X X-gal (Table 5) backgrounds all had a negative effect on colony count except for the $CuSO_4$ treatment in the 1X IPTG + 1X X-gal background. The $CuSO_4$ treatment in both backgrounds gave higher p-values than the 0.05 cut-off, making the data insignificant. All other single parameter treatments in the 1X IPTG + 1X X-gal and 1X IPTG + 0.75X X-gal backgrounds gave significant p-values. For both backgrounds, the hydrogen peroxide treatment caused the greatest significant change in colony counts compared to the controls, with very similar C values of -2.05×10^4 for the 1X IPTG + 1X X-gal background and -2.50×10^4 for the 1X IPTG + 0.75X X-gal background. Both backgrounds when treated with EDTA had the next greatest consequence and then HCl had the third greatest for both backgrounds. The C values were again comparable for both treatments. The $CuSO_4$ treatments had the least effect in both backgrounds and may have not had an effect at all, as neither caused a significant change in the colony counts when compared to the controls. Both the C absolute value was lower than 100 and the p-value was higher than 0.05 for the $CuSO_4$ treatments.

The 0.5X IPTG + 1X X-gal background (Table 7) gave unique results for colony counts of singular stress treatment plates when contrasted to the 1X IPTG + 1X X-gal and 1X IPTG + 0.75X X-gal single treatment plates. Unlike the other two backgrounds, all four single parameter treatments had a positive affect on colony count for this background. All four gave significant p-values. The amount of change due to a single

stress followed a similar pattern as the other two backgrounds. Hydrogen peroxide again had the largest influence on colony count, with a C value of $2.00x10^4$, except it was the opposite effect. Again, EDTA had the second largest C value magnitude. $CuSO_4$ and HCl switched positions for this background, with HCl causing the least amount of change in the colony count.

For the 1X IPTG + 1X X-gal and 1X IPTG + 0.75X X-gal backgrounds, all of the two stress systems proved to follow the "sign-switching" pattern except for the $CuSO_4$ + HCl plates, which still gave a negative C value (Table 6). All double treated plates gave significant p-values except the 1X IPTG + 1X-gal background CuSO4 + H_2O_2 plates, which still followed the pattern. The double stress plate with the biggest influence on colony count C values was the combination of hydrogen peroxide and EDTA for both backgrounds. This means that the addition of both EDTA and hydrogen peroxide caused a much different stress response than the model expected the bacteria to have if additive. The plates that caused the least amount of change in C value were the $CuSO_4$ + HCl plates, however there is still proof here that the two stresses together triggered a separate response than seen in both individual treatments. These were not just additive responses but rather new stress response(s) either different or as a result of cross-protection of an individual stress response.

The triple stress plate colony counts were a little more unpredictable when it comes to the sign of the C value for these two backgrounds. For the 1X IPTG + 0.75X X-gal background, only the $CuSO_4$ + HCl + EDTA plate gave a positive C value (Table 6). All triple stress sets gave significant C values, including the $CuSO_4$ + HCl + EDTA plates.

These sets of plates also had the smallest absolute C value of all triple parameter sets for this background. $CuSO_4$ + EDTA + H_2O_2 plates had the biggest absolute C value for this background for any set of plates.

The 1X IPTG + 1X X-gal background had two triple stress sets that gave positive C values and two that gave negative C values (Table 5). $CuSO_4$ + HCl + EDTA and $CuSO_4$ + EDTA + H_2O_2 were the two sets where the addition of these stresses had significant positive C values, while $CuSO_4$ + HCl + H_2O_2 and HCl + EDTA + H_2O_2 had insignificant negative C values. For this background, HCl + EDTA + H_2O_2 had the largest influence on absolute value of the C value for any set of plates.

The 0.5X IPTG + 1X X-gal background followed the same pattern, except in the opposite order (Table 7). All the single treatment plates had a positive effect on colony count. Most of the double treatment plates had a negative C value for colony count. The exceptions here are EDTA + H_2O_2 and HCl + H_2O_2. The HCl + H2O2 treated plates gave an insignificant p-value, meaning the HCl and H_2O_2 individual stress responses in the 0.5X IPTG +1X X-gal background could be additive. All single and triple treatment plates gave significant p-values. For the triple treatment plates, all of the combinations have a positive C value except for HCl + EDTA + H_2O_2. These plates have a negative effect on the C value for colony count and also have the largest magnitude on the 0.5X IPTG + 1X X-gal background of any set of plates, meaning the double treatments made up of HCl +EDTA, HCl + H_2O_2, and EDTA + H_2O_2 were the least additive and had a new response or some cross-protection taking place.

The fact that the 0.5X IPTG + 1X X-gal background gave opposite results than the other two backgrounds for colony count could mean that IPTG and therefore the cell's ability to turn on the *lac* operon, could be essential to assist *E. coli* in initial stages of survival and reproduce to form colonies under stress. Due to the fact that *E. coli* does grow without an active *lac* operon, this cannot be a major factor, but perhaps it could be supportive to the growth. The lessening of X-gal does not seem to have much of an effect when it comes to colony count, as the same patterns and very similar values were seen as plates with 1X X-gal as in the 0.75X X-gal plates.

For the 1X IPTG + 1X X-gal background, it appears that $CuSO_4$ caused a bit of a strange outcome when compared to the almost universal pattern of all the single stress plates having one sign of the C value, the double stress plates having the opposite sign, and the triple stress plates having the same sign as the single stress plates. $CuSO_4$ was in every plate set that deviated from this pattern in the 1X IPTG + 1X X-gal background (Table 5). It also was in all four insignificant data sets. For the 1X IPTG + 0.75X X-gal background, again $CuSO_4$ was found in both plate sets that broke the pattern but HCl was also in both plate sets (Table 6).

Evaluating the 0.5X IPTG + 1X X-gal background, it was noticeable that this background too had a single stress that caused a departure from the pattern (Table 7). Hydrogen peroxide was seen in all three plate sets that moved away from the pattern. What causes $CuSO_4$ and H_2O_2 to go against the pattern here is unclear. What is clear is that these stresses and combination of stresses are influencing the colony count almost every time. In particular, the combination of stresses is usually having a non-additive

effect on colony count, no matter the background. The non-additive effect of the combinations of stresses is a reason to believe that these stresses together are influencing how these colonies grow and the ability of the cell to reproduce when compared to the individual stress responses.

Section 4E: Area Data

Area data was collected for every single colony for every plate. When data was analyzed, mean area of the bacteria for each plate was used in the model (Section 4B) to compare data. A normal distribution was assumed for the model and was seen in the control data. For the mean area C value data, the backgrounds did not differentiate as much as the data for colony count did. The only major differences were the amount of significant mean area data that treatments gave for the three backgrounds. The mean area for the 1X IPTG + 1X X-gal background (Table 8) gave the most significant p-values, with only two insignificant data points for mean area, the treatments of $CuSO_4$ + H_2O_2 + EDTA and EDTA + H_2O_2 + HCl. The 1X IPTG + 0.75X X-gal (Table 9), on the other hand, had only one significant data point for mean area, treated with $CuSO_4$ + HCl. The 0.5X IPTG + 1X X-gal background (Table 10) had four significant data points for mean area, all with $CuSO_4$ in the treatment.

All three backgrounds follow the same basic data pattern as the colony count data did, where all single treatments had an effect on each background controls, all of the double treatments were overestimated and had to give a negative C value to compensate for this, and most of the triple treatments again had the same sign C value as the individual treatments, with a few exceptions. The three backgrounds shared the

exact same pattern this time, with the majority of individual stresses giving a positive C value. There were no exceptions to this pattern for the 1X IPTG + 1X X-gal background. The only exception for the 1X IPTG + 0.75X X-gal background was the $CuSO_4$ + H_2O_2 + EDTA treatment, which had a C value of -2.02×10^{12}. The 0.5X IPTG + 1X X-gal background also had one exception, again with the $CuSO_4$ + H_2O_2 + EDTA treatment having an insignificant C value of -3.28×10^{11}. This data truly supports the idea that the pattern is indicating something significant is happening, even though the data points themselves are sometimes insignificant. The pattern is seen multiple times using both significant, insignificant, and combinations of both significant and insignificant C values.

As in the colony count 1X IPTG + 1X X-gal and 1X IPTG + 0.75X X-gal data, the magnitudes of the C values also were relatively consistent for all three backgrounds when looking at mean area. Of the single parameters, H_2O_2 treated plates had the biggest positive influence on C values for all backgrounds, while HCl treated plates changed the mean area C values the least when comparing to the control plates for all backgrounds. EDTA + H_2O_2 always had the highest absolute C value for each double parameter treated plates in every background, while $CuSO_4$ + HCl had the smallest absolute C values for the double treatments in every background. As in the sign patterns, the consistency lessens when looking at the triple parameter plates magnitudes. For the 1X IPTG + 1X X-gal and 1X IPTG + 0.75X X-gal backgrounds, the $CuSO_4$ + H_2O_2 + EDTA plates had the biggest influence on the absolute C value. The 0.5X IPTG + 1X X-gal background, however, had to change the model with the largest absolute C value when treated with H_2O_2 + EDTA +HCl. All three backgrounds changed

the C value the least of any triple parameter treated plates when treated with $CuSO_4$ + EDTA + HCl.

The data from the model (see Section 4B) for the average area showed that all four stresses when added individually caused reactions that created larger average colonies. Larger colonies could be a result of one of two different responses, either the *E. coli* themselves grew larger or the *E. coli* reproduced quicker than in the controls, or perhaps a mix of the two. When two of the treatments were added, the model needed to be changed in all conditions, proving once again that what was being observed were non-additive stress responses when a new second stress was present. Then when three treatments were added, most of the time the signs of the C values changed again.

Section 4F: Intensity data

The larger that a colony was the more intensity was seen from the Kodak Molecular Imaging software. There was a high correlation for every plate when plotting area vs. intensity for each colony (Figure 6). To fix this issue, corresponding area values were divided out of every intensity value for each colony before data analysis, giving a data point called the "adjusted intensity". This completely destroyed the correlation of data (Figure 7). The means of area when plotted against the means of intensity again showed a correlation for all plates (Figure 8). The means of area plotted against the means of adjusted intensity showed that the correlation was gone from both the 1X IPTG + 1X X-gal and 0.5X IPTG + 1X X-gal backgrounds (Figure 9). However, the 1X IPTG + 0.75X X-gal background, while still having a relatively low correlation at 0.562, still had a significant p-value. So to see whether the 1X IPTG + 0.75X X-gal background was really

still correlated, each plate for each control background was plotted from lowest to highest correlation for each individual plate (Figure 10). This plot showed that there was not a real difference between the 1X IPTG + 0.75X X-gal background and the other two backgrounds.

The adjusted intensity C values from the above equation never resulted in a significant p-value for any sample in any background. The same sign pattern was still noticed here for the C value data though, with a few exceptions again. The adjusted intensity data for the backgrounds was split again into two groups, though unlike colony count, here 1X IPTG + 1X X-gal (Table 11) and 0.5X IPTG + 1X X-gal (Table 13) both gave positive values for the single parameter treatments, while 1X IPTG + 0.75X X-gal (Table 12) acted differently, giving negative values for the single treatments. There were no exceptions to the pattern in the 1X IPTG + 1X X-gal background, as all single treatments were positive C values, all double treatments negative, and all triple treatments were again positive. The 0.5X IPTG + 1X X-gal background only had one exception, the $CuSO_4$ + H_2O_2 + EDTA plates gave negative C values. The 1X IPTG + 0.75X X-gal background data showed the same but opposite pattern, with a few more exceptions than the other two backgrounds. The single treatments had all negative C values, the double treatments had mostly positive C values, and the triple treatments were half negative and half positive. The exceptions from the pattern were $CuSO_4$ + HCl giving a negative C value and $CuSO_4$ + HCl + EDTA and $CuSO_4$ + H_2O_2 + HCl both having positive C values. A difference between these two sets of backgrounds was also seen in the b value, with both the 1X IPTG + 1X X-gal and 0.5X IPTG + 1X X-gal having negative b values, while 1X

IPTG + 0.75X X-gal had a positive b value. This means the control plates had a higher intensity in the 1X IPTG + 0.75X X-gal plates than in the other two backgrounds.

The largest absolute C value for single treatments in all three backgrounds for adjusted intensity was H_2O_2. The smallest was HCl. EDTA + H_2O_2 had the largest absolute C value for all backgrounds for all double treatment plates. $CuSO_4$ + HCl gave the smallest absolute C value for all backgrounds in the double treatment plates. For the triple treatments, the consistency lowers slightly. For the 1X IPTG + 0.75X X-gal and 0.5X IPTG + 1X X-gal plates, the $CuSO_4$ + H_2O_2 + EDTA plates have the greatest effect on the C value for adjusted intensity. This plate also has a very high effect on the 1X IPTG + 1X X-gal background but the H_2O_2+ EDTA + HCl plate has a little bit larger absolute C value. The $CuSO_4$ + HCl + EDTA treatments always had the smallest absolute C value for adjusted intensity in all three backgrounds for the triple parameter treatments.

The fact that the 1X IPTG + 0.75X X-gal background acted differently than the other two backgrounds suggests that the X-gal substrate is essential to making these colonies more blue. Again, treatment data was deemed non-additive, as the pattern was mostly observed here, even though all of the data was insignificant.

Section 4G: Modeling Accuracy Data

The models run with the equation in Section 4B when assuming a normal curve were given both a p-value and an adjusted R^2 value to show how close accurate the model was when determining C values. Due to the nature of the data available for colony count (only whole numbers, one per plate), only area and adjusted intensity data could be compared to the normal curve and therefore were the only outputs to get

these values. All p-values for every output and every background were significant, meaning the models created with the R software were affective. The models did vary in significance and R^2 values, changing the amount of efficacy that the models created for each background and output.

The best models were made for the area output for the 0.5X X-gal + 1X IPTG and 1X X-gal + 1X IPTG backgrounds. For the 1X X-gal + 1X IPTG background for the area output gave an adjusted R^2 value of 0.6241 and a p-value of $1.420e^{-05}$. The 0.5X X-gal + 1X IPTG background area output's model gave an R^2 value of 0.6883 and a p-value of $1.17e^{-06}$. The 0.75X X-gal + 1X IPTG background area output gave an adjusted R^2 value of 0.4425 and p-value of 0.001964, which is still a significant model but not quite the same level of accuracy as the models for the two other backgrounds.

The adjusted intensity models were all less significant than the area models in all cases. A different order of backgrounds was observed when compared to the area, with the 0.75X X-gal + 1X IPTG background giving the best model for adjusted intensity, the 0.5X X-gal + 1X IPTG background giving the second best and the 1X X-gal + 1X IPTG background giving the least accurate model for the adjusted intensity output. All three are again considered significant. The R^2 value for the 1X X-gal + 1X IPTG background adjusted intensity output was 0.3686, while the p-value was 0.00813. The 0.5X X-gal + 1X IPTG background gave an R^2 value of 0.3821 and a p-value of 0.006398. The 0.75 X-gal + 1X IPTG background gave an R^2 value of 0.469 and a p-value of 0.001105.

Knowing how these models rank in significance, it gives an idea of why the adjusted intensity gives less significant C values than the other two outputs. Also, the

0.75X X-gal + 1X X-gal + 1X IPTG background for the area output gave fewer significant results than the other two backgrounds, possibly due to the lack of consistency in the model. Due to the significance of the models, the assumption of normal curves was validated.

Section 4H: Conclusions

Colony count showed the most significant data and was the most affected by the stressors. Colony count data displayed non-additive interactions at the two-way and three-way level. The other outputs, area and adjusted intensity, also showed non-additive interactions, even though the data was not significant as in colony count. The overall general pattern seen of change in response sign whenever a new stress was added sustains this theory as well. For every single treatment with a significant effect, that treatment when put into a combination with another significant treatment, had a significant and opposite C value for every background and output.

The 1X IPTG + 1X X-gal, the 1X IPTG + 0.75X X-gal, and the 0.5X IPTG + 1X X-gal backgrounds all showed similar patterns for both the stressor and combination of stressors area, suggesting similar interaction patterns. Differences were seen by the 0.5X IPTG + 1X X-gal background for colony count, indicating a separation of how this background initially grows and reproduces to create colonies under stress due to its lack of IPTG and therefore, active *lac* operon and transcribed and translated, functional β-galacatosidase. The treatments, however, did not result in any differences from the 1X IPTG + 1X X-gal background for area or intensity for the 0.5X IPTG + 1X X-gal background, suggesting similar interaction patterns once growth was initiated. The 1X

IPTG + 0.75X X-gal background reacted differently for both the stressors and combination of stressors when looking at adjusted intensity, which is most likely due to the lack of X-gal substrate to react with β-galactosidase to form the insoluble blue product. This suggests that the treatments may have interacted with the X-gal itself, causing the lowering of intensity from the control plates to the experimental plates.

EDTA + H_2O_2 had the greatest influence of any double parameter treatments for every background and every output on the C values, meaning that the EDTA + H_2O_2 double treated plates had to adjust the C value the most, giving a strong indication that these two stress responses were not additive in any way. $CuSO_4$ + HCl had the least effect on the C values of all backgrounds and all outputs for the double treatments. However, $CuSO_4$ + HCl gave significant C values in colony count and average area for all backgrounds, suggesting non-additive interactions for at least these two inputs.

EDTA + H_2O_2 actually was a significant exception to the overall sign pattern seen when looking at the C values for the 0.5X IPTG + 1X X-gal background in colony count yet still had the largest of all double treatment absolute C values. This was the only significant exception to the pattern that did not include an insignificant single treatment C value in all backgrounds and all inputs. This suggests that the data observed is correct but that there is an indication that this treatment that caused a pattern exception is causing a very different response in the cell compared to how the cells react to the individual treatments. It was not found to deviate from the pattern in any other background or input, no matter if it was significant or insignificant.

Samples of all four treatments added at once were done but data for these experiment plates was not analyzed in the linear model in the same fashion as the other treatments and combinations. No p-value for the C value was produced in the four treatment interaction because the degrees of freedom does not allow it to truly be calculated. A C value instead was "set" based on the other values of the other terms when doing the modeling.

The model data proves that non-additive interactions are taking place for these treatments. These non-additive interactions could be a result of responses for one stress reacting with another stress. This has been studied and observed before, as noted in Section 1A. For example, Dps, a DNA-binding protein, assists in oxidative and acid tolerance stress, as well as starvation (62). *E. coli* uses *rpoS* to respond to both osmotic and oxidative stresses (65). Osmotic stress itself is known to increase thermotolerance and oxidative-stress resistance in *E. coli* at least partially by upregulation of genes in OxyR and SoxRS (102). The sigma factor, σ^B, in *Listeria monocytogenes* provides a role in heat, ethanol, acid, starvation, and oxidative stress (5). Other proteins and responses are also known to cross-respond to multiple stressors in *E. coli* and other organisms. It is very conceivable that many more stress response proteins and entire systems respond to a plethora of stressors and the combinations of stressors.

Section 4I: Future Work

Now knowing that these combinations of stresses cause non-additive interactions, it is time to look closer at how *E. coli* are responding at the molecular level.

Doing the same experiment with *E. coli* with knockouts of genes (like *copA, oxyR, fur, dps*, etc.) and combinations of these genes can help narrow down whether any of these genes are responsible for handling multiple stressors.

Multiple new stressors can be done in the same fashion or can be introduced right into the next step of looking at knockouts in order to see if other stress responses are non-additive. Different levels of IPTG and X-gal can be observed with these knockouts to try and figure out what exactly causes a change in size or intensity. *E. coli* without the ability to produce β-galactosidase or even turn on the *lac* operon can be done in the exact same manner and comparisons of colony counts and colony size can be monitored to show if the blue/white screening affects either. Different strands of *E. coli*, different *lacZ* containing plasmids or different bacteria altogether could be tested to test if any of these parameters affect the results seen here.

Mainly however, this experiment was done to show that combinations of stressors can have non-additive responses. This has not been truly shown before and was proven with these sets of stressors. There is not much research available that addresses if stress responses are really additive or not done in a quantitative way. It is theorized that all living organisms have multiple ways to handle stress and that some of these responses cross-talk and assist on stress relief to a number of different stressors.

Figure 5. Kodak Molecular Imaging photographs.

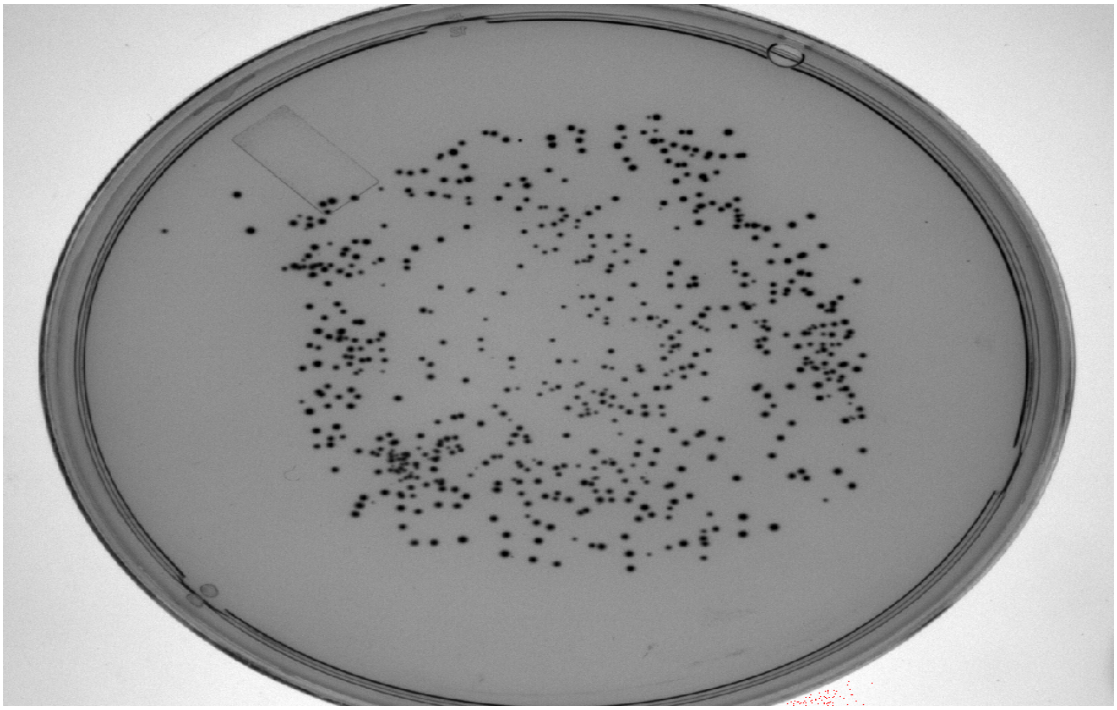

A 1X IPTG + 1 X-gal plate with EDTA and $CuSO_4$ as the stresses.

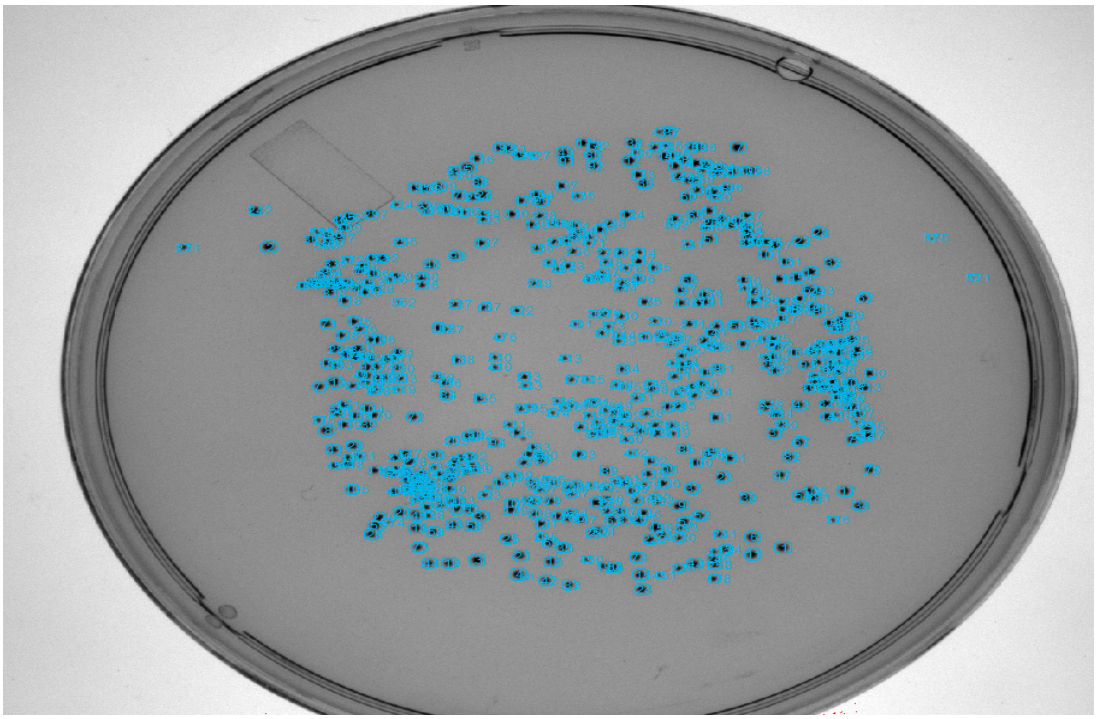

The same plate, after being counted by the Kodak Molecular Imaging system.

Figure 6. Plot showing high correlation between intensity and area for plates.

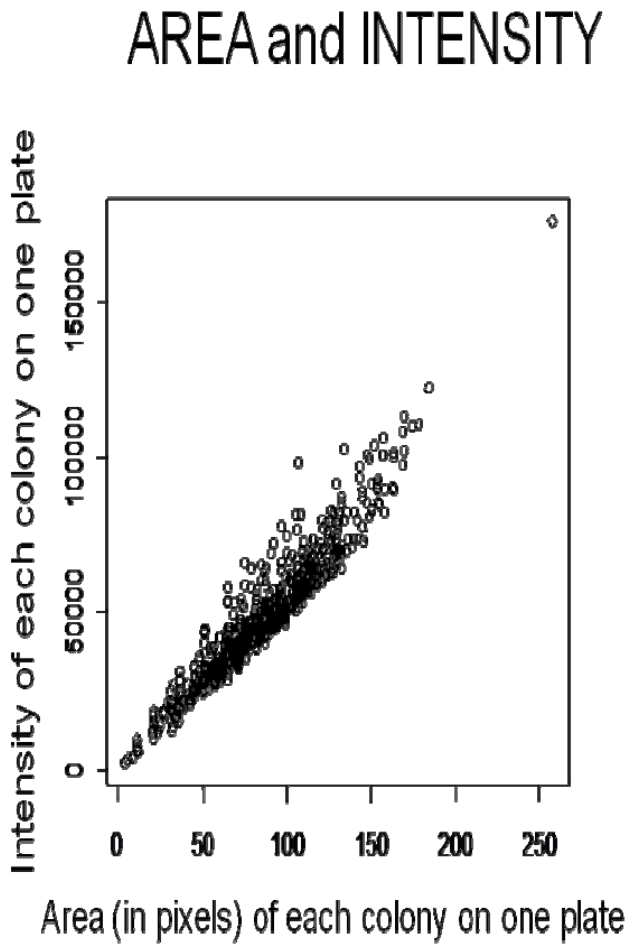

Pearson's Correlation = 0.95 (p-value < 2.2X10-16)
This plate shows the lowest correlation out of all 240 plates (35.c file).

High correlation was seen when area was plotted against intensity for every plate.

Plates were corrected to fix this by dividing the intensity values by the area values.

Figure 7. Adjusted intensity removed correlation between intensity and area for plates.

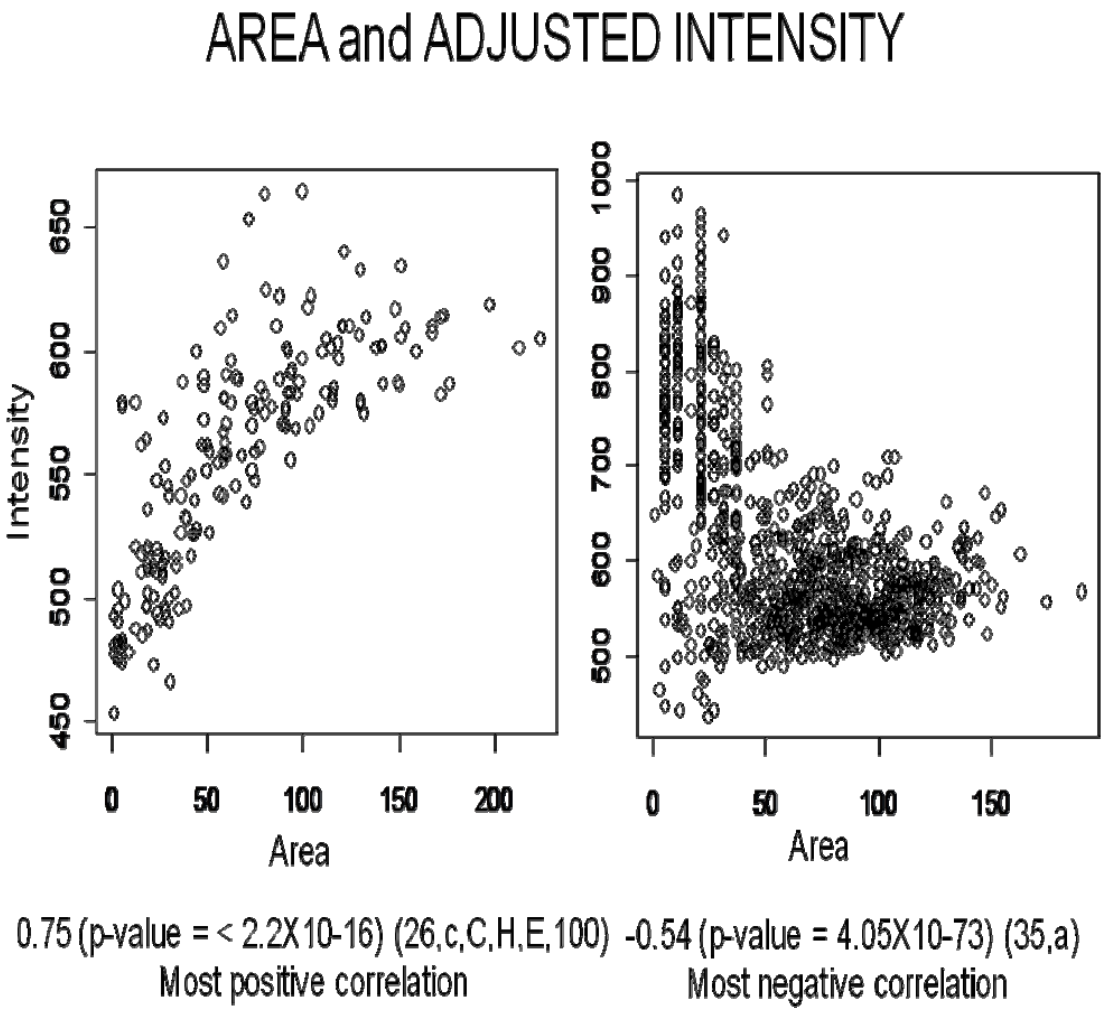

The adjusted intensity, as shown below in two examples of two separate plates intensity vs. area histograms, removes all correlation to the area from the data. The figure on the left shows a 0.5X IPTG + 1X X-gal plate with $CuSO_4$+HCl+EDTA, the plate with the highest correlation after the intensity was adjusted. Some plates even end up with negative correlation, like the plate on the right, a 1X IPTG + 1X X-gal control plate.

Figure 8. Correlation was also seen when plotting means of unadjusted intensity against means of areas for plates.

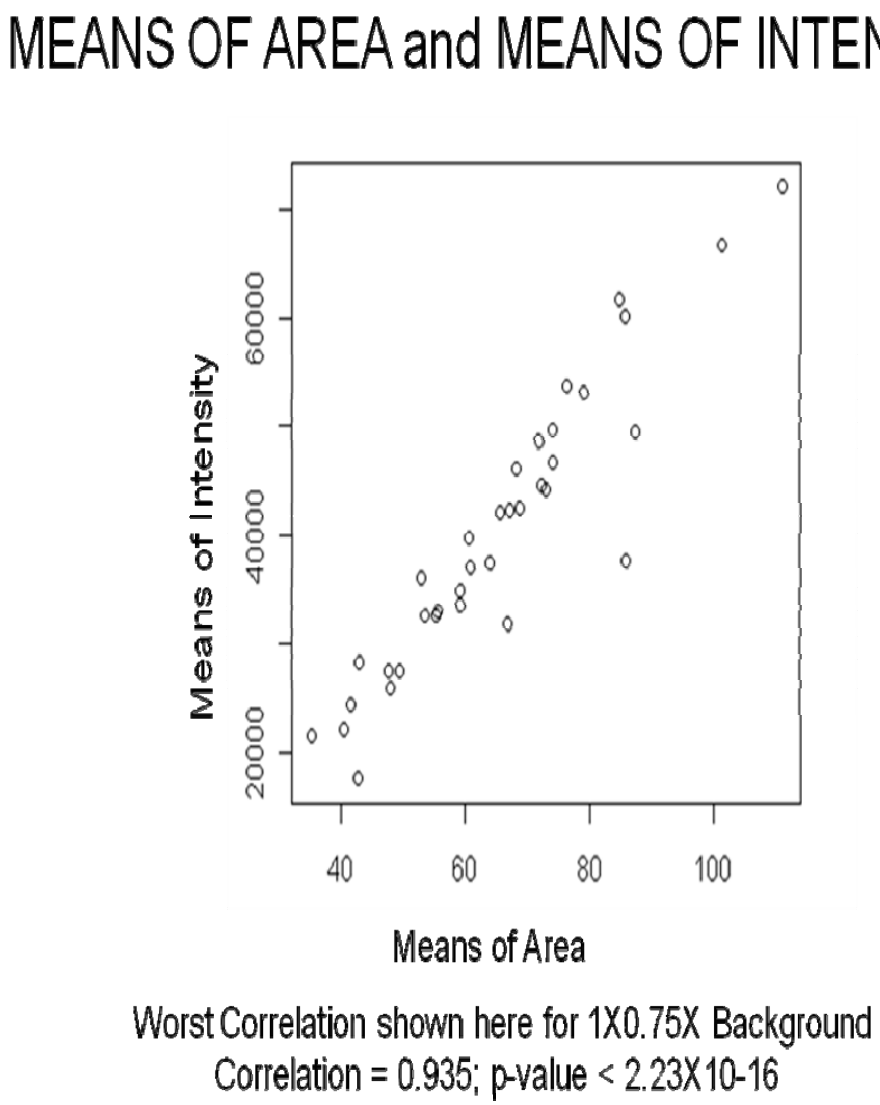

The means of area and means of intensity also had too high of a correlation, so the mean of adjusted intensities were used for data analysis. This chart shows that correlation by plotting the 1X IPTG + 0.75X X-gal control plates mean unadjusted intensity vs. the mean areas of entire plates.

Figure 9. Means of adjusted intensity removed correlation between mean intensity and mean area for plates.

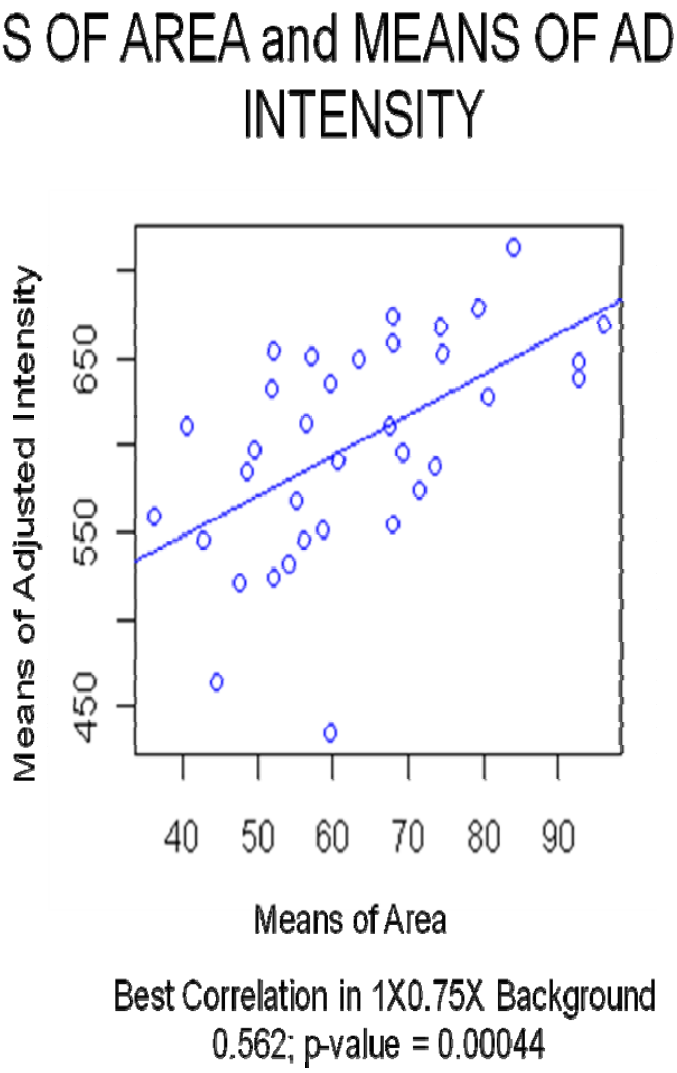

The mean adjusted intensities vs. the mean of the areas fixed the correlation issue. Here is the highest correlation set of mean adjusted intensity vs. mean area, the 1X IPTG + 0.75X X-gal control plates, yet still much lower than the mean unadjusted vs. mean area correlation.

Figure 10. Correlation comparisons between different backgrounds.

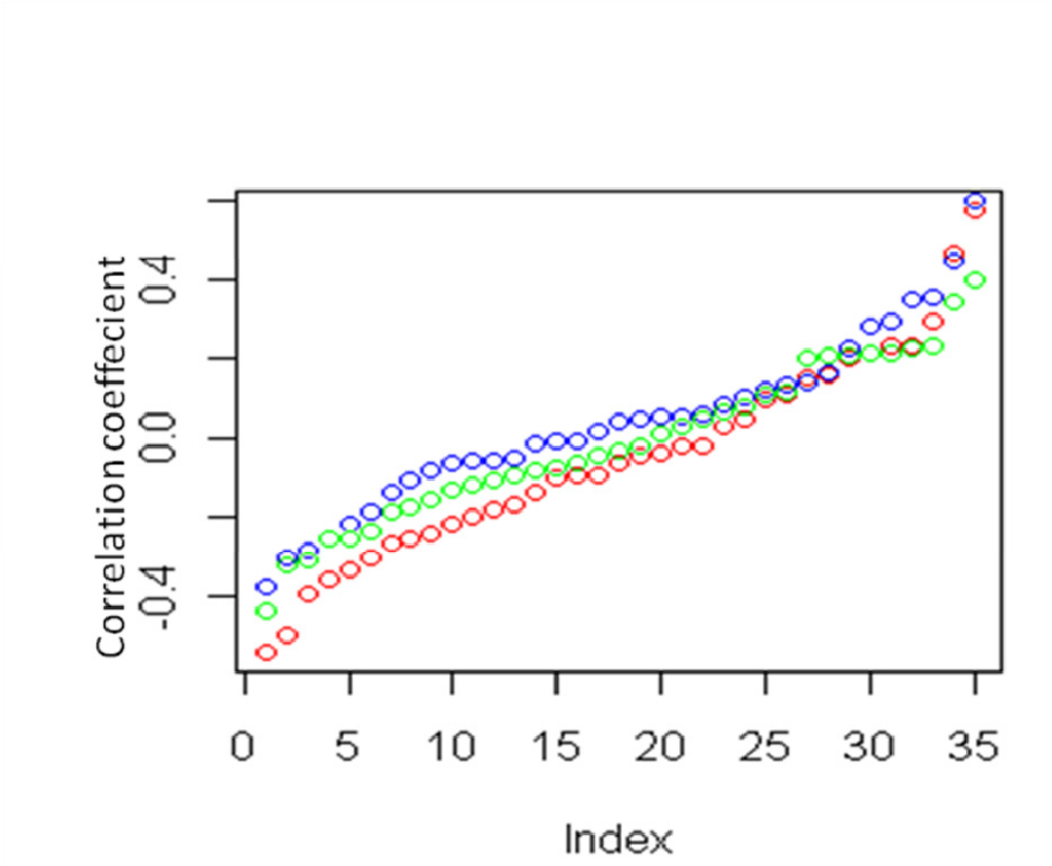

The colors represent each type of background. The green and red are 1X IPTG + 1X X-gal and 0.5X IPTG + 1X X-gal, while the blue is 1X IPTG+0.75X X-gal. This displays how each correlation between mean size and mean adjusted intensity are similar, even though the 1X IPTG + 0.75X X-gal was the only of the three backgrounds to show a significant correlation. When plotted, the blue is clearly not significantly different than the red or green. There is no significant difference in backgrounds. The controls are sorted in this graph by size of correlation, not in order by date.

Table 5. Table of colonies counted for the background 1X IPTG + 1X X-gal with C constants and relative p-values.

Stress Added	Estimate (C constant)	Pr<|t| (P-value)
None (b value, ideal control value)	6.84	$< 2x10^{-16}$
$CuSO_4$	$5.67x10^{+01}$	0.26528
EDTA	$-6.62x10^{+03}$	$3.80x10^{-14}$
HCl	$-1.34x10^{+02}$	$5.47x10^{-12}$
H_2O_2	$-2.05x10^{+04}$	$4.76x10^{-09}$
$CuSO_4$ + EDTA	$1.22x10^{+06}$	0.00345
$CuSO_4$ + HCl	$-5.26x10^{+04}$	$5.37x10^{-09}$
EDTA + HCl	$6.59x10^{+05}$	$1.90x10^{-05}$
$CuSO_4$ + H_2O_2	$1.41x10^{+06}$	0.39898
EDTA + H_2O_2	$3.26x10^{+08}$	$< 2x10^{-16}$
HCl + H_2O_2	$5.21x10^{+06}$	$2.52x10^{-16}$
$CuSO_4$ + HCl + EDTA	$2.90x10^{+08}$	$3.40x10^{-06}$
$CuSO_4$ + EDTA + H_2O_2	$4.94x10^{+09}$	0.70389
$CuSO_4$ + HCl + H_2O_2	$-9.80x10^{+07}$	0.7083
EDTA + H_2O_2 + HCl	$-7.78x10^{+10}$	$< 2x10^{-16}$

Stresses labeled yellow are considered significant data.

Table 6. Table of colonies counted for the background 1X IPTG + 0.75X X-gal with C constants and relative p-values.

Stress Added	Estimate (C constant)	Pr<|t| (P-value)
None (b value, ideal control value)	6.89	$< 2x10^{-16}$
$CuSO_4$	$-7.71x10^{+01}$	0.13342
EDTA	$-6.85x10^{+03}$	$1.07x10^{-14}$
HCl	$-1.48x10^{+02}$	$4.60x10^{-14}$
H_2O_2	$-2.50x10^{+04}$	$1.69x10^{-12}$
$CuSO_4$ + EDTA	$1.29x10^{+06}$	0.00216
$CuSO_4$ + HCl	$-4.46x10^{+04}$	$6.23x10^{-07}$
EDTA + HCl	$2.61x10^{+05}$	0.08794
$CuSO_4$ + H_2O_2	$9.81x10^{+06}$	$7.04x10^{-09}$
EDTA + H_2O_2	$4.48x10^{+08}$	$< 2x10^{-16}$
HCl + H_2O_2	$7.38x10^{+06}$	$< 2x10^{-16}$
$CuSO_4$ + HCl + EDTA	$9.10x10^{+08}$	$< 2x10^{-16}$
$CuSO_4$ + H_2O_2 + EDTA	$-1.03x10^{+11}$	$3.09x10^{-15}$
$CuSO_4$ + H_2O_2 + HCl	$-1.79x10^{+09}$	$7.85x10^{-12}$
EDTA + H_2O_2 + HCl	$-8.37x10^{+10}$	$< 2x10^{-16}$

Stresses labeled yellow are considered significant data.

Table 7. Table of colonies counted for the background 0.5X IPTG + 1 X-gal with C constants and relative p-values.

Stress Added	Estimate (C constant)	Pr<|t| (P-value)
None (b value, ideal control value)	5.66	$< 2x10^{-16}$
$CuSO_4$	$5.06x10^{+02}$	$< 2x10^{-16}$
EDTA	$1.98x10^{+03}$	0.0182
HCl	$8.62x10^{+01}$	$4.22x10^{-06}$
H_2O_2	$2.00x10^{+04}$	$3.55x10^{-09}$
$CuSO_4$ + EDTA	$-2.70x10^{+06}$	$6.34x10^{-12}$
$CuSO_4$ + HCl	$-1.34x10^{+05}$	$< 2x10^{-16}$
EDTA + HCl	$-6.07x10^{+05}$	$3.91x10^{-05}$
$CuSO_4$ + H_2O_2	$-1.14x10^{+07}$	$1.35x10^{-12}$
EDTA + H_2O_2	$1.53x10^{+08}$	$3.16x10^{-08}$
HCl + H_2O_2	$9.09x10^{+05}$	0.1411
$CuSO_4$ + HCl + EDTA	$8.19x10^{+08}$	$< 2x10^{-16}$
$CuSO_4$ + H_2O_2 + EDTA	$4.89x10^{+10}$	$6.01x10^{-05}$
$CuSO_4$ + H_2O_2 + HCl	$1.47x10^{+09}$	$8.87x10^{-09}$
EDTA + H_2O_2 + HCl	$-7.37x10^{+10}$	$< 2x10^{-16}$

Stresses labeled yellow are considered significant data.

Table 8. Table of mean area measured for the background 1X IPTG + 1X X-gal with C constants and relative p-values.

Stress Added	Estimate (C constant)	Pr<|t| (P-value)
None (b value, ideal control value)	$-6.00 \times 10^{+01}$	0.020565
$CuSO_4$	$2.95 \times 10^{+04}$	0.018528
EDTA	$4.64 \times 10^{+05}$	0.033252
HCl	$1.42 \times 10^{+04}$	0.004516
H_2O_2	$1.90 \times 10^{+06}$	0.028937
$CuSO_4$ + EDTA	$-1.81 \times 10^{+08}$	0.070115
$CuSO_4$ + HCl	$-9.46 \times 10^{+06}$	0.000116
EDTA + HCl	$-1.15 \times 10^{+08}$	0.0046
$CuSO_4$ + H_2O_2	$-7.78 \times 10^{+08}$	0.051665
EDTA + H_2O_2	$-1.70 \times 10^{+10}$	0.01726
HCl + H_2O_2	$-3.37 \times 10^{+08}$	0.031755
$CuSO_4$ + HCl + EDTA	$5.21 \times 10^{+10}$	0.001871
$CuSO_4$ + H_2O_2 + EDTA	$3.51 \times 10^{+12}$	0.212938
$CuSO_4$ + H_2O_2 + HCl	$1.24 \times 10^{+11}$	0.05199
EDTA + H_2O_2 + HCl	$1.60 \times 10^{+12}$	0.143403

Stresses labeled yellow are considered significant data.

Table 9. Table of mean area measured for the background 1X IPTG + 0.75X X-gal with C constants and relative p-values.

Stress Added	Estimate (C constant)	Pr<|t| (P-value)
None (b value, ideal control value)	$-1.44x10^{+01}$	0.5994
$CuSO_4$	$1.02x10^{+04}$	0.4445
EDTA	$1.09x10^{+05}$	0.6398
HCl	$5.73x10^{+03}$	0.2704
H_2O_2	$3.92x10^{+05}$	0.6723
$CuSO_4$ + EDTA	$-5.07x10^{+07}$	0.6377
$CuSO_4$ + HCl	$-4.70x10^{+06}$	0.0561
EDTA + HCl	$-4.94x10^{+07}$	0.2421
$CuSO_4$ + H_2O_2	$-1.72x10^{+08}$	0.6888
EDTA + H_2O_2	$-3.63x10^{+09}$	0.6292
HCl + H_2O_2	$-1.68x10^{+08}$	0.3181
$CuSO_4$ + HCl + EDTA	$2.04x10^{+10}$	0.2373
$CuSO_4$ + H_2O_2 + EDTA	$-2.02x10^{+12}$	0.5128
$CuSO_4$ + H_2O_2 + HCl	$6.35x10^{+10}$	0.355
EDTA + H_2O_2 + HCl	$7.48x10^{+11}$	0.5306

Stresses labeled yellow are considered significant data.

Table 10. Table of mean area measured for the background 0.5X IPTG + 1X X-gal with C constants and relative p-values.

Stress Added	Estimate (C constant)	Pr<|t| (P-value)
None (b value, ideal control value)	$-3.16x10^{+01}$	0.19728
$CuSO_4$	$2.60x10^{+04}$	0.03222
EDTA	$1.03x10^{+05}$	0.61439
HCl	$6.26x10^{+03}$	0.17432
H_2O_2	$1.16x10^{+06}$	0.16327
$CuSO_4$ + EDTA	$-1.14x10^{+08}$	0.23457
$CuSO_4$ + HCl	$-6.35x10^{+06}$	0.00482
EDTA + HCl	$-3.98x10^{+07}$	0.28469
$CuSO_4$ + H_2O_2	$-7.44x10^{+08}$	0.05633
EDTA + H_2O_2	$-6.47x10^{+09}$	0.33298
HCl + H_2O_2	$-2.28x10^{+08}$	0.12887
$CuSO_4$ + HCl + EDTA	$3.19x10^{+10}$	0.0406
$CuSO_4$ + H_2O_2 + EDTA	$-3.28x10^{+11}$	0.90386
$CuSO_4$ + H_2O_2 + HCl	$7.86x10^{+10}$	0.19726
EDTA + H_2O_2 + HCl	$8.39x10^{+11}$	0.42631

Stresses labeled yellow are considered significant data.

Table 11. Table of mean intensity measured for the background 1X IPTG + 1X X-gal with C constants and relative p-values.

Stress Added	Estimate (C constant)	Pr<|t| (P-value)
None (b value, ideal control value)	$-2.35 \times 10^{+02}$	0.173
$CuSO_4$	$1.29 \times 10^{+05}$	0.124
EDTA	$2.00 \times 10^{+06}$	0.172
HCl	$4.49 \times 10^{+04}$	0.167
H_2O_2	$6.71 \times 10^{+06}$	0.248
$CuSO_4$ + EDTA	$-6.14 \times 10^{+08}$	0.361
$CuSO_4$ + HCl	$-1.80 \times 10^{+07}$	0.229
EDTA + HCl	$-3.49 \times 10^{+08}$	0.185
$CuSO_4$ + H_2O_2	$-3.84 \times 10^{+09}$	0.156
EDTA + H_2O_2	$-5.13 \times 10^{+10}$	0.276
HCl + H_2O_2	$-1.19 \times 10^{+09}$	0.255
$CuSO_4$ + HCl + EDTA	$6.24 \times 10^{+10}$	0.557
$CuSO_4$ + H_2O_2 + EDTA	$9.33 \times 10^{+12}$	0.626
$CuSO_4$ + H_2O_2 + HCl	$5.38 \times 10^{+11}$	0.21
EDTA + H_2O_2 + HCl	$9.37 \times 10^{+12}$	0.211

Stresses labeled yellow are considered significant data.

Table 12. Table of mean intensity measured for the background 1X IPTG + 0.75X X-gal with C constants and relative p-values.

Stress Added	Estimate (C constant)	Pr<|t| (P-value)
None (b value, ideal control value)	$8.09x10^{+01}$	0.559
$CuSO_4$	$-1.25x10^{+04}$	0.851
EDTA	$-5.09x10^{+05}$	0.664
HCl	$-4.79x10^{+03}$	0.853
H_2O_2	$-4.15x10^{+06}$	0.376
$CuSO_4$ + EDTA	$1.56x10^{+08}$	0.773
$CuSO_4$ + HCl	$-3.60x10^{+06}$	0.765
EDTA + HCl	$1.26x10^{+08}$	0.551
$CuSO_4$ + H_2O_2	$2.01x10^{+09}$	0.354
EDTA + H_2O_2	$3.62x10^{+10}$	0.343
HCl + H_2O_2	$1.00x10^{+08}$	0.905
$CuSO_4$ + HCl + EDTA	$5.88x10^{+08}$	0.995
$CuSO_4$ + H_2O_2 + EDTA	$-1.88x10^{+13}$	0.23
$CuSO_4$ + H_2O_2 + HCl	$2.75x10^{+11}$	0.426
EDTA + H_2O_2 + HCl	$-5.47x10^{+12}$	0.365

Stresses labeled yellow are considered significant data.

Table 13. Table of mean intensity measured for the background 0.5X IPTG + 1X X-gal with C constants and relative p-values.

Stress Added	Estimate (C constant)	Pr<|t| (P-value)
None (b value, ideal control value)	$-6.78 \times 10^{+01}$	0.698
$CuSO_4$	$7.01 \times 10^{+04}$	0.408
EDTA	$3.33 \times 10^{+05}$	0.822
HCl	$1.63 \times 10^{+04}$	0.62
H_2O_2	$1.81 \times 10^{+06}$	0.759
$CuSO_4$ + EDTA	$-1.93 \times 10^{+08}$	0.778
$CuSO_4$ + HCl	$-1.48 \times 10^{+07}$	0.333
EDTA + HCl	$-1.05 \times 10^{+08}$	0.694
$CuSO_4$ + H_2O_2	$-8.65 \times 10^{+08}$	0.751
EDTA + H_2O_2	$-5.14 \times 10^{+09}$	0.914
HCl + H_2O_2	$-7.12 \times 10^{+08}$	0.504
$CuSO_4$ + HCl + EDTA	$8.72 \times 10^{+10}$	0.425
$CuSO_4$ + H_2O_2 + EDTA	$-7.25 \times 10^{+12}$	0.711
$CuSO_4$ + H_2O_2 + HCl	$5.45 \times 10^{+11}$	0.215
EDTA + H_2O_2 + HCl	$1.20 \times 10^{+12}$	0.874

Stresses labeled yellow are considered significant data.

Table 14. Examples of the C values signs following the pattern.

Inputs that have the same sign*	Background	Output	Doubles that have opposite sign**	Triples with same sign as singles
HCl, EDTA, H_2O_2	1X IPTG + 1X X-gal	Colony Count	Yes	Yes
HCl, EDTA, H_2O_2	1X IPTG + 0.75X X-gal	Colony Count	Yes	Yes
HCl, EDTA, $CuSO_4$	1X IPTG + 0.75X X-gal	Colony Count	No	No
HCl, H_2O_2, $CuSO_4$	1X IPTG + 0.75X X-gal	Colony Count	No	Yes
EDTA, H_2O_2, $CuSO_4$	1X IPTG + 0.75X X-gal	Colony Count	Yes	Yes
HCl, EDTA, H_2O_2	0.5X IPTG + 1X X-gal	Colony Count	No	No
HCl, EDTA, $CuSO_4$	0.5X IPTG + 1X X-gal	Colony Count	Yes	Yes
HCl, H_2O_2, $CuSO_4$	0.5X IPTG + 1X X-gal	Colony Count	No	Yes
EDTA, H_2O_2, $CuSO_4$	0.5X IPTG + 1X X-gal	Colony Count	No	Yes
HCl, EDTA, H_2O_2	1X IPTG + 1X X-gal	Size	Yes	Yes
HCl, EDTA, $CuSO_4$	1X IPTG + 1X X-gal	Size	Yes	Yes
HCl, H_2O_2, $CuSO_4$	1X IPTG + 1X X-gal	Size	Yes	Yes
EDTA, H_2O_2, $CuSO_4$	1X IPTG + 1X X-gal	Size	Yes	Yes
HCl, EDTA, H_2O_2	1X IPTG + 0.75X X-gal	Size	Yes	Yes
HCl, EDTA, $CuSO_4$	1X IPTG + 0.75X X-gal	Size	Yes	Yes
HCl, H_2O_2, $CuSO_4$	1X IPTG + 0.75X X-gal	Size	Yes	Yes
EDTA, H_2O_2, $CuSO_4$	1X IPTG + 0.75X X-gal	Size	Yes	No
HCl, EDTA, H_2O_2	0.5X IPTG + 1X X-gal	Size	Yes	Yes
HCl, EDTA, $CuSO_4$	0.5X IPTG + 1X X-gal	Size	Yes	Yes
HCl, H_2O_2, $CuSO_4$	0.5X IPTG + 1X X-gal	Size	Yes	Yes
EDTA, H_2O_2, $CuSO_4$	0.5X IPTG + 1X X-gal	Size	Yes	No
HCl, EDTA, H_2O_2	1X IPTG + 1X X-gal	Intensity	Yes	Yes
HCl, EDTA, $CuSO_4$	1X IPTG + 1X X-gal	Intensity	Yes	Yes
HCl, H_2O_2, $CuSO_4$	1X IPTG + 1X X-gal	Intensity	Yes	Yes
EDTA, H_2O_2, $CuSO_4$	1X IPTG + 1X X-gal	Intensity	Yes	Yes
HCl, EDTA, H_2O_2	1X IPTG + 0.75X X-gal	Intensity	Yes	No
HCl, EDTA, $CuSO_4$	1X IPTG + 0.75X X-gal	Intensity	No	Yes
HCl, H_2O_2, $CuSO_4$	1X IPTG + 0.75X X-gal	Intensity	No	Yes
EDTA, H_2O_2, $CuSO_4$	1X IPTG + 0.75X X-gal	Intensity	Yes	No
HCl, EDTA, H_2O_2	0.5X IPTG + 1X X-gal	Intensity	Yes	Yes
HCl, EDTA, $CuSO_4$	0.5X IPTG + 1X X-gal	Intensity	Yes	Yes
HCl, H_2O_2, $CuSO_4$	0.5X IPTG + 1X X-gal	Intensity	Yes	Yes
EDTA, H_2O_2, $CuSO_4$	0.5X IPTG + 1X X-gal	Intensity	Yes	No

*3 inputs with same the same sign. **All possible combinations need to have opposite sign for a “yes”.

CHAPTER 5

Skew and Kurtosis Data

Section 5A: Skew and Kurtosis Method

This chapter takes a look at the distribution data of the area and adjusted intensity and how it compares to a normal distribution. More data is available for the area and adjusted intensity when looking at distributions. Due to the amount of data available per plate in the area and intensity outputs, the ability to compare the data points to a normal distribution (a normal distribution curve is a bell curve) exists. A way to view differences in distributions from a normal distribution is by using histograms.

Skew (Figure 11) is a term to describe a deviation away from a normal distribution. A normal distribution is where the mean and median are equal in a histogram, the largest portion of the curve is in the center, and the distribution slowly declines as the curve goes to the right and left of the center. There are two types of skew, positive skew, where the right (or larger number on the x-axis) tail is longer and negative skew, where the left (or smaller number on the x-axis) tail is longer. The mean is always found much farther out on the longer tail than the median for skewed distributions. Colony areas and intensities were plotted in a histogram for every plate see the skew for each input and background per set of triplicates. It is possible to calculate the skew for area and intensity by comparing the actual distributions to a normal curve using the following equation for *n* samples:

$$g_1 = \frac{\frac{1}{n}\sum_{i=1}^{n}(x_i - \bar{x})^3}{\frac{1}{n}\left(\sum_{i=1}^{n}(x_i - \bar{x})^2\right)^{3/2}}$$

where x_i is the i[th] value, $\bar{x}$ is the sample mean, and g_1 is the sample skewness (103). A normal distribution gives a zero skew value.

Another way a histogram can differ from a normal distribution curve is if the data shows kurtosis. A positive kurtosis is when data has infrequent extreme sections of data. This differs from normal distribution because the large peaks are not necessarily in the center of the data and also do not smoothly tail off. A negative kurtosis is seen when the data has frequent modestly-sized distributions. The data does not tail off but rather plateaus and sharply ends.

Colony areas and intensities were plotted in a histogram for every plate to see the kurtosis for each input and background per set of triplicates. It is possible to calculate the kurtosis for area and intensity by comparing the actual distributions to a normal curve using the following equation for *n* samples:

$$g_2 = \frac{\frac{1}{n}\sum_{i=1}^{n}(x_i - \bar{x})^4}{\frac{1}{n}\left(\sum_{i=1}^{n}(x_i - \bar{x})^2\right)^2} - 3$$

where x_i is the i[th] value, $\bar{x}$ is the sample mean, and g_1 is the sample kurtosis (103). A normal distribution gives a zero kurtosis value.

P-values were also calculated using R for every plate to determine the probability of a normal distribution with the same mean and number of data points as the plate. P-values helped determine if the values for skew and kurtosis were

significantly different than zero. This was done by comparing the possible skews and kurtosis from a normal distribution with the same mean but limited to the number of data points (one for each colony) per plate (103). P-values less than 0.05 were considered to be significantly different than a normal distribution.

For every set of plates with the same input, background, and set of treatments, skew and kurtosis were calculated. Corresponding controls also had skew and kurtosis calculated. The treated sets were compared to the corresponding controls using a t-test to see significant differences in treated plates compared to the controls.

Section 5B: Area Skew Data

The area output gave mostly positive skews, with 226 total plates showing positive skew and 14 having negative skew. Of the 226 positive skew plates, 207 were significant. Of the 14 negative skew plates, 5 were significant. Skew was seen in the control plates as well. For the 1X IPTG + 1X X-gal background, most control plates had positive skews (Figure 12) but some had a negative skew as well. When looking at every colony in the entire set of controls for a background, all three backgrounds displayed an average positive skew for area (Figure 13). For the 1X IPTG + 1X X-gal background, three treatments (H_2O_2 + EDTA, $CuSO_4$ + HCl, and $CuSO_4$ + HCl + H_2O_2) resulted in a significantly different skew for area when compared to the corresponding three controls done the same day. All three showed a more positive skew than the corresponding controls, as well as the average skew for the entire set of 1X IPTG + 1X X-gal controls (Figure 14).

When all four treatment colonies were plotted in a histogram to see if they significantly affected the distribution, they were shown to do so when compared to the corresponding controls with a positive skew for area in the 1X IPTG + 1X X-gal background.

Two treatments ($CuSO_4$ +HCl and $CuSO_4$ + HCl + H_2O_2) were shown to significantly affect the skews positively for mean area when compared to the skews of both the corresponding controls and the average of all of the 1X IPTG + 0.75X X-gal plates skews together (Figure 15). Again, all four treatments displayed significantly more positive skew for area than both the corresponding controls and the average skew of all the 1X IPTG + 0.75X X-gal controls.

For the 0.5X IPTG + 1X X-gal background, no treatments that were analyzed showed a significant change in skew for area. However, again, the four treatments together demonstrated a significant larger positive skew for area when compared to both the corresponding controls and the average skew of the 0.5X IPTG + 1X X-gal control set plates together (Figure 16).

Section 5C: Area Kurtosis Data

Both types, positive and negative, of kurtosis were seen in the area data for these plates (Figure 17). There were 166 plates that showed a negative kurtosis, while 74 showed a positive kurtosis. Of the 166, 122 plates showed a significant p-value for negative kurtosis being significantly different than a normal distribution. Of the 74, 56 were significant for positive kurtosis.

When all control data was plotted, it showed an average negative kurtosis for each background. As noted above, the goal of choosing background IPTG and X-gal concentrations was to lower both the X-gal alone and the IPTG alone without affecting the appearance of the plate. This was believed to be accomplished, until a reasonable number of plates were available and data for kurtosis was plotted. The 0.5X IPTG + 1X X-gal control plates showed a much higher kurtosis on certain days than both the 1X IPTG + 1X X-gal and 1X IPTG + 0.75X X-gal plates (Figure 18). Two days in particular showed major differences in the control data when it came to kurtosis for area. Paired t-tests backed up this data, as area average kurtosis for 0.5X IPTG +1X X-gal was compared to both other backgrounds average kurtosis and resulted in significant p-values for both. Even with the removal of the two large difference days, these p-values still were significant meaning that the average kurtosis for these three backgrounds was in fact different, even if the highly unlikely chance that both large sets were random error. This was the only significant differences observed in the different background control sets.

To test if this difference in kurtosis was affecting the data from the equation in Section 4B, the differences in the mean areas were looked at for the control sets of each background (Figure 19). The means of the area are not different, even on the same days where the kurtosis differed significantly. Paired t-tests backed up that the mean areas were not significantly different than a normal distribution and that the data was useful in the equation still. The overall average distribution for the area is normally distributed in each of the backgrounds. The distribution on these plates were changed but the

mean area was not changed, nor the entire distribution of the mean area across all plates.

Two treatments caused a significant change in kurtosis for area when compared to both the average kurtosis of the entire control set and the kurtosis for the corresponding controls for the treatments in the 1X IPTG + 1X X-gal background (Figure 20). HCl + $CuSO_4$ and H_2O_2 + HCl + $CuSO_4$ both caused a significant average increase in kurtosis. No treatments altered kurtosis significantly for area in the 1X IPTG + 0.75X X-gal background. The 0.5X IPTG + 1X X-gal background area kurtosis was only significantly changed by H_2O_2 alone (Figure 21). H_2O_2 lowered the kurtosis to an even lower negative value.

Section 5D: Intensity Skew Data

Skew was measured for adjusted intensity (Figure 22). As in the area data, both positive and negative skew was observed. There were 179 plates that showed positive skew, while 61 plates showed negative skew for adjusted intensity. Of the 179, 110 plates were significant for positive skew. Of the 61, 32 showed significance for negative skew. The addition of four stressors (HCl, H_2O_2 + EDTA, EDTA + HCl + H_2O_2, and $CuSO_4$+ HCl) in the 1X IPTG + 1X X-gal background caused a shortening in tail toward the more intense colonies, resulting in significant negative skews (Figure 23). The corresponding controls for all of these plates had positive skews for adjusted intensity, as well as the average skew of the complete collection of all 1X IPTG + 1X X-gal controls. For the 1X IPTG + 0.75X X-gal and 0.5X IPTG + 1X X-gal backgrounds, no significant changes in skew were observed for adjusted intensity.

Section 5E: Intensity Kurtosis Data

Just as in area, kurtosis was measured for adjusted intensity. Unlike area however, the plates showed more positive kurtosis than negative (Figure 24). There were 149 plates that showed a positive kurtosis, while 91 plates showed a negative kurtosis. Of the 149, 116 plates showed significant positive kurtosis. Of the 91, 49 plates displayed significant negative kurtosis.

For the 1X IPTG + 1X X-gal background data, addition of two stressors (H_2O_2 + EDTA and EDTA + H_2O_2 + HCl) resulted in significant change to give negative kurtosis when compared to the corresponding controls and the average kurtosis of the 1X IPTG + 1X X-gal controls as a whole (all positive kurtosis) (Figure 25) . All four treatments together also changed the kurtosis negatively significantly. No significant changes occurred in kurtosis of adjusted intensity for the 1X IPTG + 0.75X X-gal background. One treatment (H_2O_2) caused a lowering in kurtosis when compared to the corresponding controls and the average kurtosis of all 0.5X IPTG + 1X X-gal controls as a whole (Figure 26).

Section 5F: Conclusions

The background conditions were very close to ideal, with the ideal plates for the 1 IPTG + 0.75X X-Gal and 0.5X IPTG + 1X X-Gal backgrounds having lower IPTG and X-gal concentrations without affecting the appearance of the plate. The only exception seen in the distributions of the backgrounds was the kurtosis curves for the area in the 0.5X IPTG + 1X X-Gal background. This was shown to not truly affect the model data as the means of the area were not significantly different in the 0.5X IPTG + 1X X-Gal

background. Stressors tended to decrease kurtosis for adjusted intensity, while both increase and decreases in kurtosis were seen for area.

Skew and kurtosis data showed that some specific interactions here affected the area and adjusted intensity data. In cases where two-way or three-way treatment interactions significantly affected the skew or kurtosis, at most only one single treatment component of the two-way or three-way treatment interaction significantly changed the skew or kurtosis on its own as a single treatment.

H_2O_2 caused significant changes in kurtosis for both area and adjusted intensity in the 0.5X IPTG + 1X X-gal background. This helps support the fact that H_2O_2 was affecting the responses of *E. coli.* The model found that the means of area change significantly in response to HCl in the 1X IPTG + 1X X-gal background. This significant change was the lowest absolute C value that the model found significant. HCl was seen to affect skew significantly for the 1X IPTG + 1X X-gal background. This significant change in distribution helps support the model's ability to indicate a significant change in response.

Though the model is reliable, looking at the means only does not give the entire story. Even in control plates there are significant changes in distributions. In some cases, the treatments specifically affect the distribution of area and intensity. In conclusion, the distribution data showed that *E. coli* grows in a stochastic manner and some of the treatments affected the nature of the stochastic effects.

Figure 11. Distribution of skew for area.

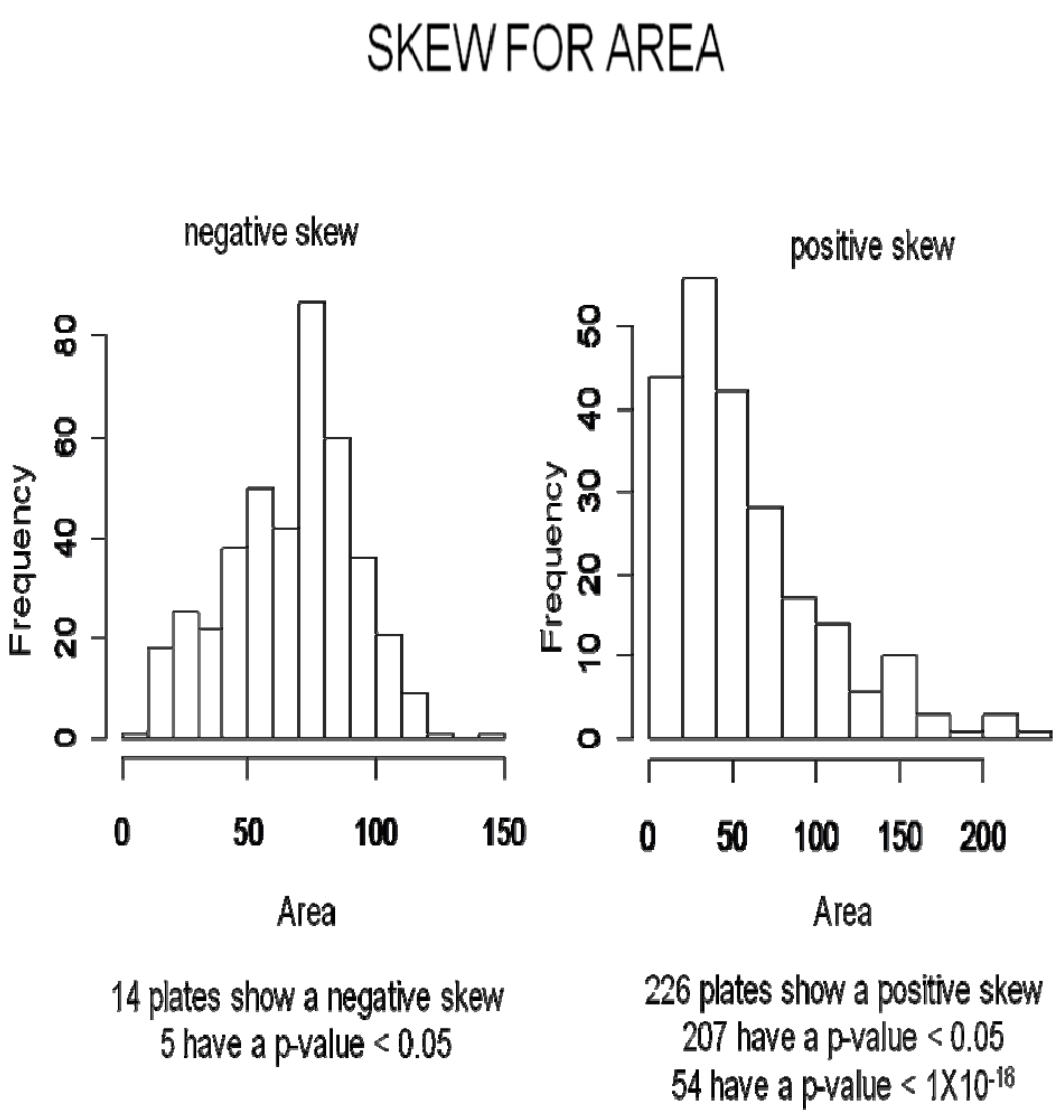

When plotting area histograms for individual plates, a normal distribution was not seen and skew for area was observed in both negative and positive forms. Almost all significant skews were positive but five plates still had significant negative skew. Frequency is number of colonies for these histograms, examples of histograms of individual plates.

Figure 12. Skew for area in controls for 1X IPTG + 1X X-gal background.

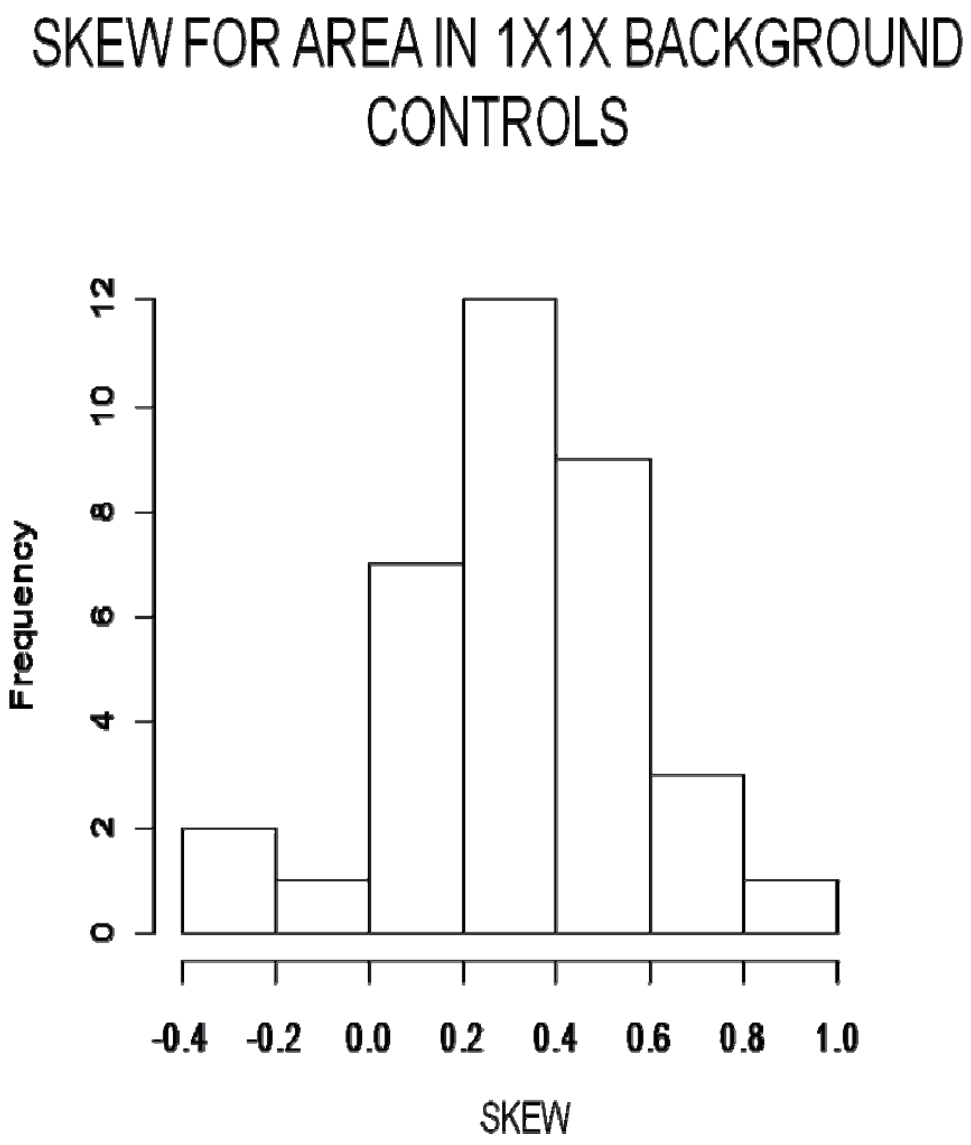

The 1X IPTG + 1X X-gal control background plate's area skews. Frequency in this histogram is number of plates. A zero skew is a normal distribution. Most plates showed a positive skew. 1X IPTG + 0.75X X-gal and 0.5X IPTG + 1X X-gal control background plates showed similar results.

Figure 13. Average skew seen in control plates according to background.

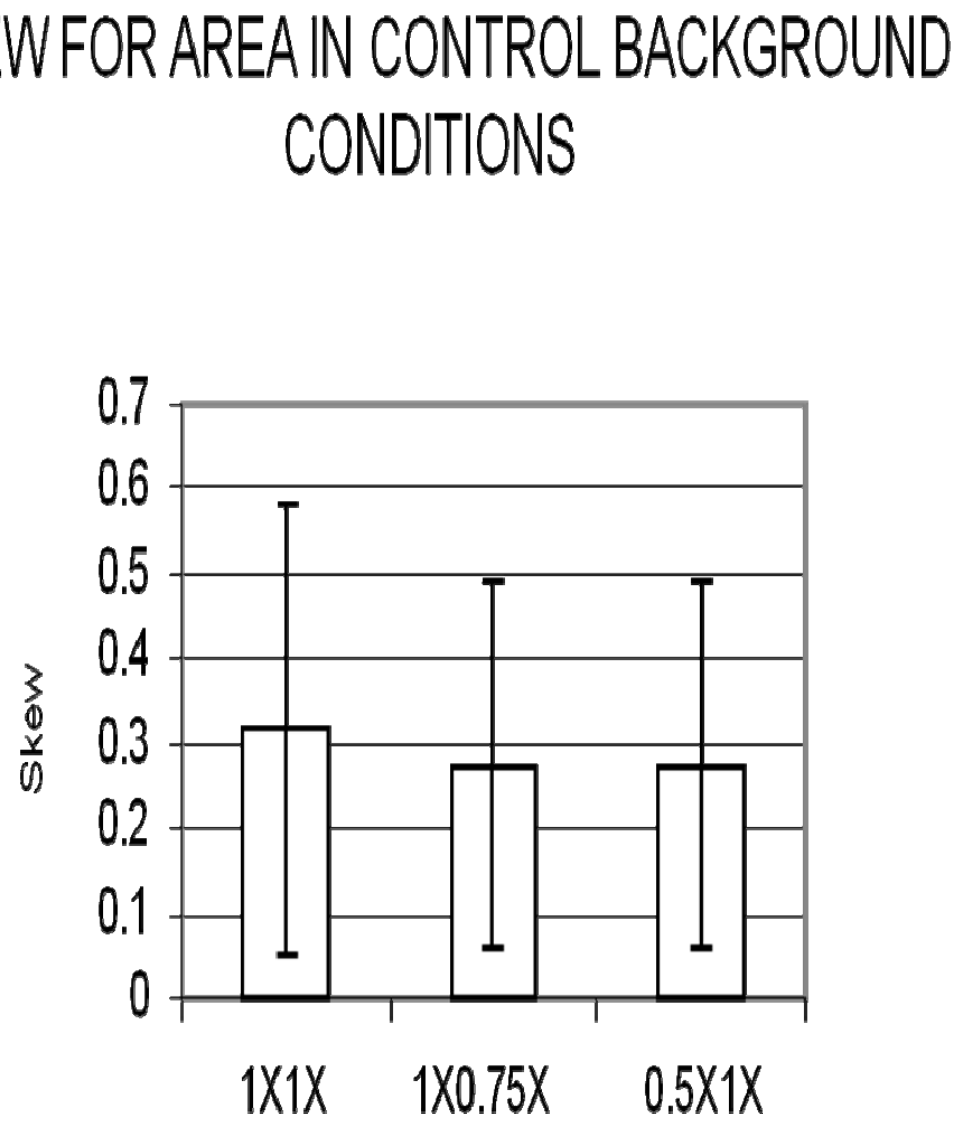

The skews seen in each background are similar, and are not significantly different from each other. Error bars are the standard deviation.

Figure 14. Inputs that show significant change in skew for area in the 1X IPTG + 1X X-gal background.

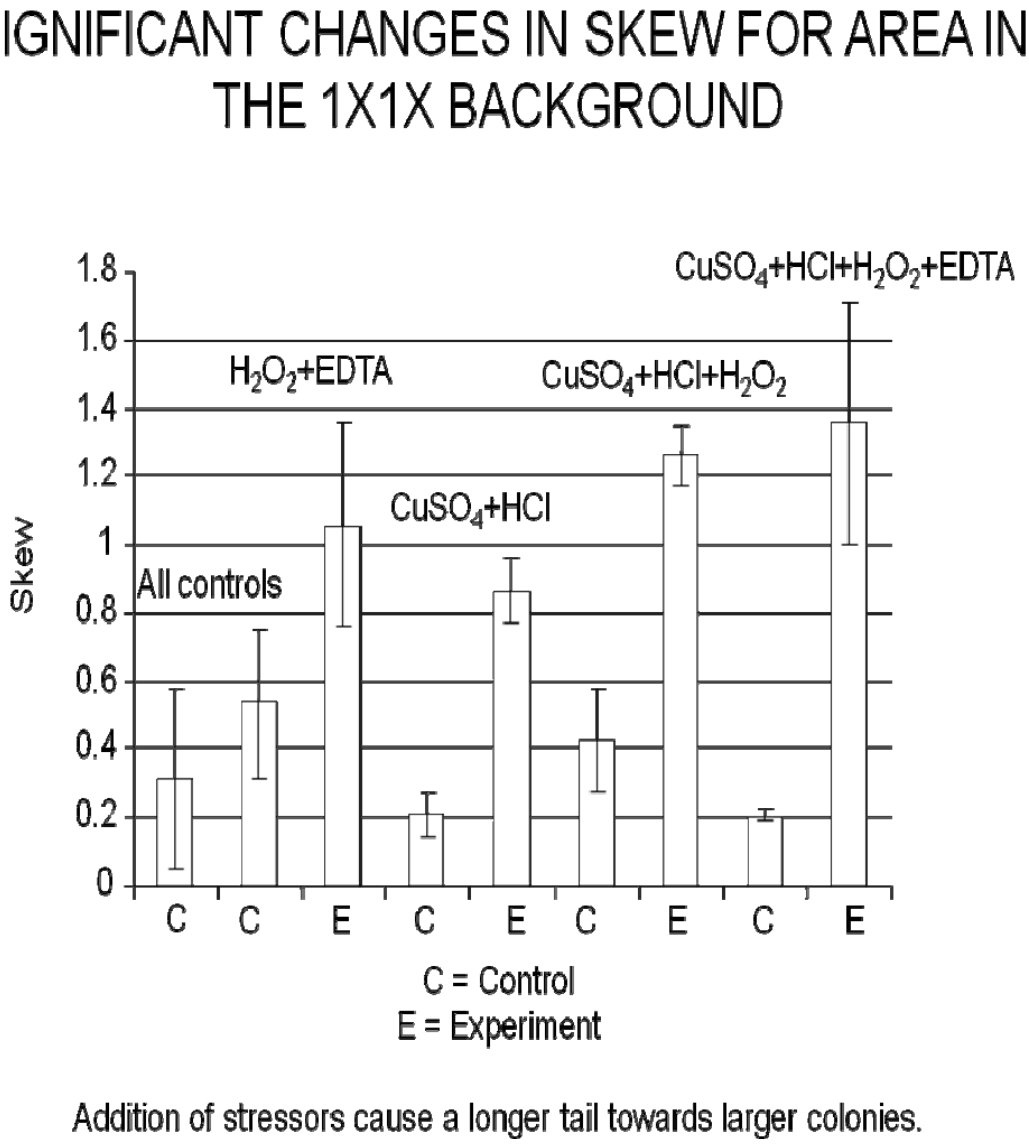

Four different treatments were observed to give significant changes in skew when added to the 1X IPTG + 1X X-gal background. Skews were compared to matching control data plates done on the same day (adjacent to experiments) and also the average skew of the entire thirty-five control data sets (bar all the way to the left). Error bars are standard deviation.

Figure 15. Inputs that show significant change in skew for area in the 1X IPTG + 0.75X X-gal background.

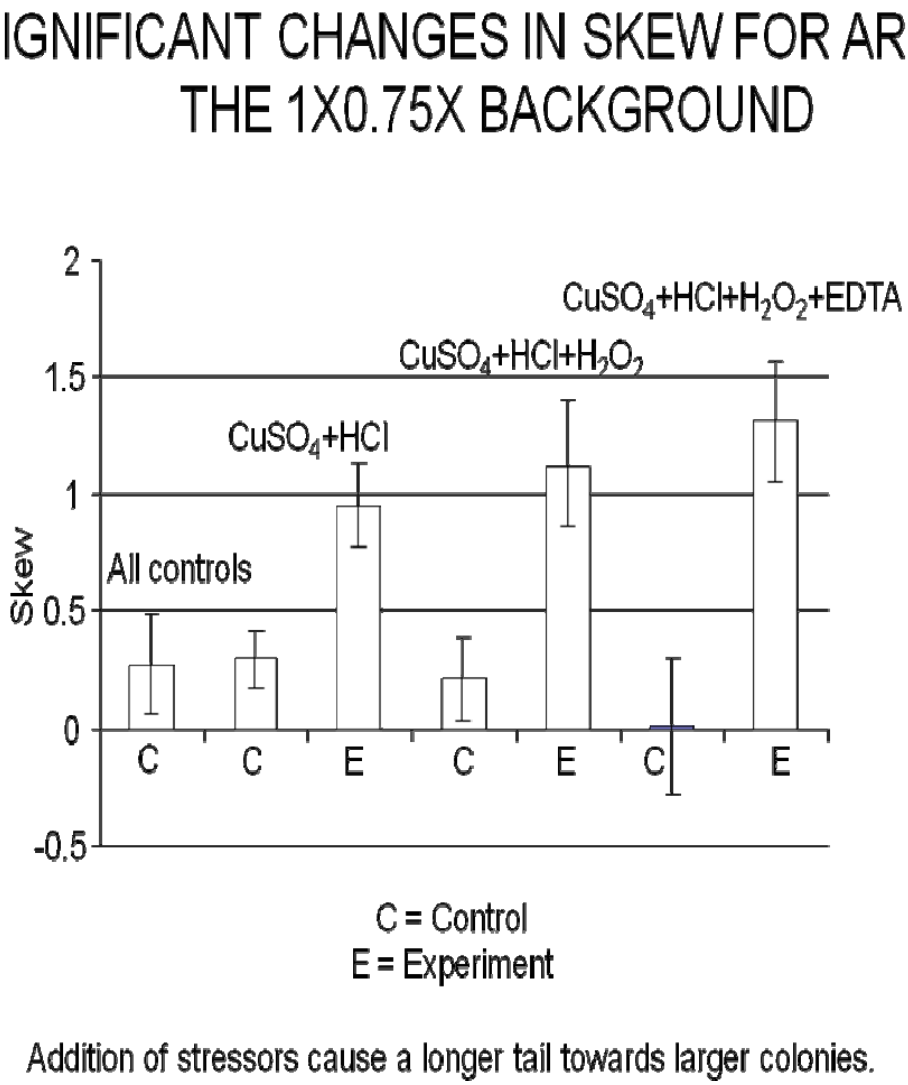

Three different treatments were observed to give significant changes in skew when added to the 1X IPTG + 0.75X X-gal background. Skews were compared to matching control data plates done on the same day, and also the average skew of the entire thirty-five control data sets. Error bars are standard deviations.

Figure 16. Inputs that show significant change in skew for area in the 0.5X IPTG + 1X X-gal background.

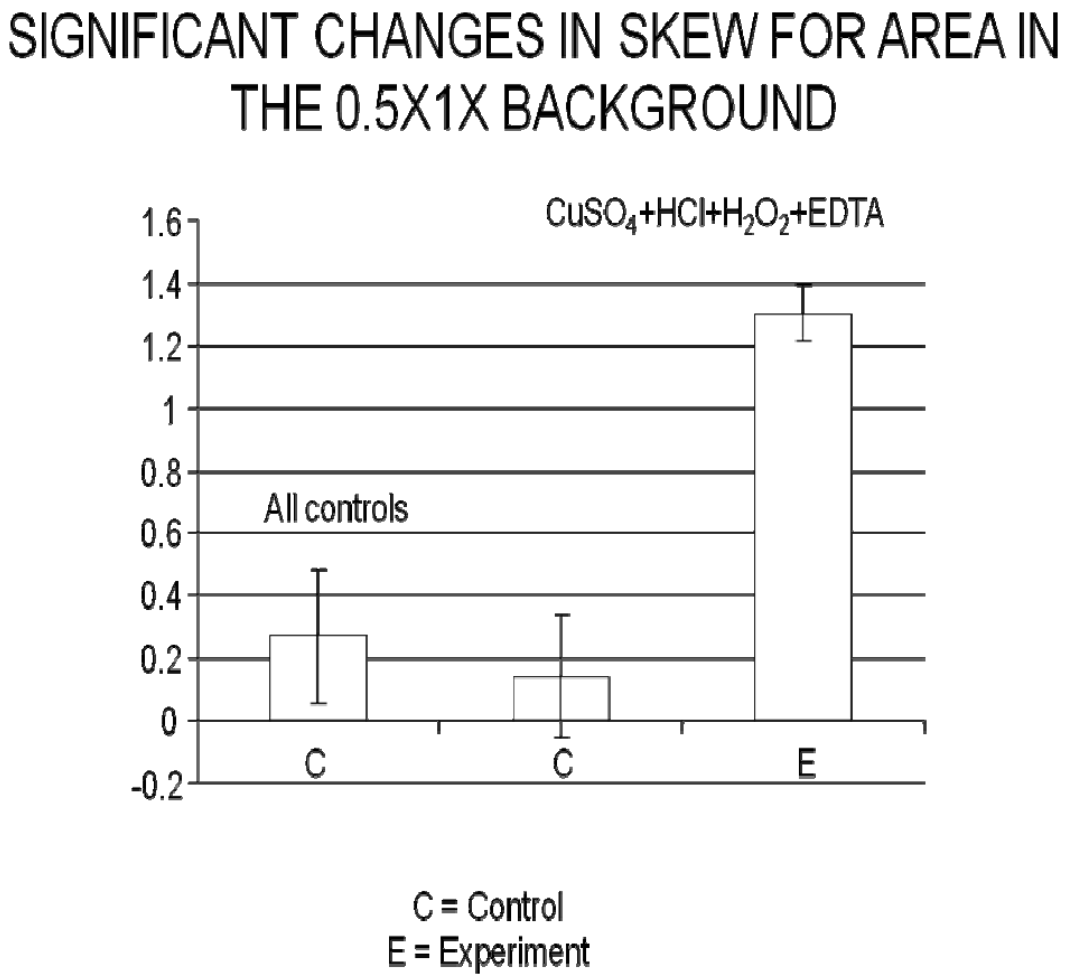

Only one treatment was observed to give significant changes in skew when added to the 0.5X IPTG + 1X X-gal background. Skews were compared to matching control data plates done on the same day, and also the average skew of the entire thirty-five control data sets. Error bars are standard deviations.

Figure 17. Distribution of kurtosis for area.

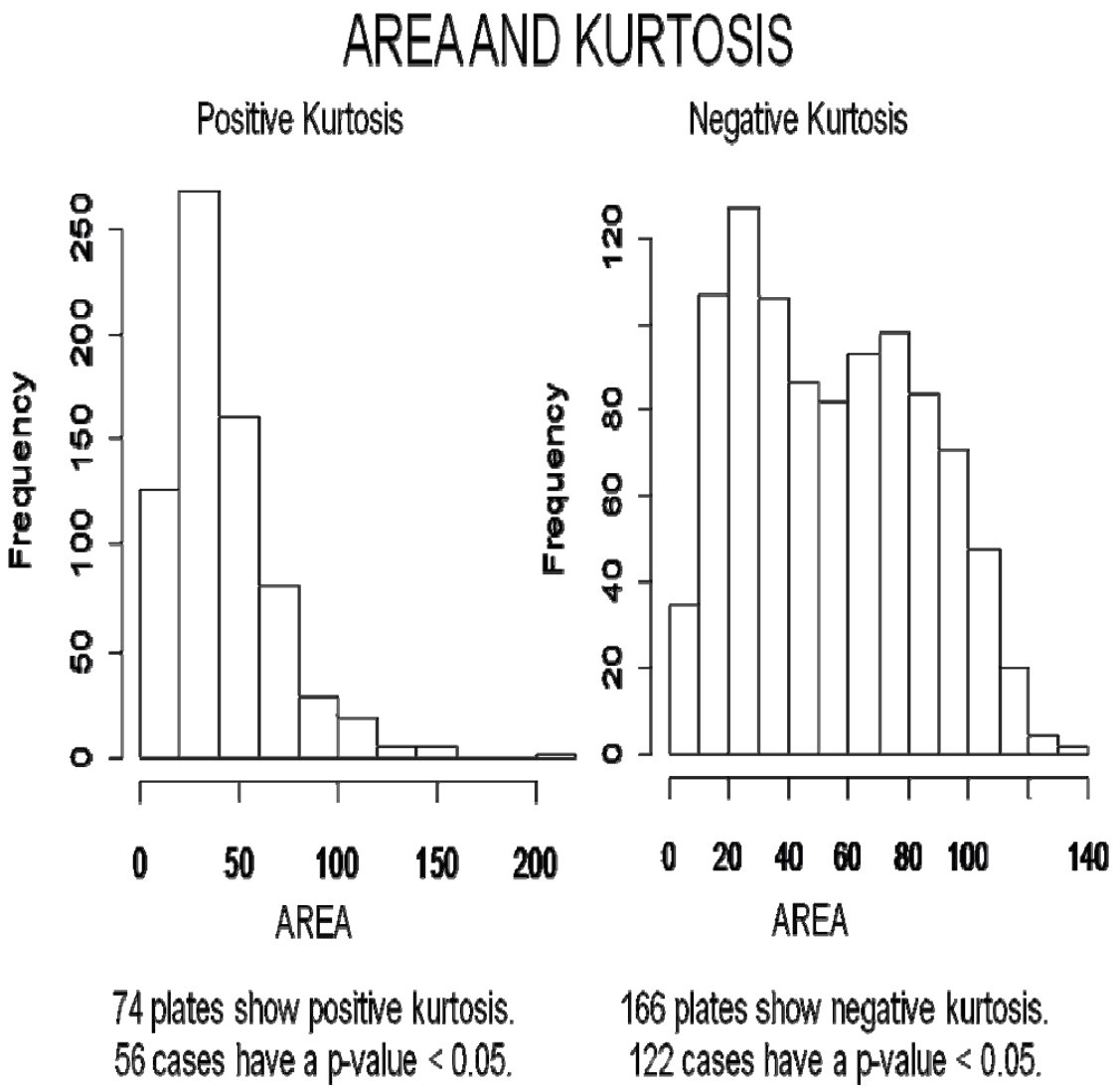

When plotting area histograms for individual plates, kurtosis for area was also observed in both negative and positive forms. Most significant kurtosis was negative. Frequency is number of colonies for these examples of histograms of individual plates.

Figure 18. Kurtosis for area differed when comparing different backgrounds.

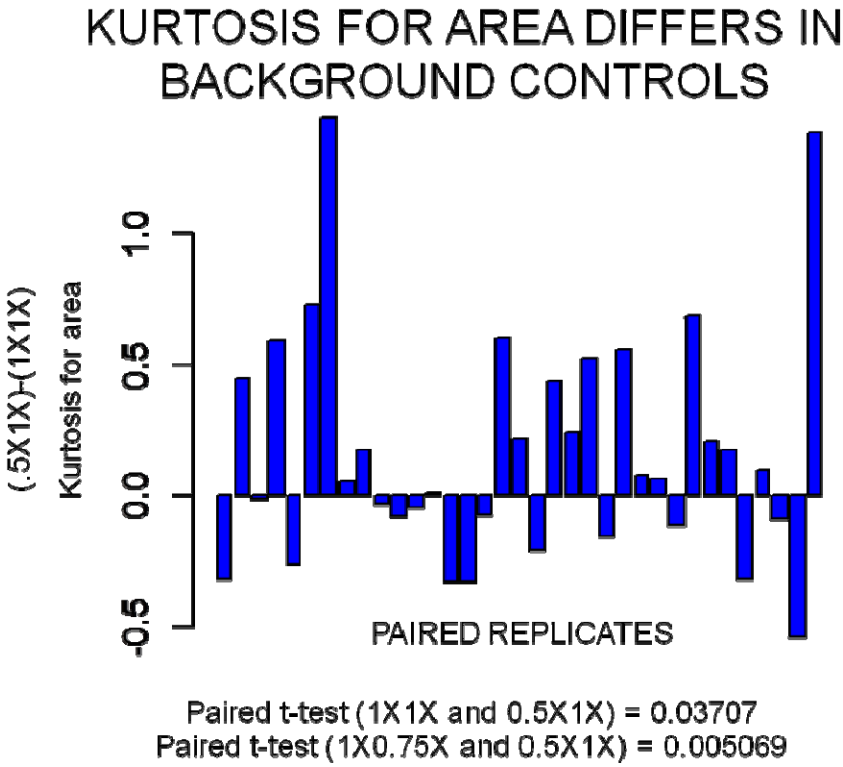

Background control plates showed both negative and positive kurtosis, but unlike skew, there were some significant differences seen when comparing different backgrounds. The 0.5X IPTG + 1X X-gal background had a significantly higher kurtosis observed when compared to both other backgrounds. Two plates gave much higher positive kurtosis in 0.5X IPTG + 1X X-gal than the same day 1X IPTG + 1X X-gal plate control plate. Paired t-tests showed that the kurtosis for the different backgrounds were significantly different, in particular the 0.5X IPTG + 1X X-gal and with both the 1X IPTG + 1X X-gal and the 1X IPTG +0.75X X-gal backgrounds. Below the chart shows the difference in kurtosis on a day by day basis from the 0.5X IPTG + 1X X-gal background controls and the 1X IPTG + 1X X-gal background controls. The 0.5X IPTG + 1X X-gal background differed even more when compared to the 1X IPTG + 0.75X X-gal background controls.

Figure 19. Mean area did not change when comparing different backgrounds.

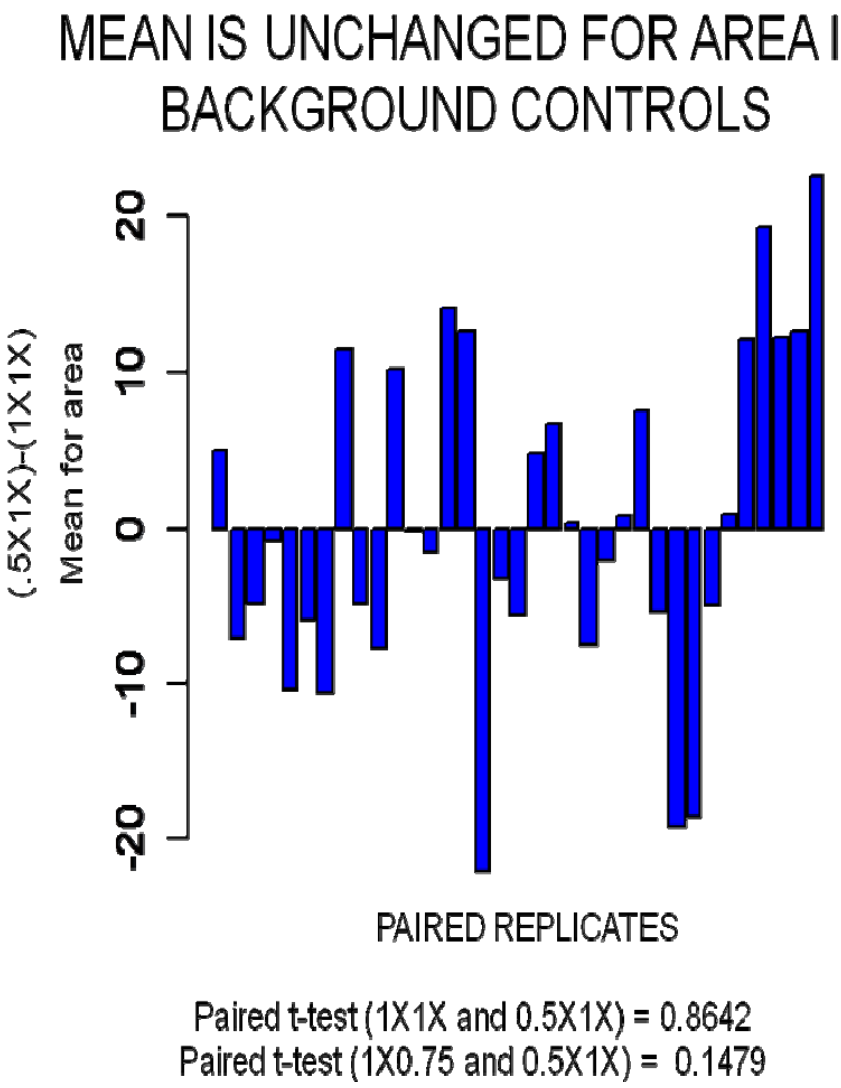

While kurtosis does change depending on background for the controls, the mean of the areas did not change significantly. This chart shows a day by day comparison of the 0.5X IPTG + 1X X-gal background controls and the 1XIPTG + 1X X-gal background controls. Paired t-tests showed no significant differences in mean of area between any backgrounds.

Figure 20. Inputs that show significant change in kurtosis for area in the 1X IPTG + 1X X-gal background.

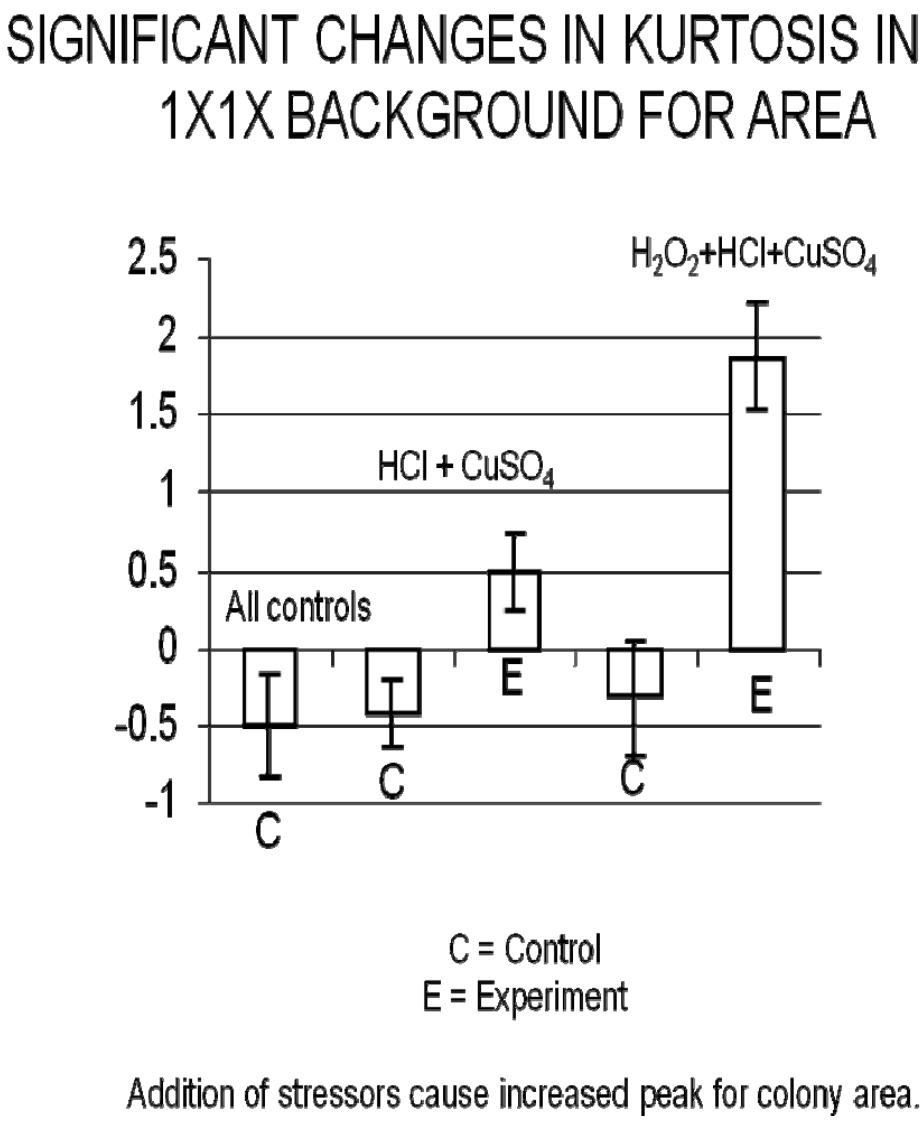

Two treatments showed significant change in kurtosis for area in the 1X IPTG + 1X X-gal background when compared to both the corresponding dates control plate data (adjacent to the experiments) and the average of all controls in the 1X IPTG + 1X X-gal background. Both added a positive kurtosis. Error bars are standard deviations.

Figure 21. Inputs that show significant change in kurtosis for area in the 0.5X IPTG + 1X X-gal background.

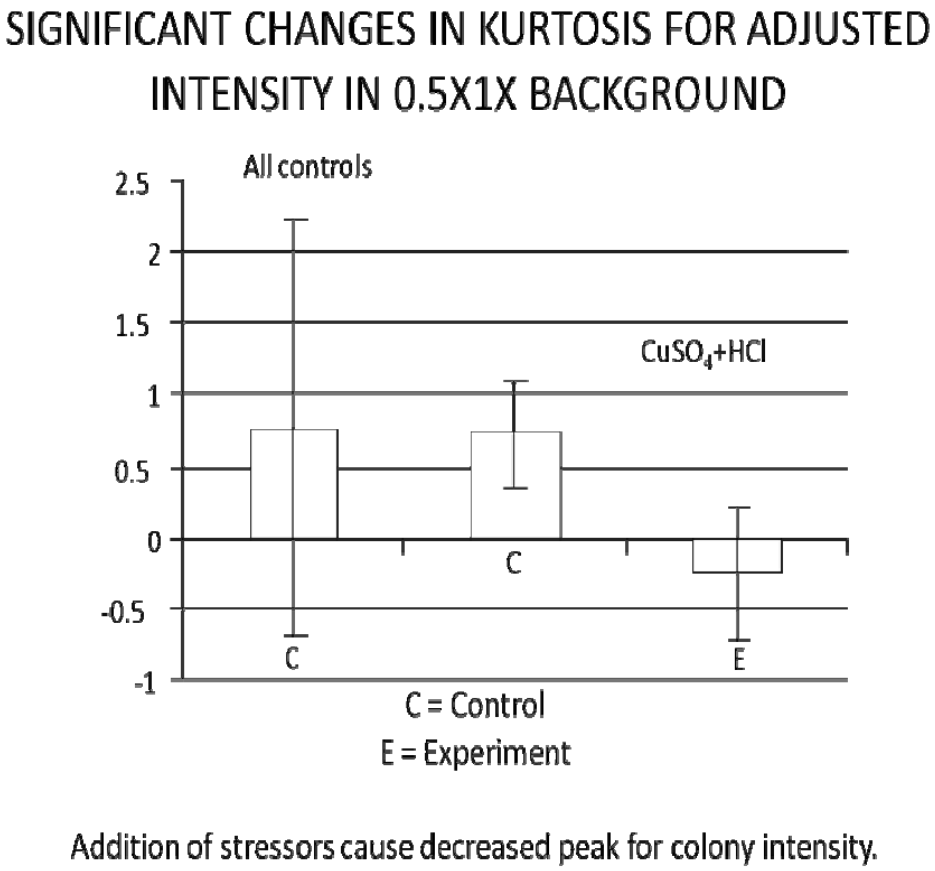

No significant changes in kurtosis were seen in area for the 1X IPTG + 0.75X X-gal background but one treatment, the hydrogen peroxide treatment, gave a significant negative change in kurtosis in area when compared to the same day controls and the average of all the controls for the 0.5X IPTG + 1X X-gal background. Error bars are standard deviations.

Figure 22. Skew distribution for adjusted intensity.

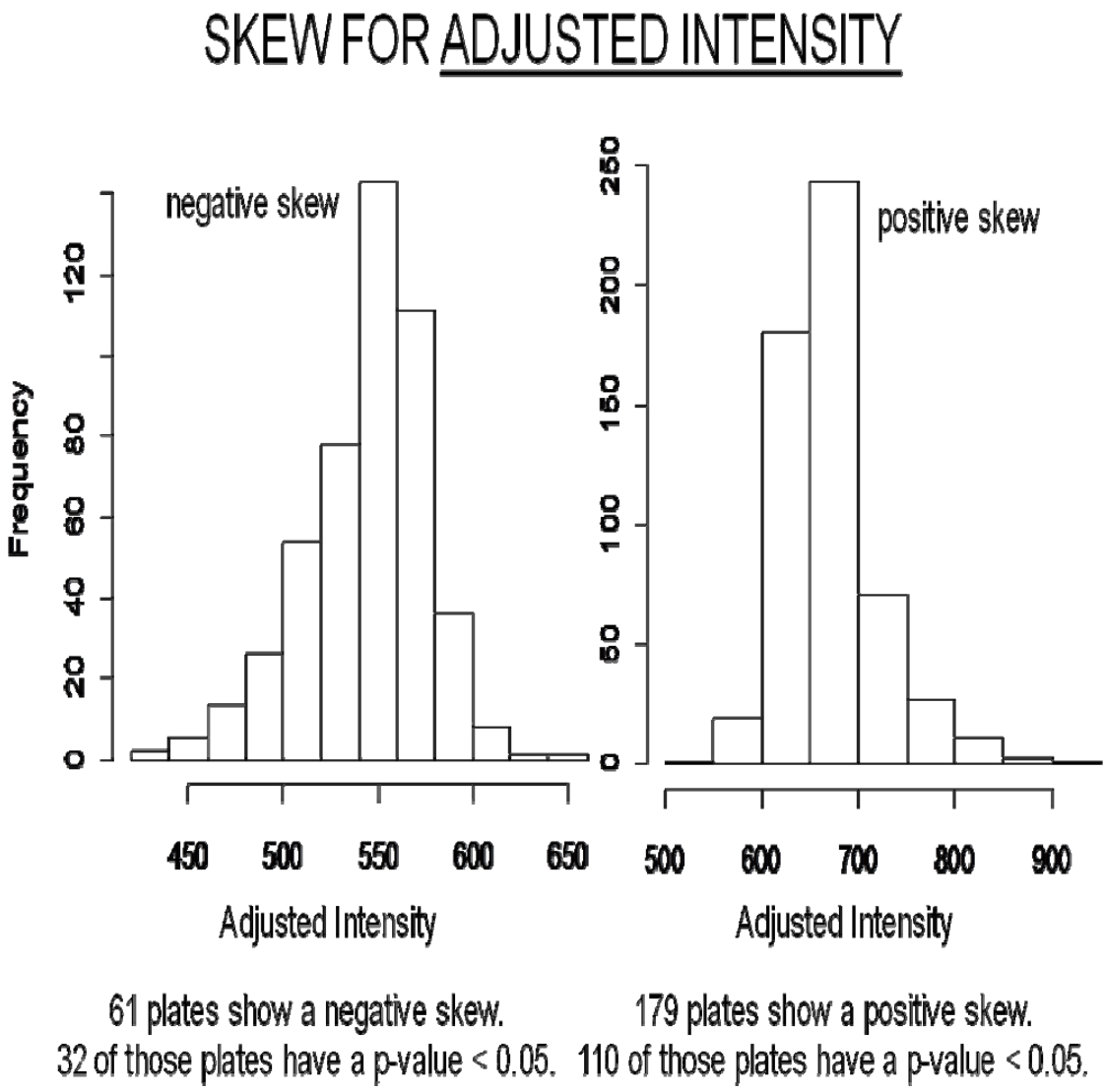

Adjusted intensity also showed both negative and positive skew, with the majority of the significant skews positive. These histograms are examples of two plates that showed skew for adjusted intensity. Frequency is number of colonies for these histograms.

Figure 23. Inputs that show significant change in skew for adjusted intensity in the 1X IPTG + 1X X-gal background.

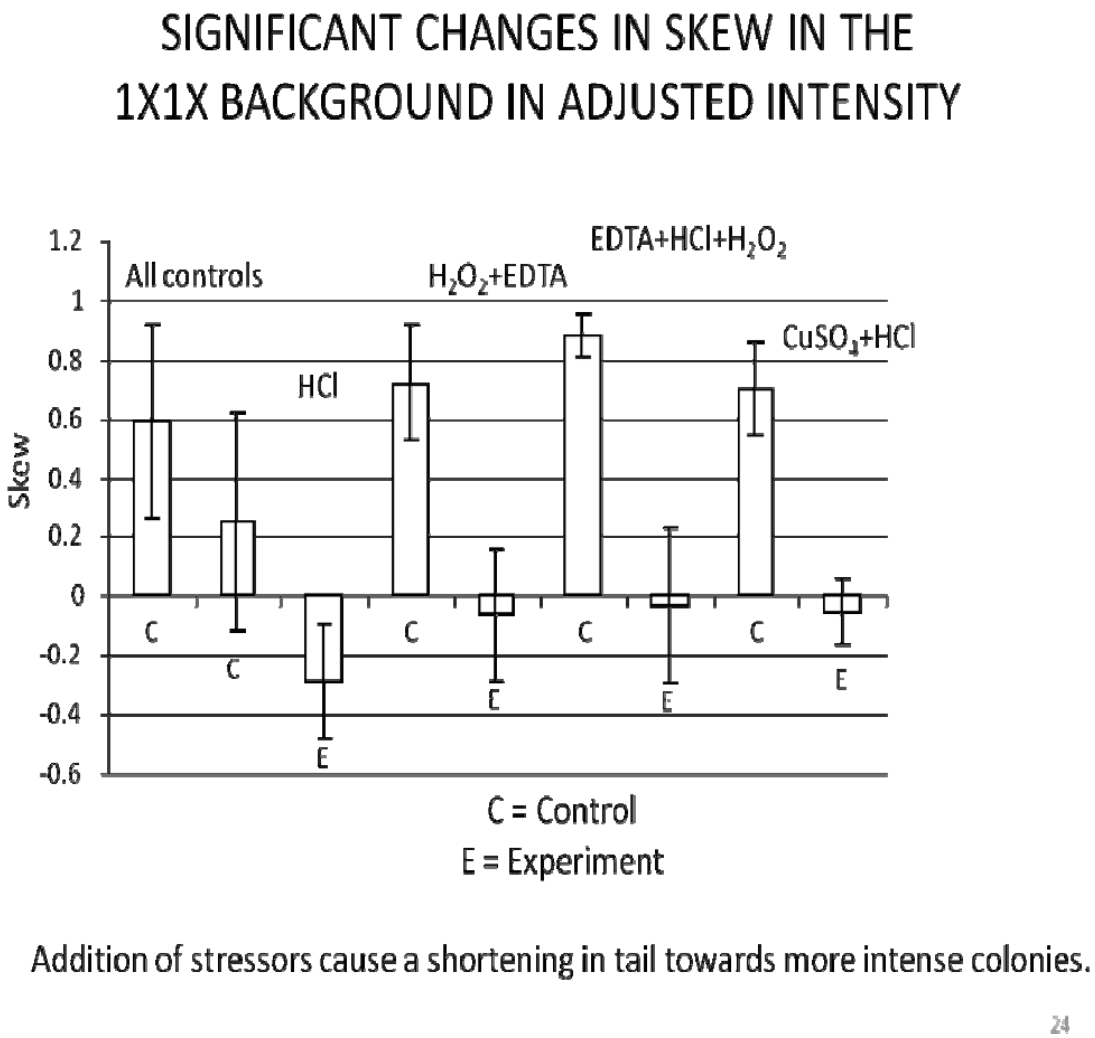

Four treatments caused significant skew changes for adjusted intensity in the 1X IPTG + 1X X-gal background. All of these treatments caused a significant change to a negative skew when compared to the same day controls (adjacent to treatments) and the average of all the controls for the 1X IPTG + 1X X-gal background (bar all the way to the left). No other backgrounds had any significant changes in skew for adjusted intensity. Error bars are standard deviation.

Figure 24. Kurtosis distribution for adjusted intensity.

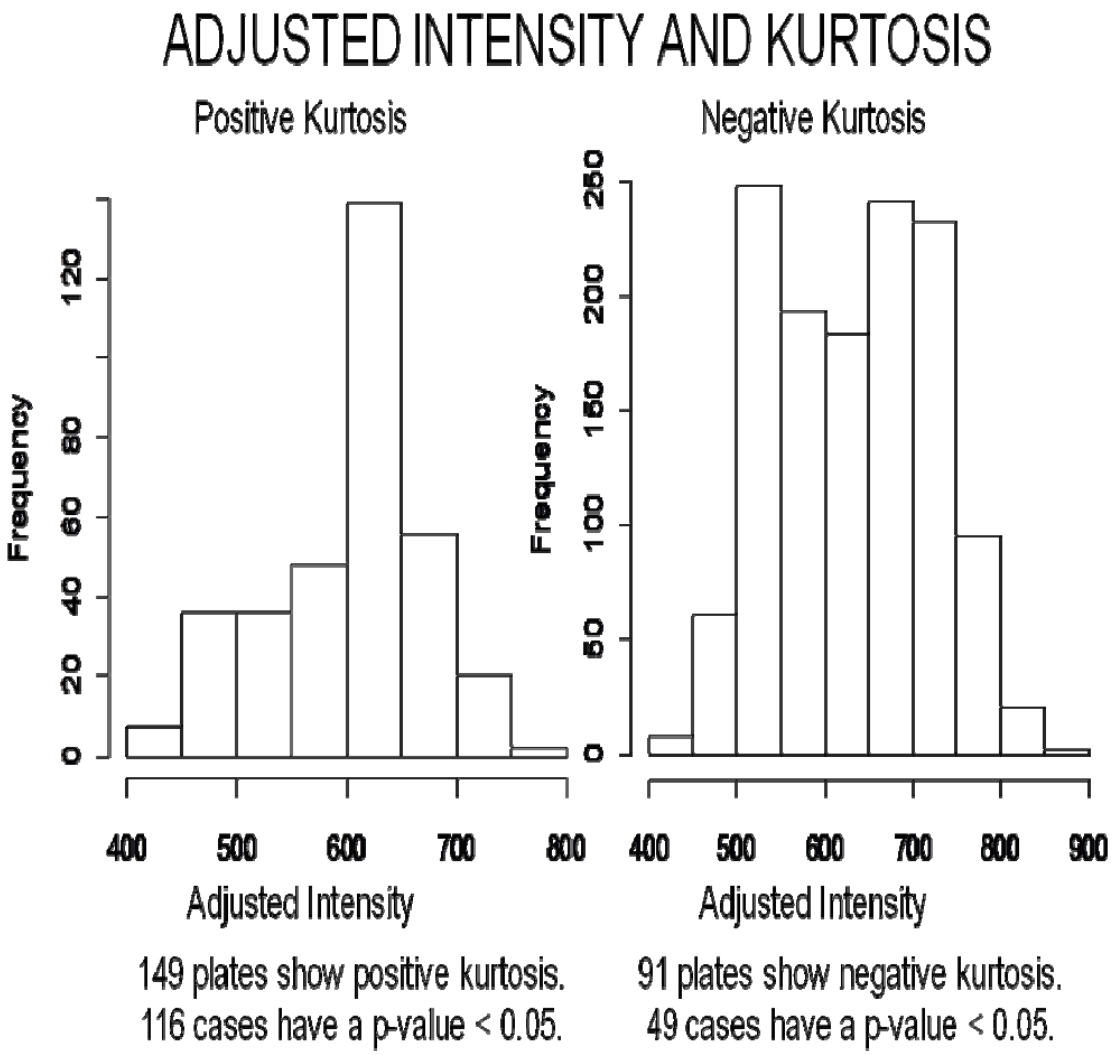

When plotting area vs. frequency for individual plates, kurtosis for adjusted intensity was also observed in both negative and positive forms. Most significant kurtosis was positive. Frequency is number of colonies for these examples of histograms, both individual plates.

Figure 25. Inputs that show significant change in kurtosis for adjusted intensity in the 1X IPTG + 1X X-gal background.

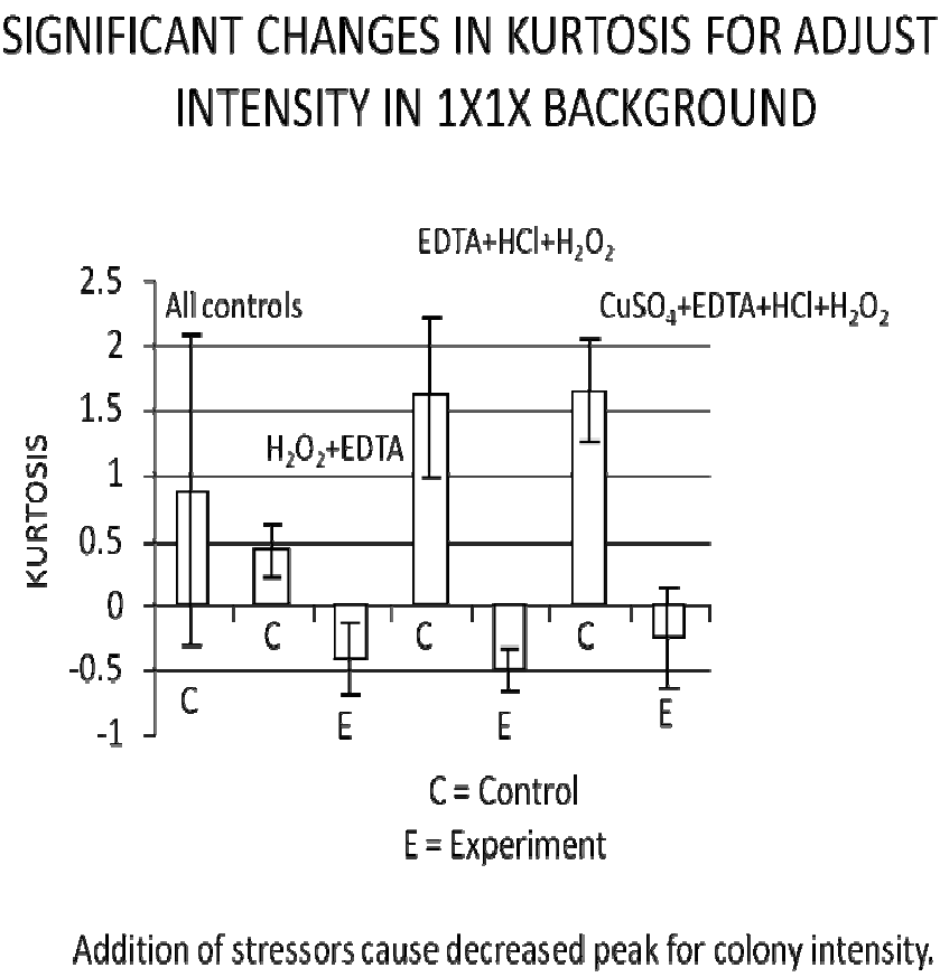

Three treatments showed significant change in kurtosis for adjusted intensity in the 1X IPTG + 1X X-gal background when compared to the same day controls (adjacent to treatments) and the average of all the controls for the 1X IPTG + 1X X-gal background (bar all the way to the left). All three caused a significant negative kurtosis change in kurtosis. Error bars are standard deviations.

Figure 26. Inputs that show significant change in kurtosis for adjusted intensity in the 0.5X IPTG + 1X X-gal background.

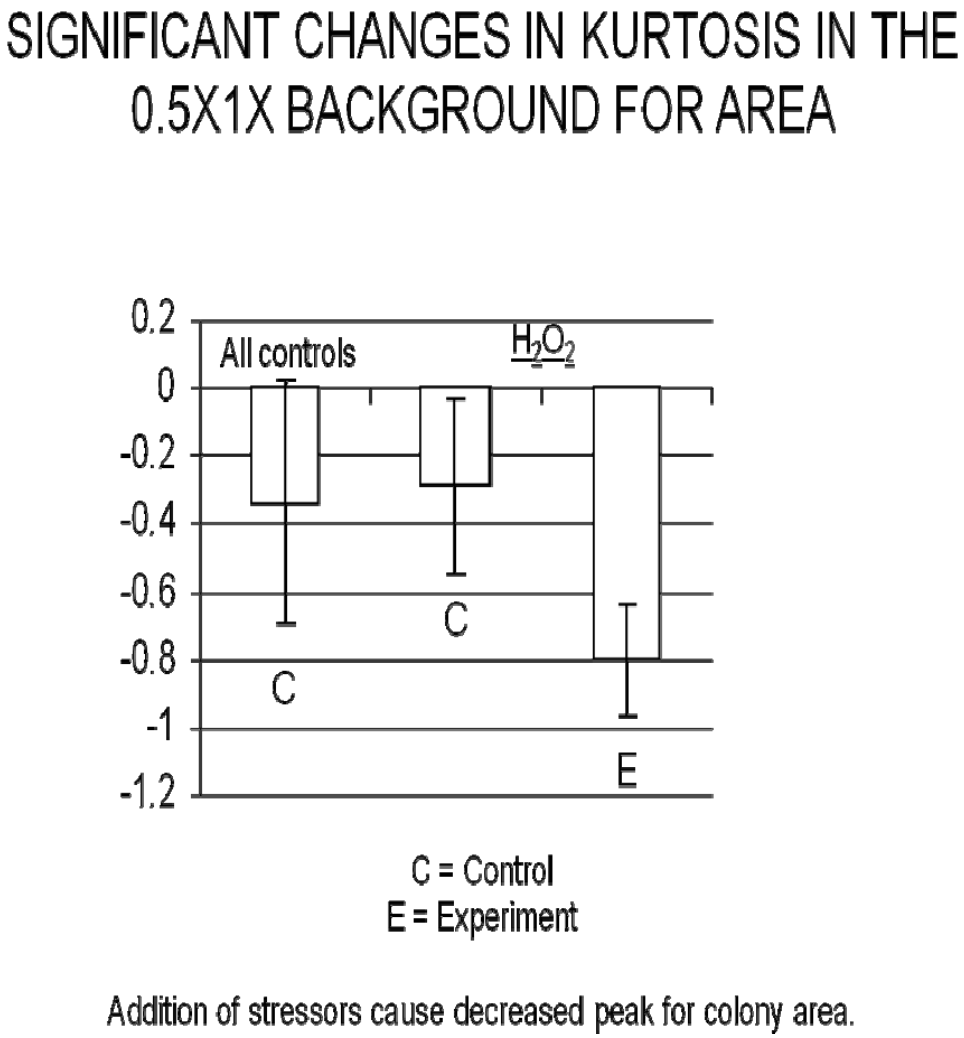

No significant changes in kurtosis were seen in adjusted intensity for the 1X IPTG + 0.75X X-gal background. One treatment, the hydrogen peroxide treatment, gave a significant negative change in kurtosis in adjusted intensity when compared to the same day controls and the average of all the controls for the 0.5X IPTG + 1X X-gal background in kurtosis. Error bars are standard deviations.

CHAPTER 6

High Performance Liquid Chromatography

Section 6A: Introduction

This chapter will discuss a separate set of experiments. These experiments used high performance liquid chromatography (HPLC) with a UV-Vis detector in an attempt to observe specific concentration changes in biomolecules in *Escherichia coli* (*E. coli*) when exposed to oxidative stress through hydrogen peroxide. HPLC has become a popular method for quantitative and qualitative analysis ever since its commercial introduction in 1969 (104). HPLC is an excellent tool for separating mixtures of chemical compounds and giving relative and sometimes direct concentrations of these compounds. HPLC can also be paired with several types of detectors (UV-Vis, Mass Spectrometry, NMR, fluorescence spectrometry, etc.) and combinations of these detectors to give the best results in the simplest manner (105). The experiments here used a UV-Vis detector in order to try to detect different biomolecules by their absorbed ultra-violet (UV) and visible light wavelengths.

This method used a Beckman Coulter System Gold 126 Solvent Module High Performance Liquid Chromatography with a System Gold UV-Vis 168 detector in order to track oxidative stress caused molecular changes in *E. coli* cells. Most amino acids (as well as many other molecules) will not absorb UV or visible light in a manner that will allow for quantification when performing HPLC with UV-Vis. The extracts of these cells were therefore put into reactions with dithionitrobenzene (DTNB), a molecule that reacts with free thiols to give a HPLC/UV-Vis readable molecule by forming a disulfide

bond with the free thiol, modifying the molecules so they can be detected based on the absorbance of ultraviolet light via an aromatic group (Figure 27). In order to locate the amino acids and other free amine carrying molecules, 2,4,6-Trinitrobenzene Sulfonic Acid (TNBSA) and a small amount of hydrochloric acid are reacted with the treated *E. coli* extracts. This compound reacts with free amines to aromatically modify these compounds as well, while not disturbing the structure of the rest of the molecule (Figure 28). As a result, all changes to molecules with a free thiol or free amine were theorized to be able to be observed under different levels of oxidative stress using HPLC with UV-Vis detection.

HPLC is a type of column chromatography and works under the same basic principles of earlier models. The column acts as the stationary phase and a mobile phase, along with the sample, passes through. The major difference between HPLC and the earlier models is that instead of gravity moving the process, HPLC uses high pressure to force through the mobile phase. The sample is then separated in the column according to the relative polarities of its molecules. The eluate, or the part of the sample released from the column at any time, is then passed through a detector at the other side of the column, which in turn gives the computer data to make a chromatogram (Figure 29). Columns are able to be packed very tightly, giving high surface area for interactions between the mobile and stationary phases, resulting in much improved separation (106). In reverse phase HPLC, long, non-polar hydrocarbon chains are attached to silica on the inside of the column and a polar mobile phase allows the more polar molecules in a mixture to get separated and arrive at the detector first

(106). In this experiment, reverse phase HPLC is achieved using a C_8 column, which is a column that has hydrocarbon chains eight carbons long attached to silica lining the inside of the column. The carbon chains and the more non-polar molecules interact with van der Waals dispersion forces, slowing the elution of these molecules (106).

The mobile phase is chosen to act as a baseline in the chromatogram that will not react with the sample. In reverse-phase with a UV-Vis detector, this should be a polar solution with a moderate pH that has a very low UV absorption wavelength. It is commonplace to use two solutions as the mobile phase in a gradient fashion, with the first solution being relatively more polar and the second solution more non-polar (106). The upside of using gradient HPLC is better separation, with more power to concentrate on specific retention times, either elongating areas of the spectrum, or shortening areas of non-activity. There are problems typical to gradient HPLC however. Long equilibrium times and long cycle times are needed due to the multiple mobile phases. Non-reproducible retention times are also more common for gradient HPLC (106).

Retention times and UV-Vis absorption are how the HPLC system used in this study differentiated between compounds. Ideally, each individual compound that is detected has its own retention time, which is the amount of time it takes from the injection of the sample to when the sample is detected. However, it is possible for two or more molecules to have the same retention time when using the same method. For example, two enantiomers may have the same retention times in an achiral column. Retention times depend on the flow used to move forward the mobile phase, the type and size of column used, the chemicals in the mobile phase, and to a lesser extent, the

temperature of the column (106). When using retention times as a way of identifying parts of the mixture, all of these parameters must be carefully monitored. In these experiments, the flow was constant and regulated by a program in the computer. The same columns were used on every experiment. The mobile phases were prepared fresh everyday with a constant pH and filtered to remove any contaminates. The temperature was always room temperature, and though was not controlled, never varied much more than 15° C.

Detection was accomplished with a diode array UV-Vis. A diode array consists of a number of photosensitive diodes placed side by side and insulated from one another in the form of a multi-layer sandwich (107). The output from each diode can be scanned, stored, and subsequently processed by a computer. The diode array monitors the ultraviolet light that has passed through the liquid sensor cell in the multi-wavelength liquid chromatography detector. The light is dispersed by a quartz prism or a diffraction grating onto the surface of the diode array, so each diode will receive light of a slightly different wavelength to that received by the others. When a given substance is eluted through the sensor cell, all the outputs from the array can be acquired and the results used to construct an absorption spectra ranging many wavelengths. If the wavelength of the light at which a compound gives maximum absorption is known, then the diode array allows for selection of this (and possibly two) wavelength(s) to provide maximum data for that substance (107). Due to the amount of computer space and time, not all of the peak areas for every wavelength are recorded

and these specific wavelengths selected give the most data, though the specific wavelengths can be changed post-run.

The computer gives a chromatogram for the results. Peaks correspond to each individual compound and the area underneath the peak is directly proportional to the concentration of that compound in the mixture. The location of the peak on the x-axis is the retention time of the compound (106). The HPLC software also has the ability to export other information, including what the peak's percentage area compared to the total area underneath all the peaks is and the maximum wavelength absorbed of the peak. The retention time, percent area, and lambda max were recorded for these experiments in an attempt to identify recurring molecules in *E. coli.*

Section 6B: Method

Reagents: DH5-α cells were a gift from Dr. Vivian Bellofatto, UMDNJ. Hydrogen peroxide (5 M) was purchased from Fisher Scientific. Lysogeny broth (LB) was bought from Teknova. Dibasic potassium phosphate buffer (50 mM in distilled water) with KOH added to adjust the pH was purchased from Fisher Scientific. Potassium chloride (100 mM), acetonitrile, sodium bicarbonate, and the methanol were all bought from Fisher Scientific. Sodium bicarbonate (30 mM) was diluted using deionized water and was adjusted to pH 8.5. Acetonitrile was diluted with deionized water to 75% acetonitrile.

DTNB: DTNB (10 mM, purchased from Sigma) was prepared in Tris buffer (bought solid from Fisher Scientific, and was diluted in deionized water and adjusted to pH 8.0). DTNB solutions were kept at -20°C in light repellent 1.5 mL plastic centrifuge tubes.

TNBSA: TNBSA preparation and HPLC method was based on Hermanson's TNBSA method (102). TNBSA (0.06% w/v) was prepared by doing a 3:50 dilution of a 5% w/v TNBSA solution in 0.1 M sodium bicarbonate adjusted to pH 8.5. TNBSA stock was bought from Pierce.

Experimental Conditions: The cultures, grown in 250 mL of LB broth, were started from 5 mL of grown bacteria in LB broth (overnights) and grown to $A_{600\ nm}$ = 0.6, with the absorbance read by the Simple Reads program using a Cary 50 Bio UV-Visable Spectrometer. *E. coli* cells were treated with 100 µL of 5 M hydrogen peroxide for 5, 30, 60, and 150 minutes once in the 250 mL of broth. *E. coli* was also cultured without treatment of hydrogen peroxide as a control. The cells were then harvested by centrifuging for 15 minutes at 4,500 rpm using the Marathon 21000R 1EC 6555C rotor centrifuge and the swinging bucket rotor at 4° C. The LB broth was removed from the pellet and the pellet was washed with 10 mL of cold 50 mM potassium phosphate buffer containing 100 mM KCl, pH 7.4. The suspended cells were then subjected to centrifugation again as described above and stored at -80° C.

For the preparation of *E. coli* cells for the HPLC, the molecules inside the cells were extracted using a methanol extraction method. Frozen *E. coli* cells were resuspended in 1 µL of methanol for every 1.25 x 10^{-4} grams of cells *E. coli* and placed in a -80° C freezer for 30 minutes. The samples were then thawed on ice. Once thawed completely, the samples were transferred into a 1.5 mL plastic centrifuge tube and centrifuged at 13,000 rpm for 15 minutes at 4° C. The supernatant was removed from the sample, and kept aside on ice. The pellets were resuspended in 100 µL methanol

and centrifuged again at 13,000 rpm for 15 minutes at 4° C. The supernatant was removed and added to the earlier removed supernatant. The supernatants were transferred to a Ultracel YM-3 microcon centrifuge filtration tube and centrifuged until complete. The YM-3 microcons are designed to have a molecular weight cutoff of 3,000, and were used to filter the samples in order to remove unwanted larger molecules, including full proteins, but keep amino acids intact and in the sample.

HPLC Method: The extracts were then treated with either DTNB or TNBSA to create convenient compounds that will give results when run in the HPLC using a C_8 column (a column packed with eight chained hydrocarbons attached to silica lining the inside of the column) and read with a UV-Vis detector. Cells extracts treated with DTNB were done so after a methanol extraction for 10 minutes at room temperature at a volume ratio of 2:1 by volume of 10 mM DTNB:Sample. Those treated with TNBSA were done so for 90 minutes at 37° C at a volume ratio of 4:2:1 by volume of sample: 0.06% w/v TNBSA: 1 M HCl. The samples were then all filtered before HPLC.

Samples are introduced into the HPLC with only liquid and absolutely no air using a glass sample syringe. A sample loop holds the sample until a valve is turned, which instantly opens the loop to be flushed with the mobile phase. When injecting samples, a 250 µL syringe and a 200 µL sample loop were utilized.

The HPLC was run with two mobile phases using a gradient method (Figure 30). The first mobile phase was 30 mM Sodium bicarbonate (pH 8.5), used to elute more polar molecules from the column. The second eluent was 75% HPLC grade acetonitrile,

used to remove more hydrophobic molecules from the column. The flow rate for the method was 1.5 mL/minute.

All runs took place using a 250 x 4.6 mm TARGA C_8 column always from Higgins Analytical using the same gradient method and flow. The HPLC produces a multi-wavelength full spectrum, reading from 190 nm – 600 nm. The machine was also set to two maximum wavelengths, reading at 260 nm and 350 nm as well as the maximum wavelength for each individual peak. Lambda max for excess DTNB was expected to be 412 nm (109), while the modified free thiols were expected to have a lambda max of 326 nm (110). Excess TNBSA was expected to absorb at 335 nm (111) and the modified amino acids were expected at around 340 nm. This value changes due to the different side chains of the amino acids and were seen at a range of 335-355 nm (112).

Section 6C: Results Introduction

The results from this experiment varied radically. The method was performed consistently, though consistent results could not be collected, even from exactly replicated runs.

Separate HPLC control runs of *E. coli* with no hydrogen peroxide were run four individual times with TNBSA added and with DTNB added. Experimental runs of *E. coli* treated with five minutes of hydrogen peroxide were also done four times with TNBSA and then again four times with DTNB.

Area under the curve, retention time, and the maximum absorbance wavelength (λ_{max}) for each peak were recorded. The area under the curve is directly proportional to the concentration of whichever molecule's elution caused the curve. In mathematical

terms, it is the integral under the curve produced by graphing time vs. absorbance. It was determined that actual values of the area under the curve were useless when exact same conditioned chromatograms gave significantly different values for the same peaks. Ideally, the area under the curve data was important because it showed whether certain molecules were increasing or decreasing in concentration due to the oxidative stress. Different numbers of *E. coli* in the preparation or slightly different volumes used in the extraction would also cause differences in the absolute amount of a molecule in a sample and therefore the area under the curve as well.

As expected, the area percent for the same peak was much more consistent from replicate reading to reading than the areas themselves. This was believed to happen due to the variation of volumes injected due to random error. The areas of each individual peak were divided by the total area of all the peaks in the run to serve as a better indicator of relative concentrations.

Section 6D: DTNB and TNBSA Blanks

DTNB and TNBSA with no cells, but rather with only pure methanol were run (Figure 31 for DTNB, Figure 32 for TNBSA). In Figure 31, the DTNB peak is assumed to be the large peak at roughly 19 minutes, given it is the only major chemical introduced and the only major peak eluted. The other two much smaller following peaks are unknown peaks. In Figure 32, the TNBSA peak is assumed to be eluted at 11 to 12 minutes. The major peak is assumed to be the TNBSA peak alone, however, contamination is obvious as multiple other smaller peaks are observed.

Every control and experimental run was lined up with these "blank" DTNB and TNBSA runs and the peaks that were seen in both were removed from the analysis. The area percents were then calculated and compared using the remaining peaks.

Section 6E: DTNB Control Results

Control samples reacted with DTNB as described in Section 6B were run four times (Figures 33-36), and experimental runs a corresponding four times (Figures 37-40). Control samples treated with DTNB gave sixty-two separate peaks from the four separate runs, plus some much smaller noise (or very low concentration molecules) peaks. Of the sixty-two, only three peaks appeared in all four runs. The first peak eluted at 8.46 minutes, with a lambda max of 275 nm (+/-2 nm). These peaks had an average area percent of 1.65. This peak is adjacent to a peak at 6.27 minutes, with a lambda max of 330 nm, the experimentally found peak for DTNB modified cysteine (Figure 63). The Cys peak is seen in all four controls, but at a much lower area percentage in the fourth day (Figure 37), where the peak was only 0.21% of the total area for the chromatogram (Table 15). The other three Cys peaks gave an average percent area of 29.60%. The third peak found in all four control runs eluted at 14.5 minutes and had an average area percent of 5.90%, the highest average percentage of any non-Cys peak. The day four control again had the lowest area percentage for this peak, at 0.17%.

Eight other peaks appeared in three of the control runs. Of these eight, six were found in two or less experimental runs. The peaks found at 45.8 minutes and 48.7 minutes were found in three experimental runs. However, of these three runs, only two

were connected by day and sample. There was an individual run included in both of these peak sets that were done with different samples on different days and these samples and days varied for both peaks.

Section 6F: DTNB Experimental Results

Experimental runs produced sixty-four separate peaks, plus some smaller noise peaks found throughout the four runs. Of these, nineteen additional peaks appeared in three or more runs, with four of these peaks seen in all four experimental runs. These include a peak found at 12.3 minutes with a percent area average of 1.98%. The lambda max of these peaks was 257 nm. This peak was also found in one run of the control samples but not the other three. The molecule that eluted here is not known. A second peak was found in all four runs at 31.2 minutes with a lambda max of 273 nm. This peak appeared in two control runs.

The peak found at 14.5 minutes was seen in all four experimental runs as well (Table 15). With a percent area average of 3.50%, it again was the highest average area percentage of any non-Cys peak (as noted in Section 6E, it was also the highest average area percentage peak of any non-Cys peak in the controls). The Cys peak itself again appeared in all four chromatograms. The average percent area of the Cys peaks in the experimental runs went down to 19.90%. It is interesting to note that the Cys peak in the day four experiment (Figure 40) had the largest area percent of all the experiments at 32.20%, while the Cys peak in the control sample for that day had by far the smallest at 0.21%. Every other day had a larger Cys peak in the control sample than in the experiment sample.

Even though all four runs in the control and experiments eluted a Cys peak, no information about how the oxidative stress affected the concentration of Cys molecules in *E. coli* could be learned. The data was far too sporadic, as the comparison of day four to the other days shows. The variation in the data is too much to be considered meaningful. The Cys peaks were the most reproducible peaks and still there was irreproducibility of the peaks from day to day.

When day four is removed from the data, the p-value from a paired t-test comparing the controls to the corresponding experiments still gives a non-significant result at 0.145. There is a chance that the Cys is not being affected by the hydrogen peroxide and that is the reason for the high p-value. If this is the case, then the DTNB experiment results are giving nothing interesting at all, as Cys peaks were the only peaks even close to being reproduced on a day to day basis and the treatments would not be changing the concentration of Cys whatsoever. Even if the Cys was consistent and showed a significant change, looking at only the Cys concentrations would not be very interesting either.

Section 6G: TNBSA Control Results

Control samples reacted with TNBSA as described in Section 6B were run four times (Figures 41-44) and experimental runs a corresponding four times (Figures 45-48). Control samples treated with TNBSA gave a total of seventy-eight different peaks seen throughout the four runs plus some smaller noise peaks. Twenty-four of these peaks appear in at least three of the four runs, with eight seen in each trial. Of these eight, six have a lambda max in the 340-350 nm range and are believed to be molecules with a

free amine modified with TNBSA. The amino acid serine modified with TNBSA gave experimental results of a peak at roughly 22 minutes. Ser was eluted in all four samples with a lambda max of 349 nm. This peak had an average percent area of 2.63 (Table 16). The amino acid cysteine modified with TNBSA was also experimentally found at approximately 30 minutes. This peak was also seen in the results, at 29.6 minutes and a lambda max of 350 nm in all four control runs with an average area percent of 3.31%. The unknown peak with the highest percent area was found at 12.1 minutes in three of the control runs. This peak was believed to be a TNBSA modified free amine with an average lambda max of 348 nm. The peaks varied tremendously in size, from 19.93% in day 2's control (Figure 38), to 1.08% in the control of day 3 (Figure 39), with an average percent area of 7.54%. It did not elute in day 4 (Figure 40).

Section 6H: TNBSA Experimental Results

Perhaps the best example of the lack of consistency in results comes from the experimental samples with TNBSA. Of the eighty-six different peaks, fourteen peaks were featured in three or more runs, with only two peaks eluting in all four runs. The first peak was the 12.1 minute peak, with an average area percent of 16.69%. It is difficult to say if this peak rising is actually a sign of oxidative stress causing an uptake of this molecule. The peak did not elute at all in the day 4 control but gave the highest area percent of all in the day 4 experiment (Figure 44) at 39.65%. Compare this number to the first day experiment (Figure 40) at 0.13% and it appears that this is a major source of where inconsistent chemistry is occurring. This peak appeared in all other control and experiment chromatograms.

The second peak found in all four experiment runs with TNBSA eluted at 36.5 minutes, with a lambda max of 331 nm. The peak had an average area percent of 2.66. This peak does not appear in any control runs and has been theorized to be a product of the hydrogen peroxide reacting with a molecule to make it available to chromatography by forming some sort of free amine that was available for TNBSA to bond with or perhaps *E. coli* itself reacting to the hydrogen peroxide and having a natural stress response that gave a free amine. This peak did give a smaller lambda max than most of the free amine-TNBSA compounds gave.

The Ser peak eluted again in three of the four experimental runs with TNBSA at an average percent area of 2.21%. The first day (Figure 41) did not elute this Ser peak. The Cys peak also diminished in the number of experimental results, with only three experimental runs producing a Cys peak with TNBSA (Table 16).

Section 6I: UV-Vis Methods and Results

The lambda maxes of the entire mixtures were measured on the UV-Vis spectrometer using a simple reads program at 412 nm. The simple reads program gives an absorbance spectrum at a specific wavelength. DTNB reactions were completed as discussed in Section 6B. Samples prepared for the HPLC were split into half right after the reactions were finished. These new samples were read in the UV-Vis using a quartz cuvette and the absorbance of each individual sample was recorded. Every sample run on the machine, both control and experiments, were read using the UV-Vis.

TNBSA reactions were also read on the UV-Vis spectrometer using a simple reads program at 335 nm for each sample run in the HPLC (Table 22). Samples prepared (see

Section 6B) for the HPLC were split into half right after the reactions were finished. These new samples were read in the UV-Vis. The absorbance of each individual sample was recorded.

A paired t-test of control ratios of DTNB:TNBSA to the experiment ratios of DTNB:TNBSA gave a p-value of 0.1197. This shows that there was not a significant difference in control and experimental maximum wavelengths.

TNBSA experiments absorbed less UV- and visible light than their control counterparts every time but these numbers and ratios varied. The p-value is slightly significant for a paired t-test of the TNBSA control to TNBSA experiment data at a value of 0.027. DTNB data is much more variable, with absorption values sometimes being higher for controls when compared to experiments and other times lower for controls when compared to experiments. From this data alone, it was obvious that there were some inconsistencies in the samples, even before the samples were injected into the HPLC.

Section 6J: Conclusion

When a peak did not appear in all of the runs, it became insufficient to give any real results. This was the majority of the TNBSA peaks and a smaller yet still substantial majority of the DTNB peaks. Major peaks were present in some runs but absent in others using the same method. There were bits and pieces of information that could be drawn from this experiment but unfortunately the results were not nearly consistent enough to prove anything about how these *E. coli* react to oxidative stress caused by hydrogen peroxide. The TNBSA itself was proved to be contaminated but in theory the

TNBSA should have reacted in the same way with *E. coli*, no matter the contamination. Of course, there could have been variation in the cultures as well, which may have caused some of the variations seen in the chromatograms.

Nevertheless, it may be possible to study these reactions in such a manner. Others have had much more success in using TNBSA and DTNB with HPLC to study biomolecules. Sulfhydral content has been discovered many times over using DTNB assays. Free amines content has been discovered using the TNBSA assays.

From the results collected, it has to be assumed that the cells themselves were not uniform or that there was an issue with the method. Results varied day to day but also run to run using the exact same sample preparation and the same cells themselves. It was difficult to explain what exactly went wrong. The same preparation from the same cells using the same reactions with the same chemicals using the same machine and method should have produced like results, but did not. The method was verified using cysteine and serine as controls reacted with TNBSA. It was concluded that DTNB would not need to be tested until the error source for the TNBSA reactions and runs were determined, as much more data could be ascertained with the TNBSA runs, due to more peaks eluting.

Section 6K: Cysteine and Serine as Controls for Error Checking

To understand where the errors were taking place, multiple HPLC runs were performed using a 50:50 mix of 10 mM DL Serine and 10 mM L-Cysteine in distilled water. The cysteine was purchased from Matheson, Coleman & Bell, and the serine from Nutritional Biochemicals Corp. To try and replicate the *E. coli* cell conditions, 300

µL of the 50:50 mixes were centrifuge filtered with 250 µL methanol. This was an educated guess, as most *E. coli* samples were centrifuged with about 200-300 µL (varying on weight of frozen *E. coli*) of methanol during extraction. After centrifuging, the serine/cysteine mix was reacted with TNBSA as described in Section 6B. Each reaction was injected with a volume of 150 µL. This was repeated three times a day on three different days (Figure 49-57).

With the two amino acids, it was expected that three peaks would elute, one for the Ser-TNBSA complex, one for the Cys-TNBSA complex, and the last as excess TNBSA. This was not the case. After the removal of the TNBSA blank peaks and peaks with insignificant areas (under 0.5% area), the data showed that seven runs had eight peaks, one had seven , and one had six (Table 17). The peak missing in the run with seven major peaks was also missing in the run with six major peaks. The other peak missing in the run with six major peaks was the average smallest major peak in every other run. The retention times were similar and the lambda maxes given were within 5 nm for a peak to be considered the same. The percent areas of these peaks were compared to each other throughout the nine runs.

For Figure 49 (day 1, sample 1 of the 50:50 mix of serine and cysteine reacted with TNBSA), the peak at 12 minutes is the TNBSA. The peak at roughly 20 minutes is the serine. The serine peak has unknown associated molecules that appear as small "sub-peaks" in every HPLC run, including the serine only run (Figure 61). The peak at roughly 28 minutes is the cysteine. All other peaks are unknown and the peak at 40 minutes is prominent. Figures 50 and 25 (day 1, samples 2 and 3 of the 50:50 mix of

serine and cysteine) are very similar. Both samples gave very comparable chromatograms when compared to Figure 49 but there are some obvious differences. The associated molecule with serine has larger area percents, 12.5% and 11.7% respectively, in these two runs in comparison to Figure 49, with the serine peak at 9.9% area. There are new peaks associated with the 40 minute peak.

The second day's first sample (Figure 52) eluted a smaller TNBSA peak. The serine peak and associated peak separated into two separate peaks. In Figure 55 (day 2, sample 2) and 28 (day 2, sample 3), the peak at 40 minutes does not have an associated peak. The serine peaks were slightly larger in Figure 52, Figure 53, and Figure 54 (22.5%, 19.1%, and 20.3% relatively) when compared to the serine peak's percent areas in the day 1 samples.

For the third day (Figures 55, 56, and 57), all three samples look almost identical but notice the scale of mAU on the y-axis. The Cys peaks are all different percent areas, with the first sample (Figure 55) giving 18.1%, the second (Figure 56) 14.2%, and the third (Figure 57) 18.3%.

It was decided that the individual days should be tested for variance. No matter how these were compared, it was obvious that there was an issue with the chemistry involved in these experiments. It was possible that the HPLC and its chemistry were contributing to the error, however if the HPLC was not working correctly it should not have affected area percents drastically or conceivably at all. If there was a leak, a malfunction, or a contaminant in the machine, the actual areas under the peaks would

reveal this but the percent areas should not have changed as all of the samples should be subject to these same problems.

To see what was causing the problem with the chemistry, a few more samples were run using the same HPLC method as described in Section 6B. A 50: 50 mixture by volume of 5 mM cysteine: 5 mM serine sample was run one time on three separate days (Figures 58-60) and compared to the runs of 10 mM Cys: 10 mM Ser samples. These runs were again prepared in the exact same way as described above. The results showed a new major peak that was not seen in any of the 10 mM Cys: 10 mM Ser sample at a retention time of roughly 31 minutes. This compound was found in all three 5 mM Cys: 5 mM Ser runs, with an average area percent of 4.5%. This was not more TNBSA complex, as again the peaks from TNBSA alone were removed for data analysis. Why this molecule was eluting under these circumstances was very curious and further defends the theory that the issue here was inconsistent chemistry from run to run.

Figure 58 shows the chromatogram for sample 1 of the 50:50 5 mM serine and 5 mM cysteine mixture reacted with TNBSA. When the amount of both amino acids goes down, as compared to Figures 49-57, the serine peak goes down, but the Cys peak does not lose much height. The “peak” at 31 minutes, which looks like a very little bump on the Cys peak, considered an associated but separate molecule, is actually read as an individual peak in this chromatogram, while in the 10 mM mixes was not. In Figure 59 (sample 2), the amount of sample that eluted before the first 5 minutes was greatly dropped in this run as compared to sample 1 (Figure 58). The Cys peak also drops in this chromatogram but the serine peak grows. The Cys peak grows again in this

chromatogram, while the Ser peak comes back down to the height it was at in sample 1 (Figure 58).

Samples of these “half (5 mM) concentration” Ser:Cys mixtures reacted with TNBSA were compared to the “full (10 mM) concentration” samples reacted with TNBSA using an unpaired t-test to show whether same day runs were giving more consistent area percent results than runs on different days. To achieve this, the half concentration samples’ major peaks were lined up against all three same day full concentration samples major peaks (Tables 16-18) and again against the first full concentration sample done on each day (3 in total), and then the second sample, and then the third sample (Tables 19-21). In theory, there should have been no significant difference in area percents between the half and full concentration runs. Of course with the additional peak seen in the half concentration samples, it was obvious that this would not be the case. All of the major peaks found in the nine separate runs done with the full concentrations were seen in all three of the half concentration runs. For the first day of full concentration runs, none of the compared peak’s p-values were below 0.1, and therefore can be considered insignificant data when compared to the half concentration data. The second day of full concentration runs provided 5 significant p-values, including both the serine and cysteine peaks. The third day gave two significant p-value peaks, including serine but not the cysteine peak. This data shows that, even though the second day gave decent results for both major peaks, the area percents were in fact inconsistent, even when performed on the same day, with the same exact chemicals, with the same exact preparation.

To show whether this data was random or not, the half concentrations were again compared with unpaired t-tests against a group of one full concentration run from each day. The first samples prepared on each day gave two significant p-value peaks when compared to the half concentration runs, including the serine peak. The second samples prepared on each day only gave one significant p-value peak when compared to the half concentrations, with neither amino acid peak giving a significant p-value. The final samples run on each day gave four significant p-values, with again the serine peak but not the cysteine peak giving a significant p-value. This data shows further that either on separate days or on the same day, the chemistry between TNBSA and even simple free amines was not reacting consistently, either prior to or inside the HPLC column.

Samples of 10 mM serine with TNBSA alone (Figure 61, prepared in the same way as described in Section 6B) and cysteine with TNBSA alone (Figure 62, also prepared in the same way as described in Section 6B) showed that the cysteine definitely had some contamination. Further proof of this came when read in the UV-Vis using a Scan program, cysteine reacted with TNBSA and HCl gave multiple lambda maxes. This was repeated with serine and TNBSA with HCl but gave only read at one wavelength.

A 50:50 mixture of 10 mM serine and 10 mM cysteine was reacted with DTNB (as described in Section 6B) and injected into the HPLC (Figure 63) to see if the cysteine contamination affected its free thiol side chain. It did not, as only the DTNB and cysteine-DTNB compound were seen in the chromatogram. A blank sample made up of 100% methanol, 0.06% w/v TNBSA and HCl in a 4:2:1 by volume ratio was reacted and

read using the Scan program. Again, multiple wavelengths were absorbed by the sample, with lambda max not being 335 nm like expected but rather at roughly 260 nm. As mentioned in Section 6D, the TNBSA only chromatogram showed some contamination as well (Figure 32).

However, even though the TNBSA appeared to be contaminated, it should not have affected the percent areas of the peaks from run to run on the same day, like what was observed. Also, the TNBSA blank peaks were always removed before runs were compared. It is conceivable that the TNBSA increased its contamination over time, however there is no data to support this, as neither percent area nor loss or gain of peaks increased over time (either hour by hour on runs done the same day or day by day).

Section 6L: Discussion

The serine and cysteine standards further proved that the issue here was in the chemical reactions with the free amines and TNBSA either prior to injection or in the HPLC column. Due to the seen differences in percent areas, and therefore concentrations, on the same reactions done on the same day with the same exact chemicals, there must be an issue with the chemistry involved here. If the method involved could not duplicate results done using set standards, there was no chance for it to work using a bacteria's entire molecular composition. There may be reactions taking place on the column, which would partially explain why there are different peaks eluting at different times (and sometimes not at all). The TNBSA may have contained a contaminate that interacted with one of the mobile phases, which in turn reacted

differently with the samples, but as stated above, this should not have mattered in quantifying the TNBSA modified molecules, as all samples would be subject to the same contaminates. Again, the same preparation using the same reactions with the same chemicals using the same machine and method should have produced like results, but did not.

Figure 27. DTNB Mechanism with a free thiol.

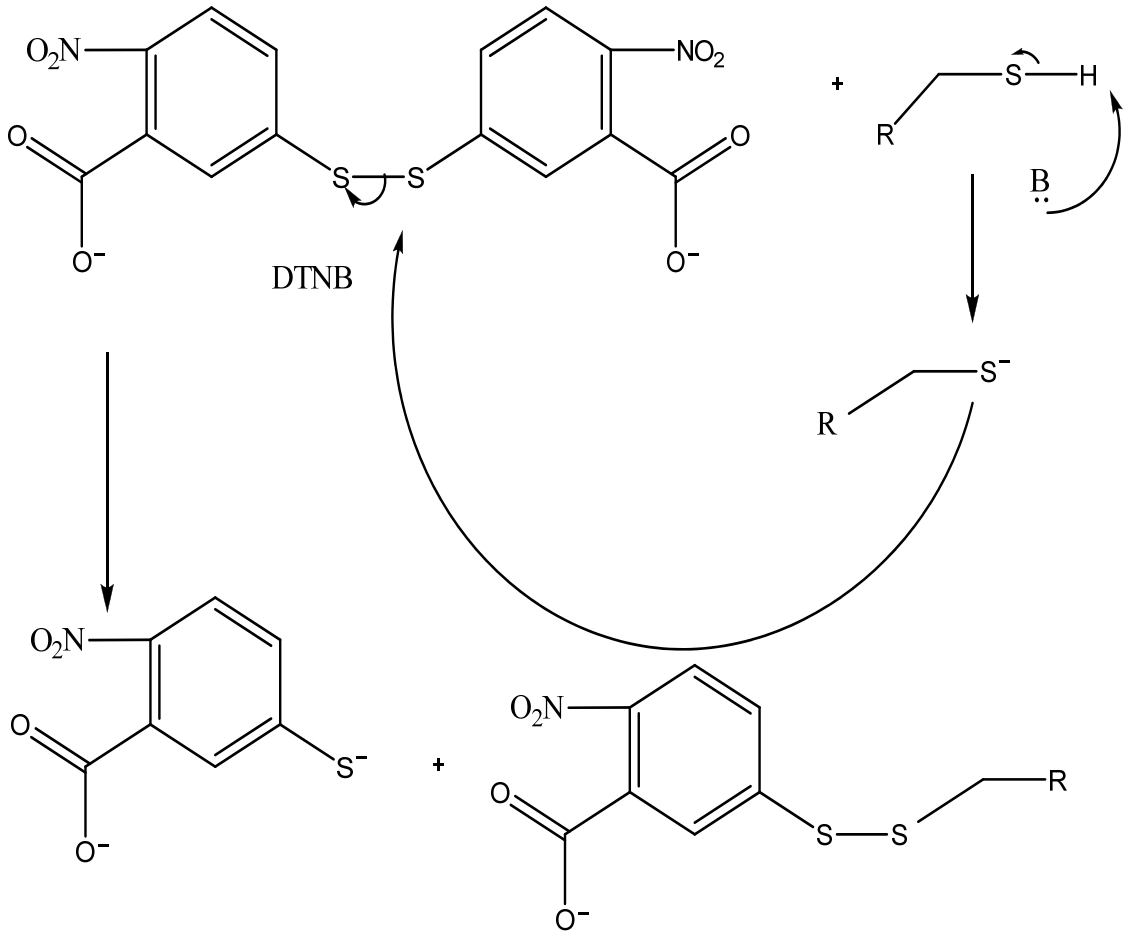

The free thiol becomes aromatically modified to give better UV-Vis detection.

Figure 28. TNBSA Mechanism with a primary amine.

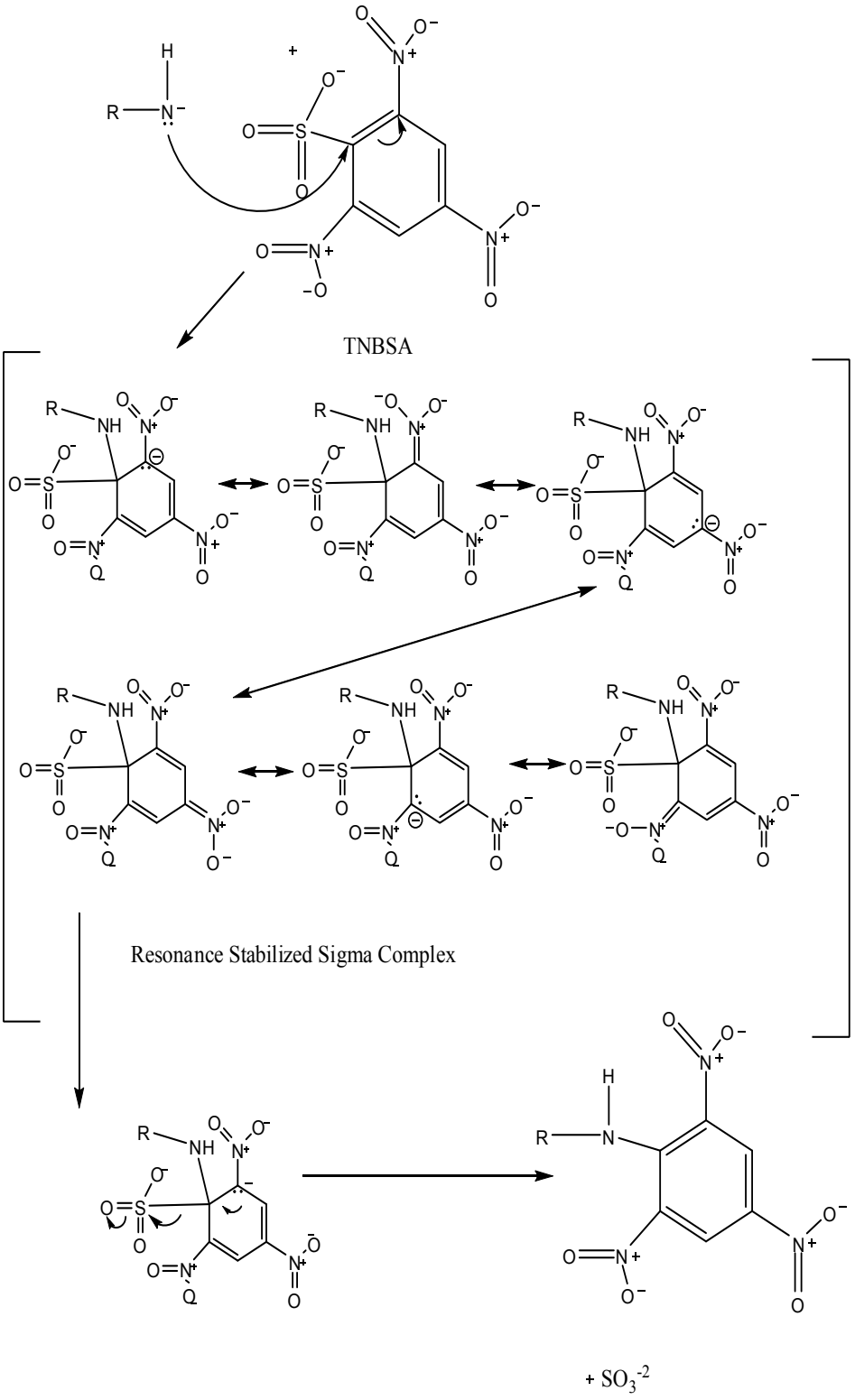

The free amine becomes aromatically modified to give better UV-Vis detection.

Figure 29. HPLC flow chart.

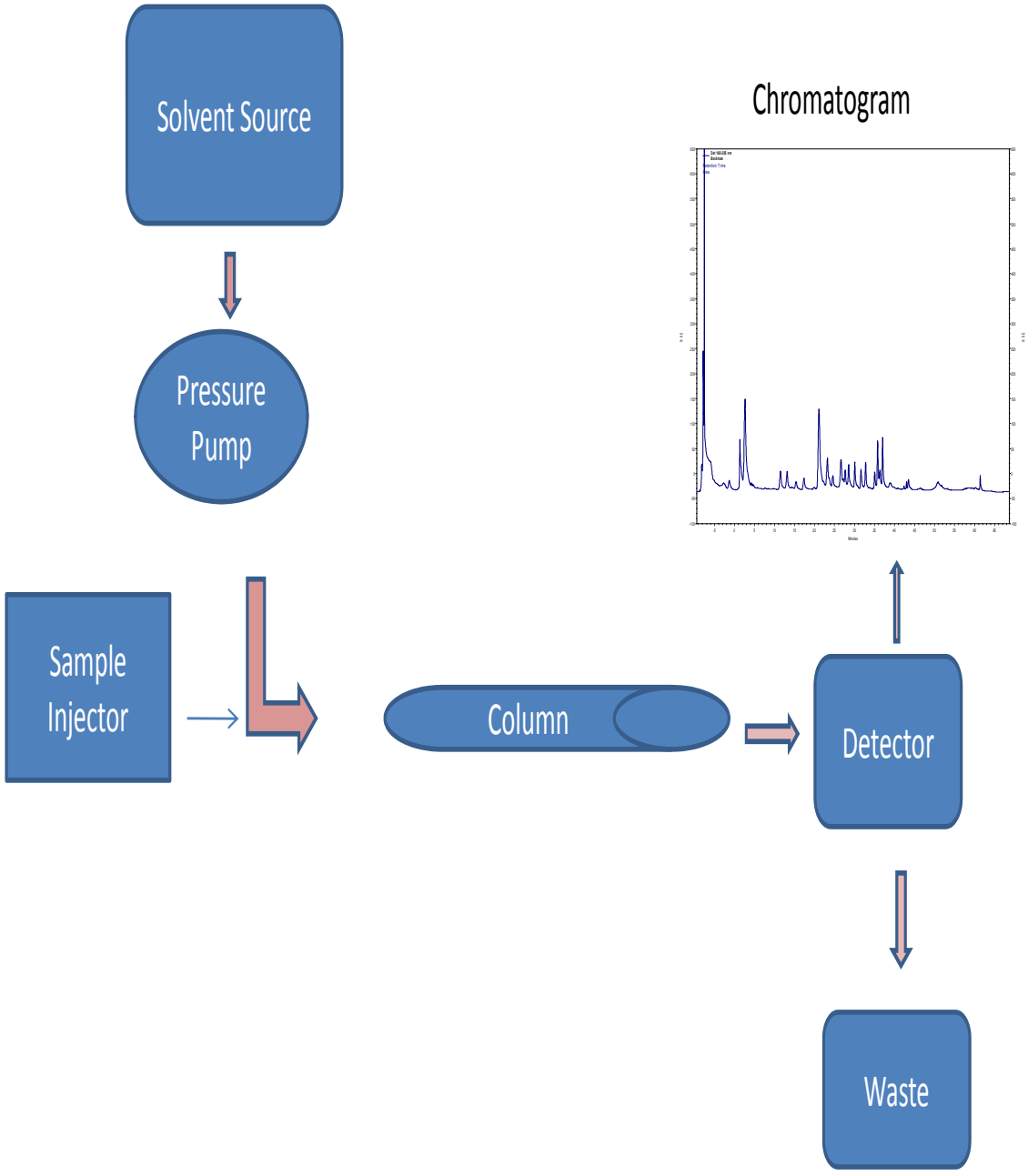

(Adapted from Clark et. al (106)).

Figure 30. Gradient method for DTNB and TNBSA with *E. coli* runs.

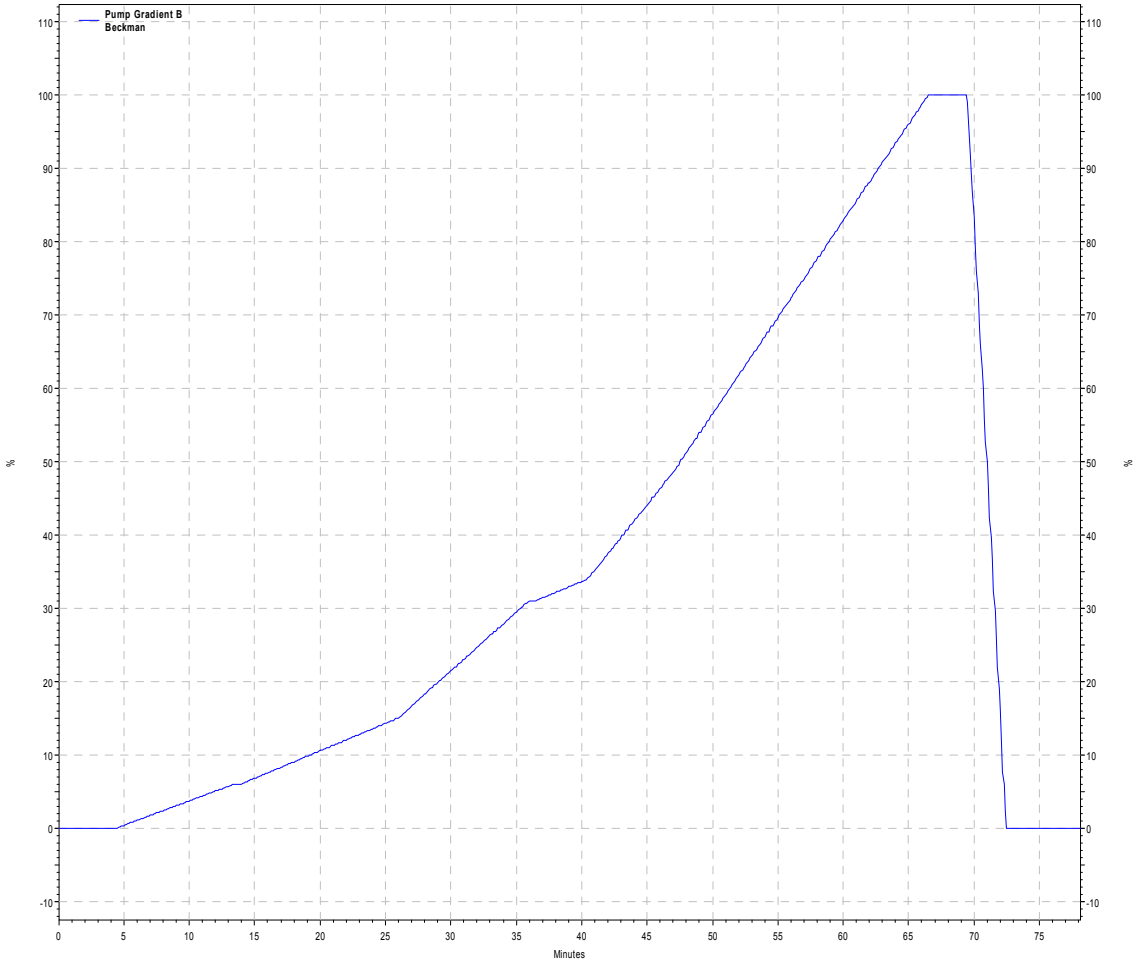

Time (min)	Module	Function	Value	Duration (Min)
0.51	Det 168	Autozero		
4.50	Pump	%B	6.00	9.00
14.00	Pump	%B	15.00	12.00
26.00	Pump	%B	31.00	10.00
36.50	Pump	%B	34.00	4.00
40.50	Pump	%B	48.50	6.50
47.00	Pump	%B	100.00	19.50
69.50	Pump	%B	0.00	3.00
78.00	Pump	Flow Rate	0.100	0.00
78.10	Det 168	Stop Data		
0.00				

Figure 31. DTNB with methanol chromatogram.

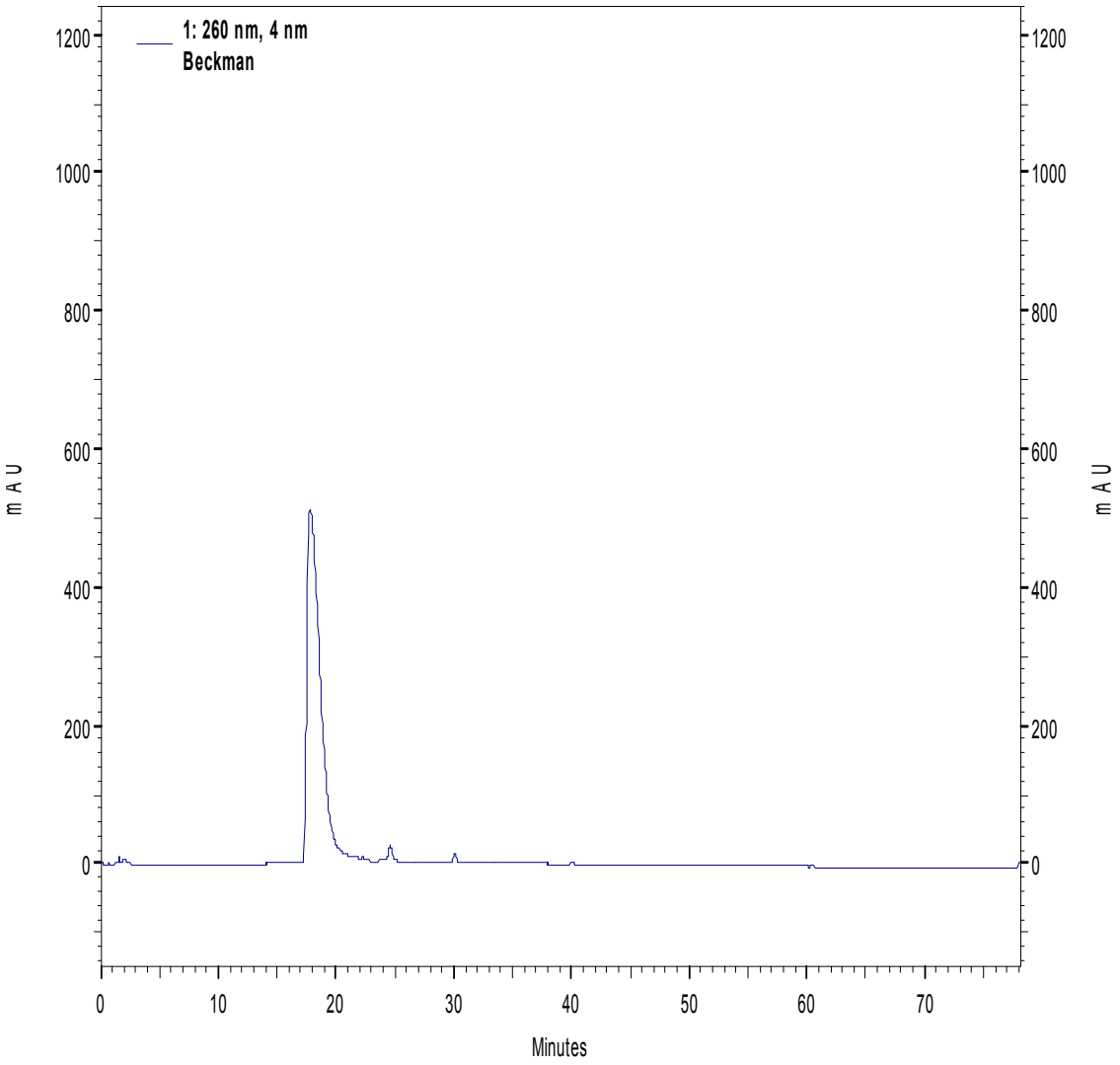

Peak at ~19 minutes is assumed to be DTNB peak.

Figure 32. TNBSA with methanol chromatogram.

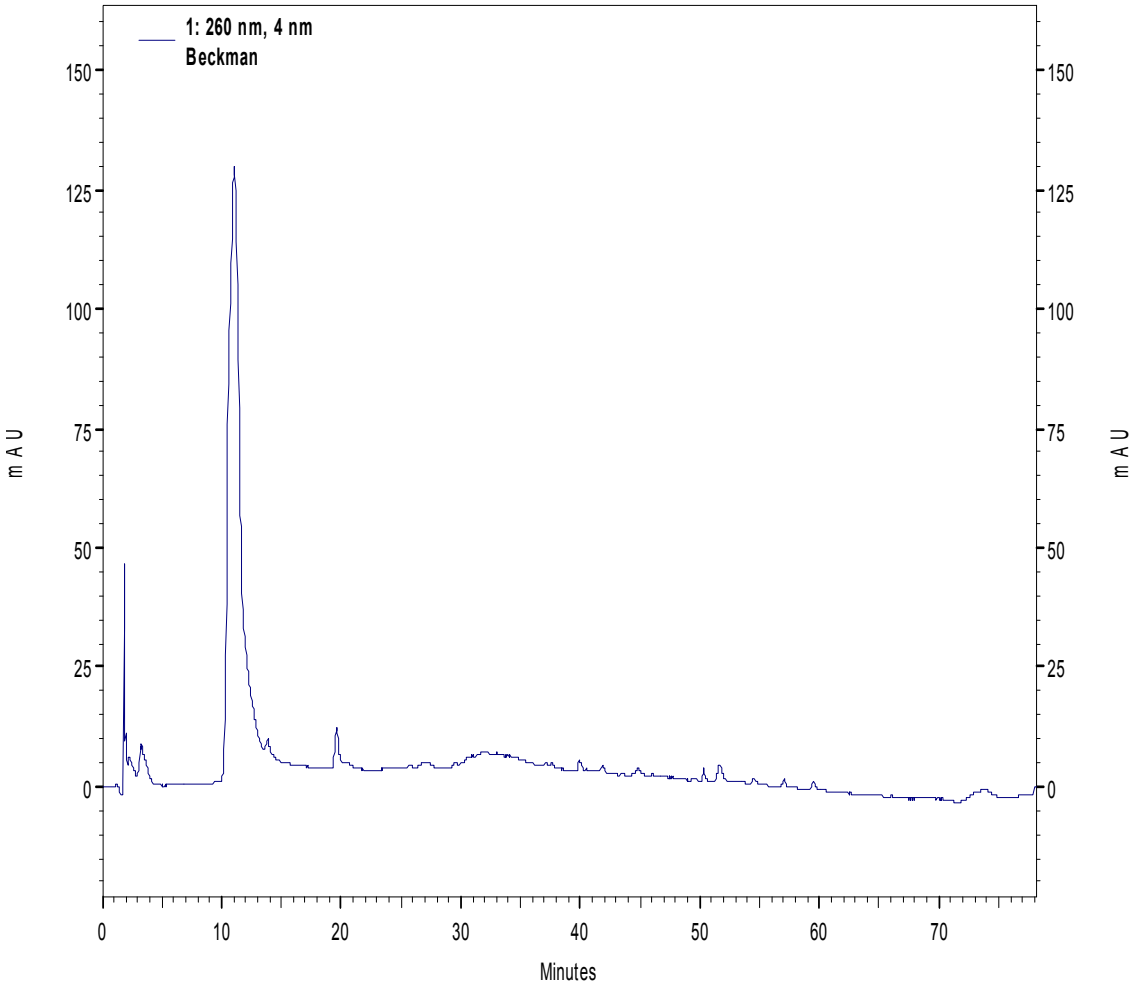

The major peak at 11-12 minutes is assumed to be the TNBSA alone peak, however, contamination is obvious as multiple other smaller peaks are observed.

Figure 33. Day 1 DTNB + *E. coli* control chromatogram.

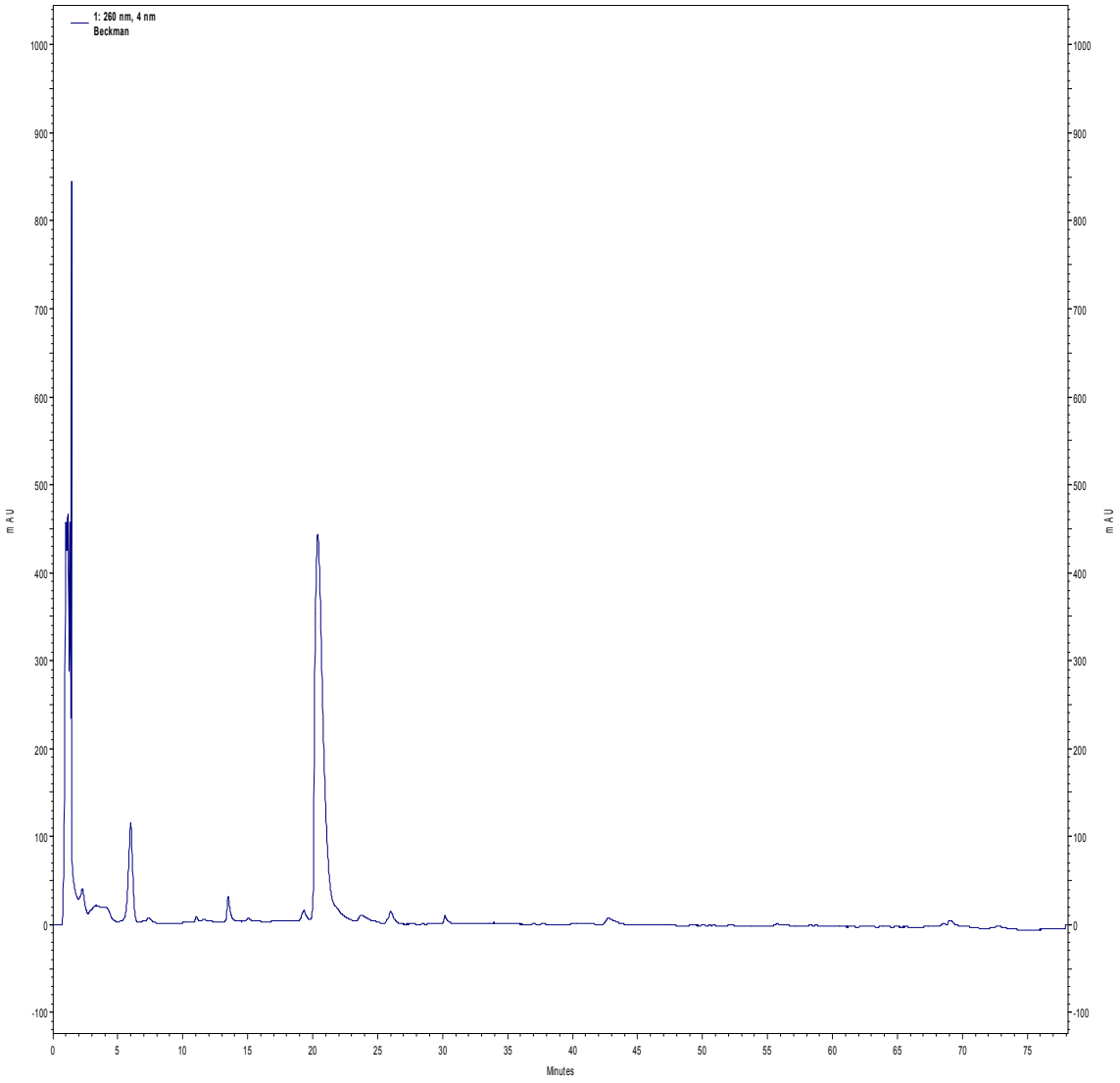

Most peaks are assumed to be caused by free thiol molecules from *E. coli* extracts not exposed to hydrogen peroxide adjusted with DTNB. Peak at ~19 minutes is assumed to be the peak eluted by DTNB alone.

Figure 34. Day 2 DTNB + *E. coli* control chromatogram.

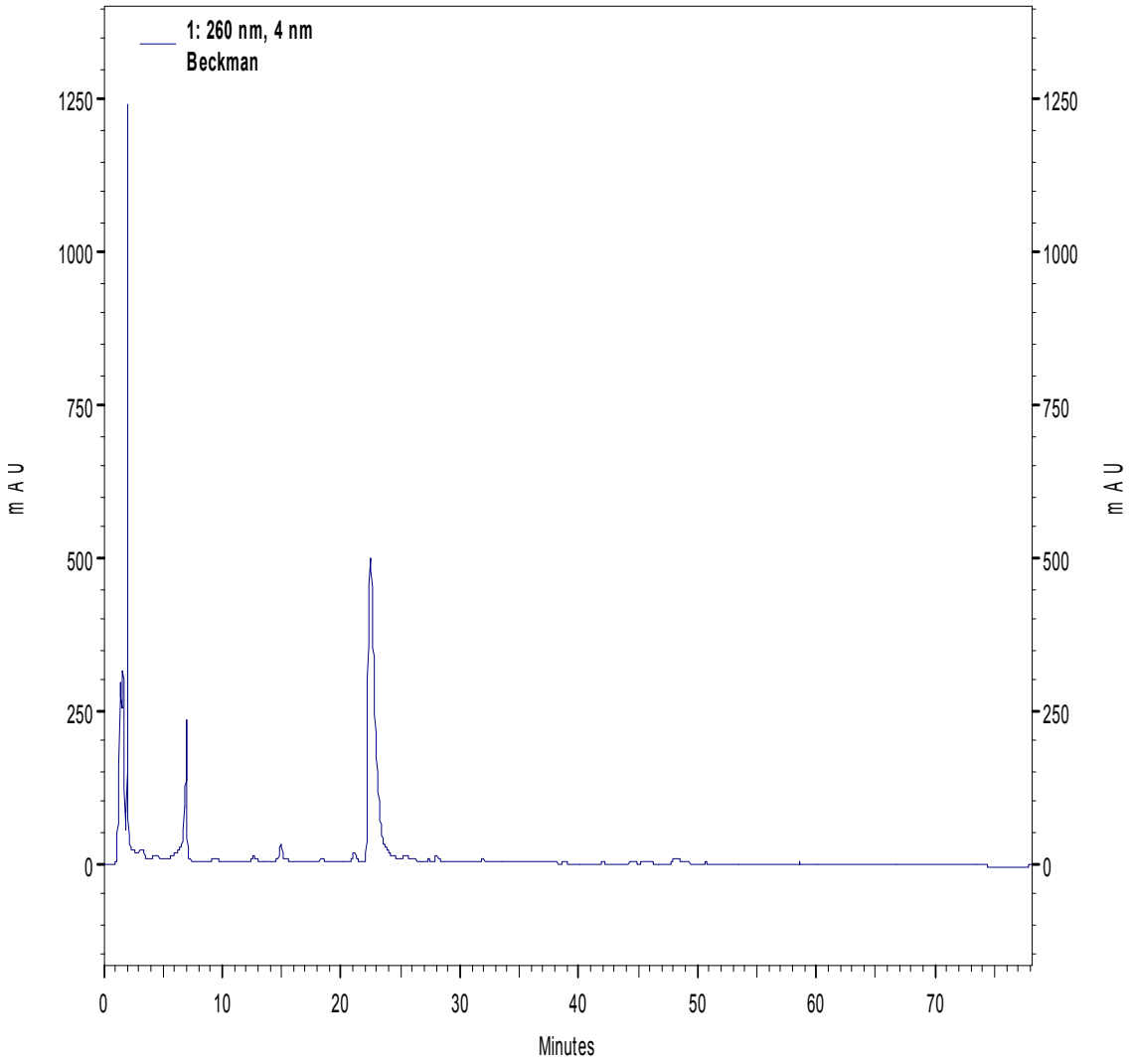

Most peaks are assumed to be caused by free thiol molecules from *E. coli* extracts not exposed to hydrogen peroxide adjusted with DTNB. Peak at ~19 minutes is assumed to be the peak eluted by DTNB alone.

Figure 35. Day 3 DTNB + *E. coli* control chromatogram.

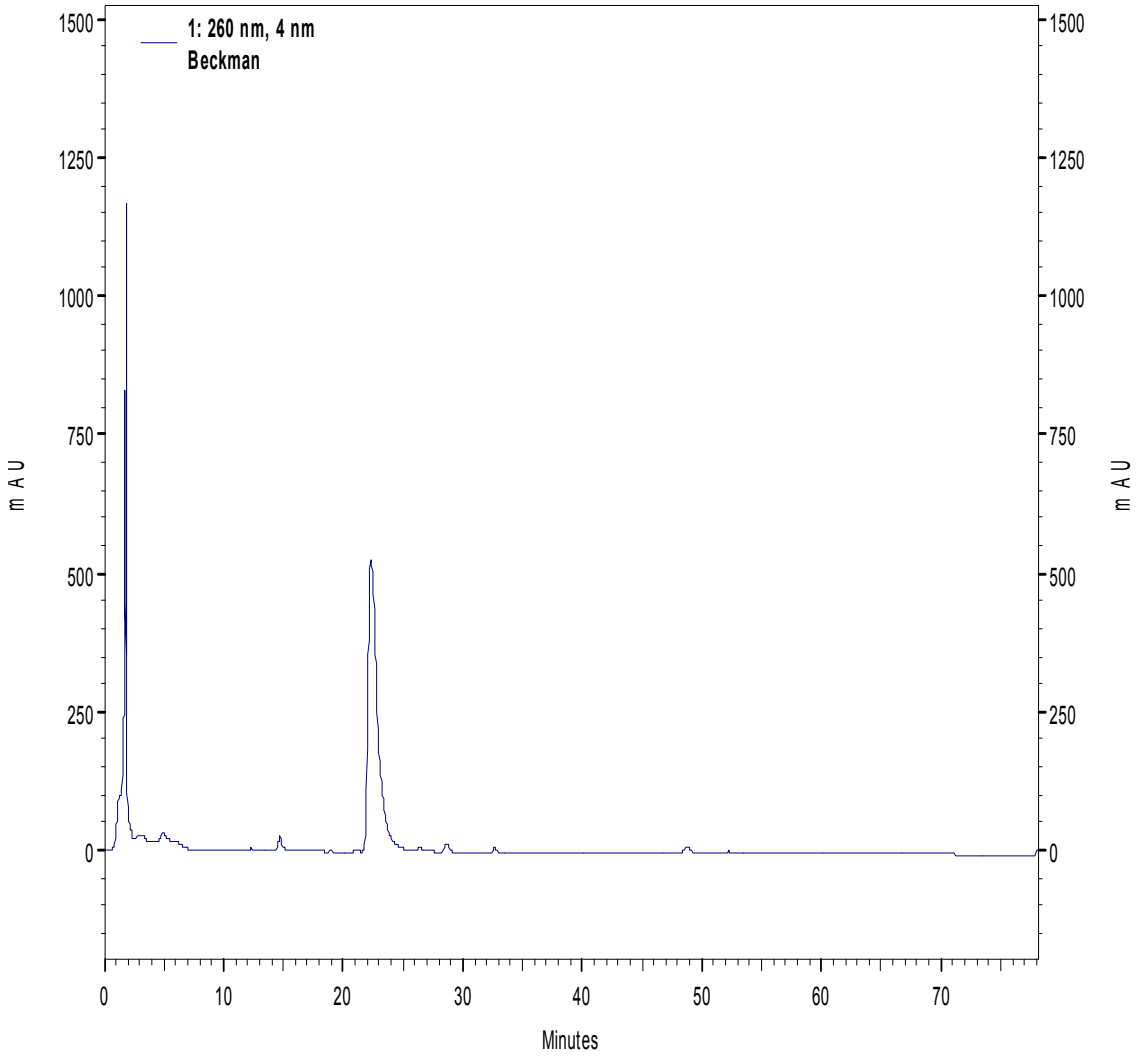

Most peaks are assumed to be caused by free thiol molecules from *E. coli* extracts not exposed to hydrogen peroxide adjusted with DTNB. Peak at ~19 minutes is assumed to be the peak eluted by DTNB alone.

Figure 36. Day 4 DTNB + *E. coli* control chromatogram.

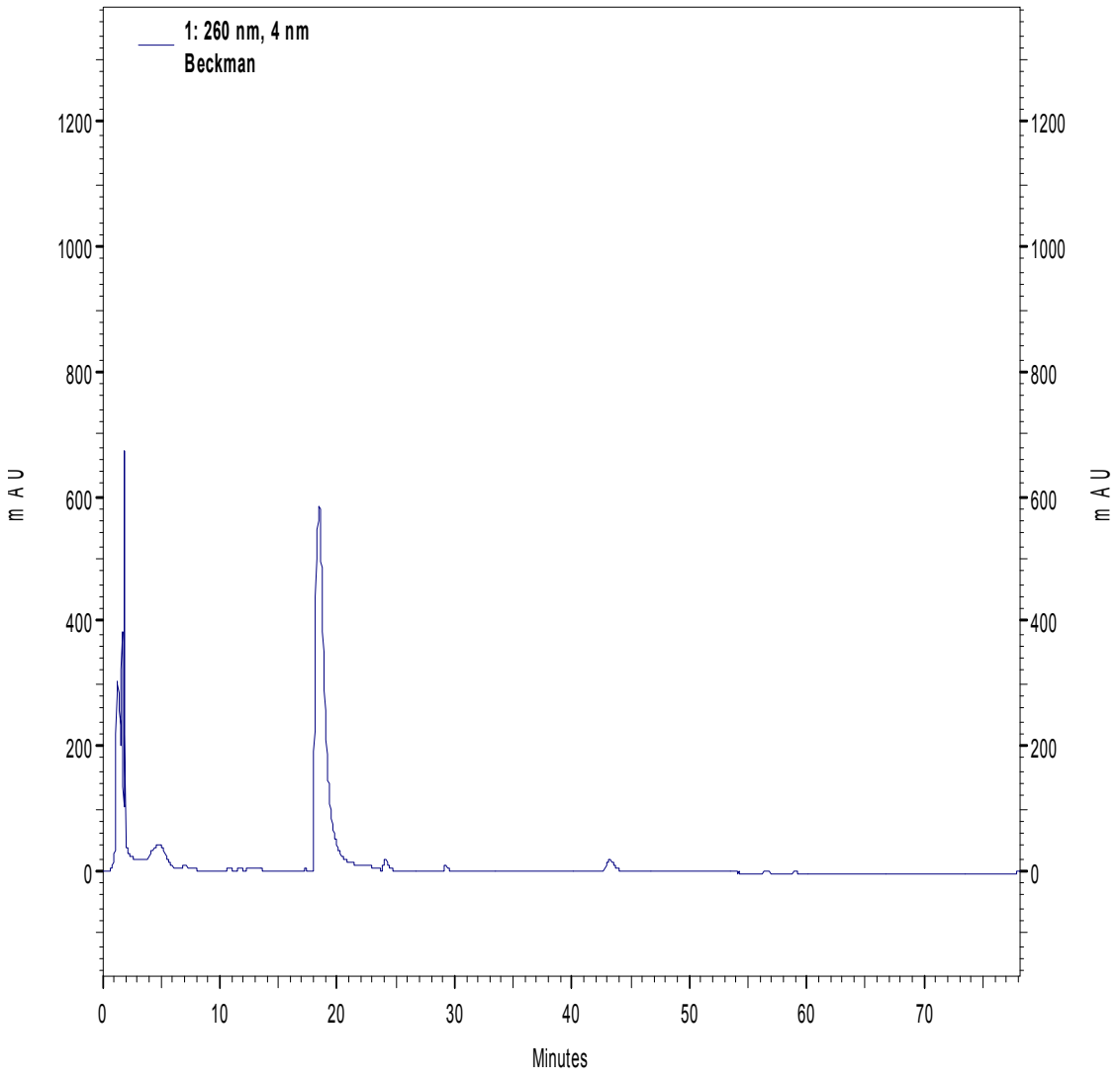

Most peaks are assumed to be caused by free thiol molecules from *E. coli* extracts not exposed to hydrogen peroxide adjusted with DTNB. Peak at ~19 minutes is assumed to be the peak eluted by DTNB alone.

Figure 37. Day 1 DTNB + *E. coli* treated with 5 min. hydrogen peroxide chromatogram.

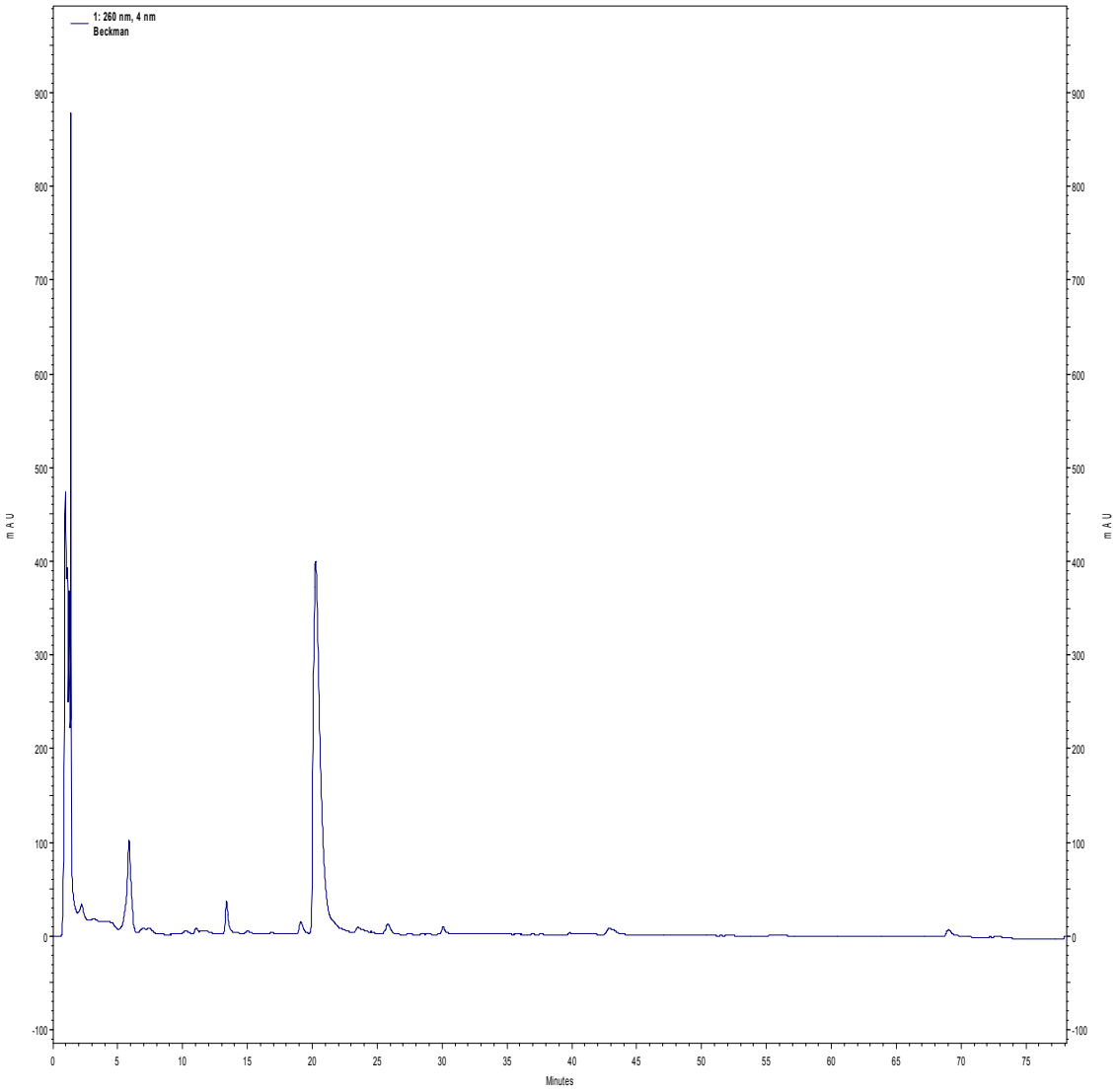

Most peaks are assumed to be caused by free thiol molecules from *E. coli* extracts exposed to 5 minutes of hydrogen peroxide adjusted with DTNB. Peak at ~19 minutes is assumed to be the peak eluted by DTNB alone.

Figure 38. Day 2 DTNB + *E. coli* treated with 5 min. hydrogen peroxide chromatogram.

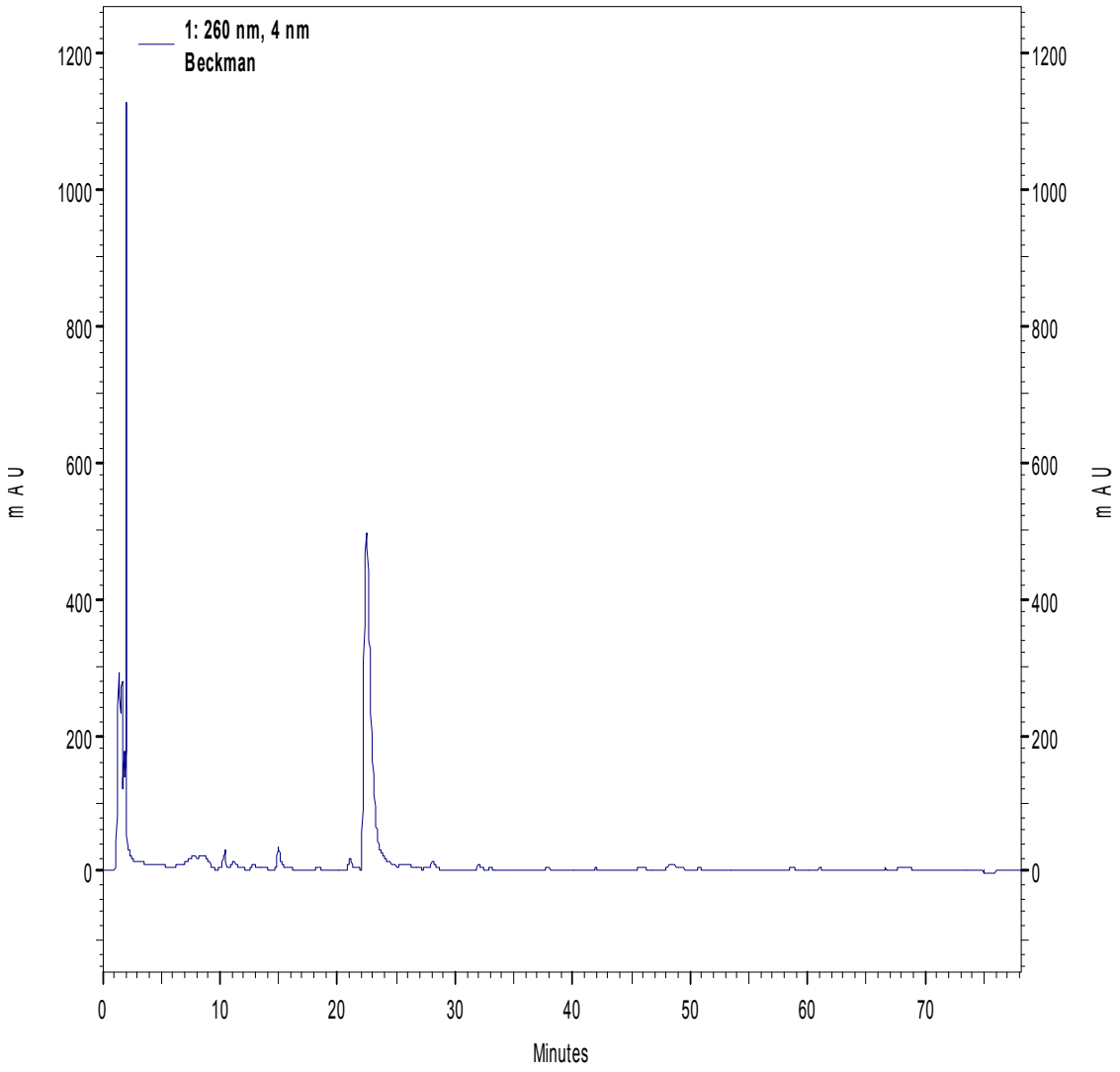

Most peaks are assumed to be caused by free thiol molecules from *E. coli* extracts exposed to 5 minutes of hydrogen peroxide adjusted with DTNB. Peak at ~19 minutes is assumed to be the peak eluted by DTNB alone.

Figure 39. Day 3 DTNB + *E. coli* treated with 5 min. hydrogen peroxide chromatogram.

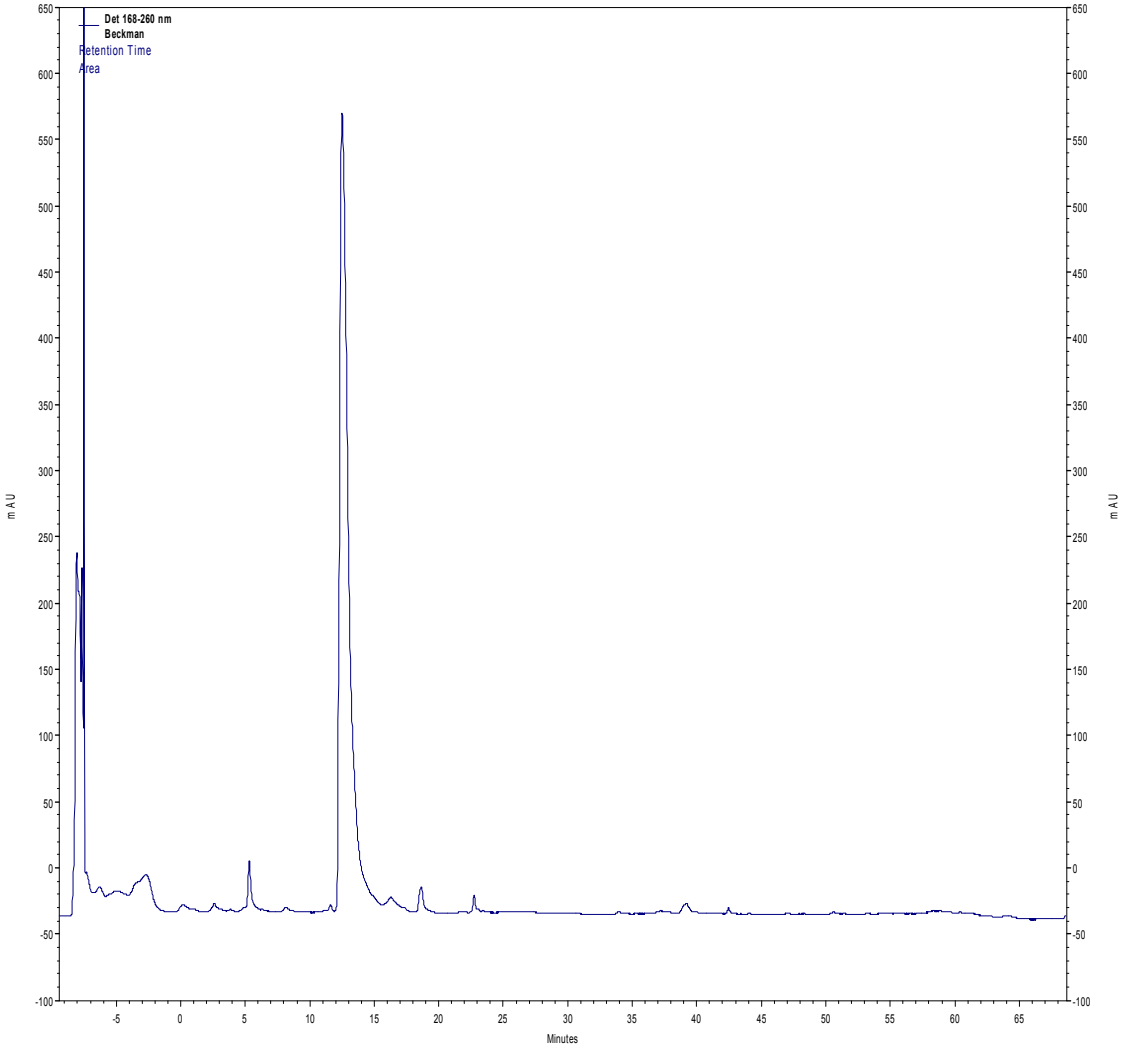

Most peaks are assumed to be caused by free thiol molecules from *E. coli* extracts exposed to 5 minutes of hydrogen peroxide adjusted with DTNB. Peak at ~19 minutes is assumed to be the peak eluted by DTNB alone.

Figure 40. Day 4 DTNB + *E. coli* treated with 5 min. of hydrogen peroxide chromatogram.

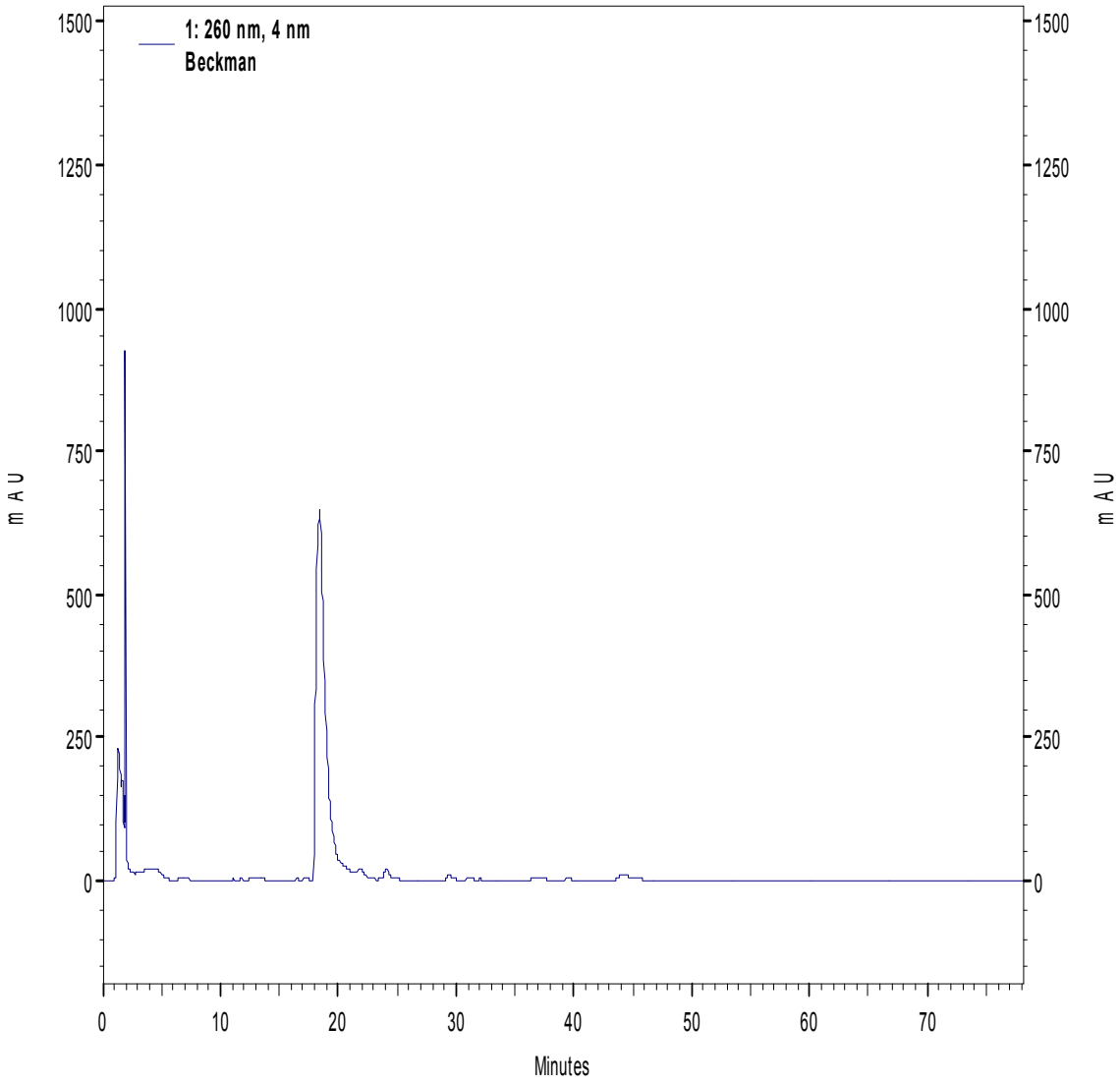

Most peaks are assumed to be caused by free thiol molecules from *E. coli* extracts exposed to 5 minutes of hydrogen peroxide adjusted with DTNB. Peak at ~19 minutes is assumed to be the peak eluted by DTNB alone.

Figure 41. Day 1 TNBSA + *E. coli* control chromatogram.

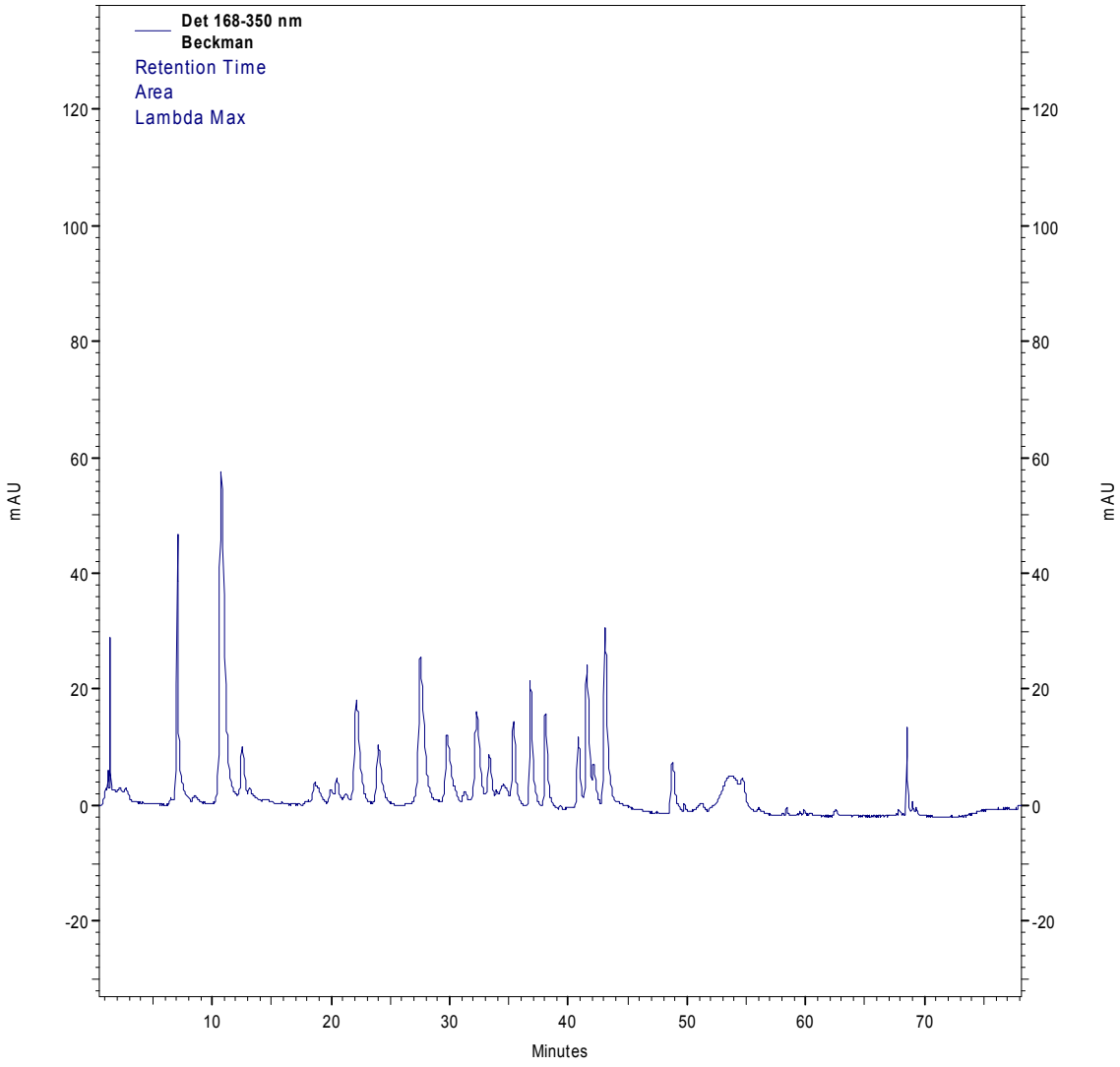

Most peaks are assumed to be caused by free amine molecules from *E. coli* extracts not exposed to hydrogen peroxide adjusted with TNBSA. Peak at ~11-12 minutes is assumed to be the peak eluted by TNBSA alone.

Figure 42. Day 2 TNBSA + *E. coli* control chromatogram.

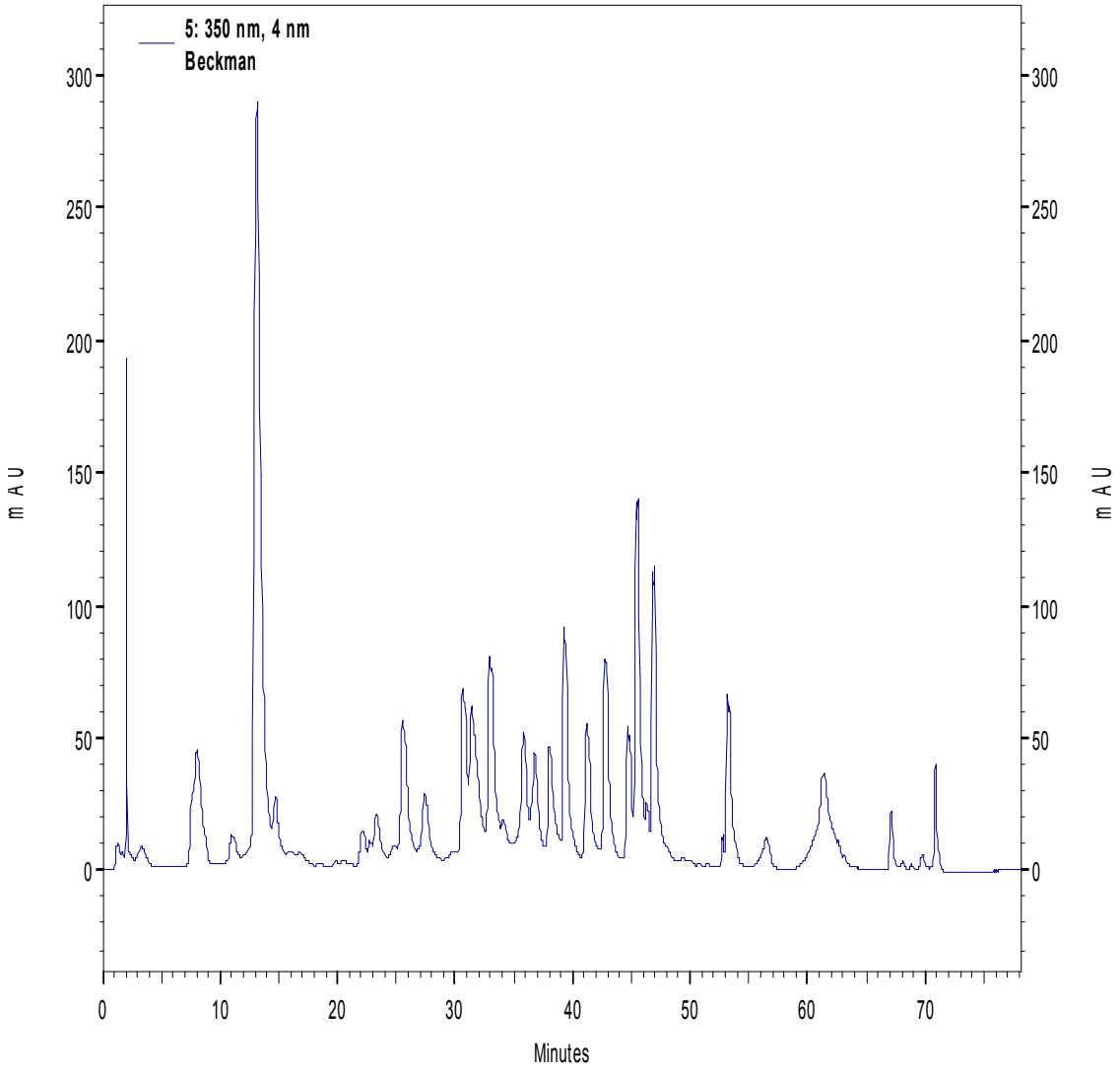

Most peaks are assumed to be caused by free amine molecules from *E. coli* extracts not exposed to hydrogen peroxide adjusted with TNBSA. Peak at ~11-12 minutes is assumed to be the peak eluted by TNBSA alone.

Figure 43. Day 3 TNBSA + *E. coli* control chromatogram.

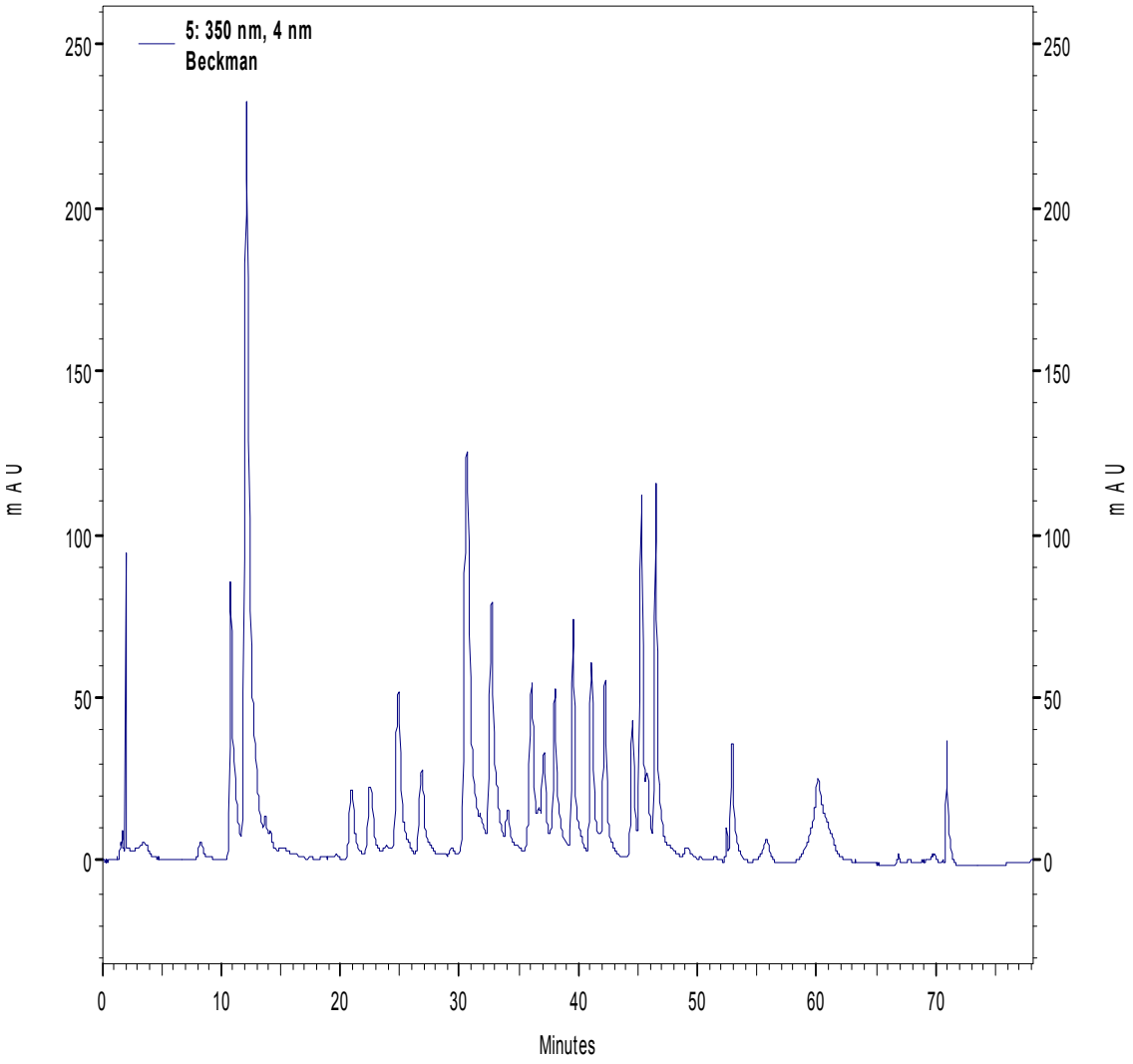

Most peaks are assumed to be caused by free amine molecules from *E. coli* extracts not exposed to hydrogen peroxide adjusted with TNBSA. Peak at ~11-12 minutes is assumed to be the peak eluted by TNBSA alone.

Figure 44. Day 4 TNBSA + *E. coli* control chromatogram.

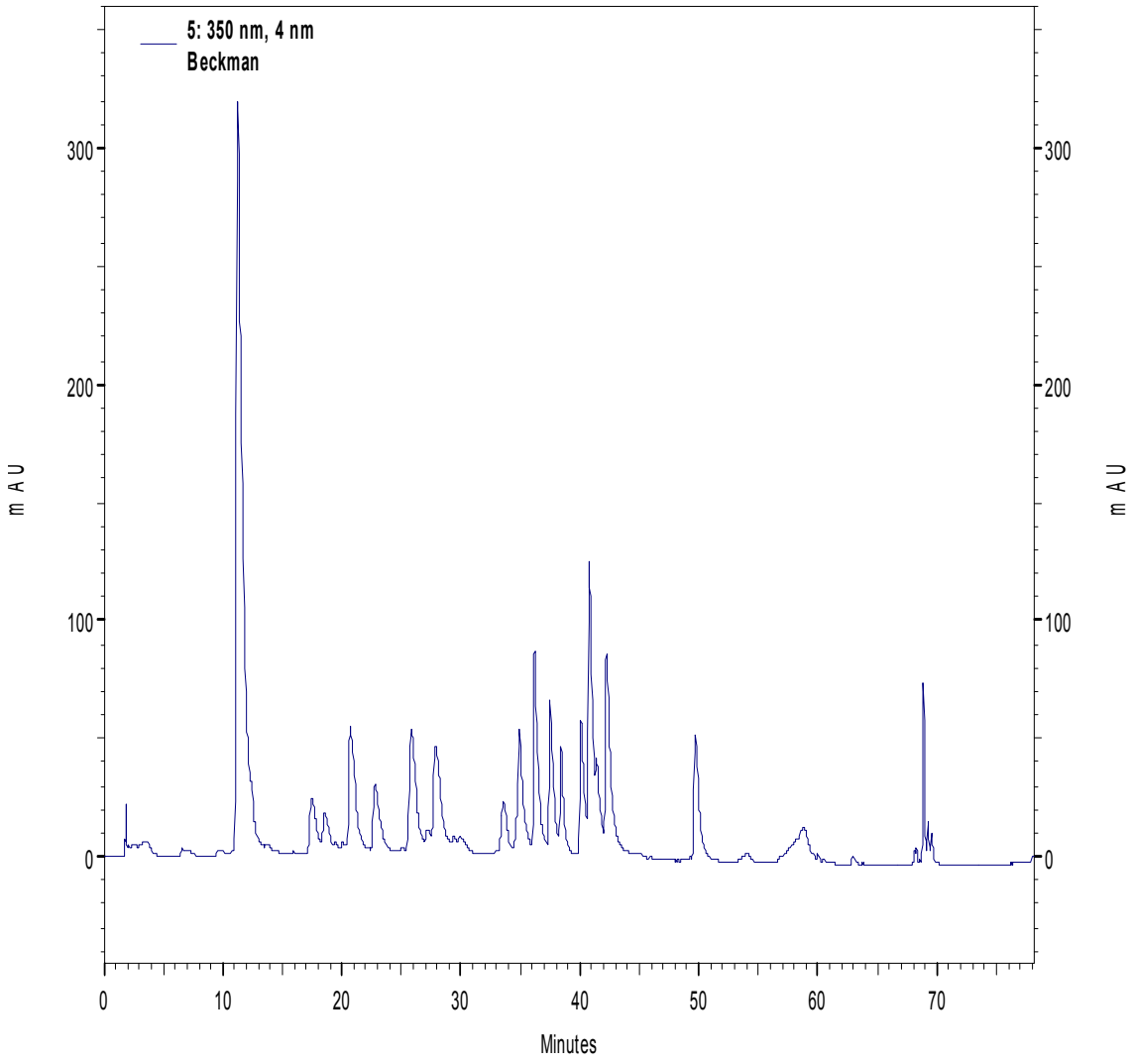

Most peaks are assumed to be caused by free amine molecules from *E. coli* extracts not exposed to hydrogen peroxide adjusted with TNBSA. Peak at ~11-12 minutes is assumed to be the peak eluted by TNBSA alone.

Figure 45. Day 1 TNBSA + *E. coli* treated with 5 min. of hydrogen peroxide chromatogram.

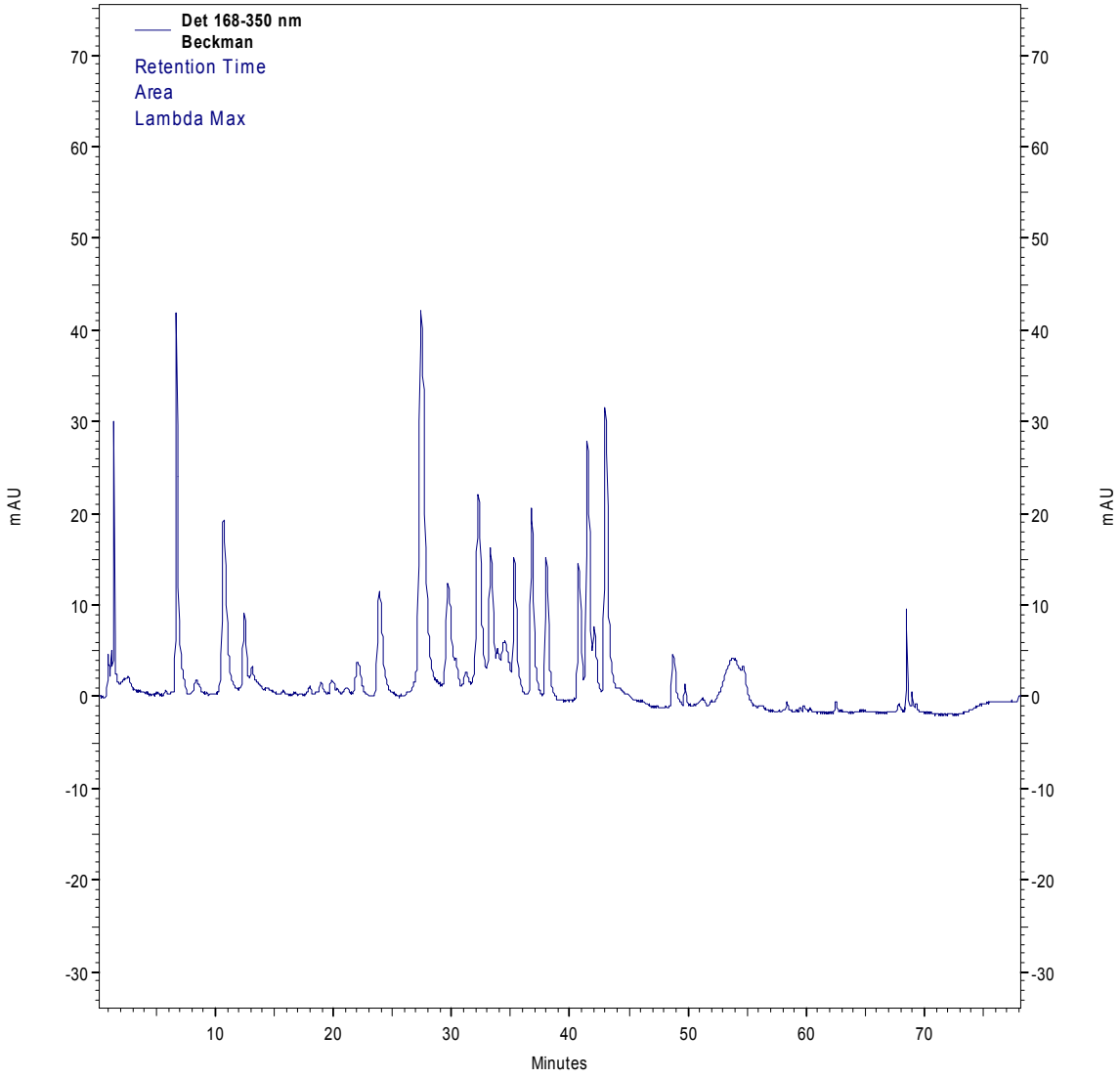

Most peaks are assumed to be caused by free amine molecules from *E. coli* extracts exposed to 5 minutes of hydrogen peroxide adjusted with TNBSA. Peak at ~11-12 minutes is assumed to be the peak eluted by TNBSA alone.

Figure 46. Day 2 TNBSA + *E. coli* treated with 5 min. of hydrogen peroxide chromatogram.

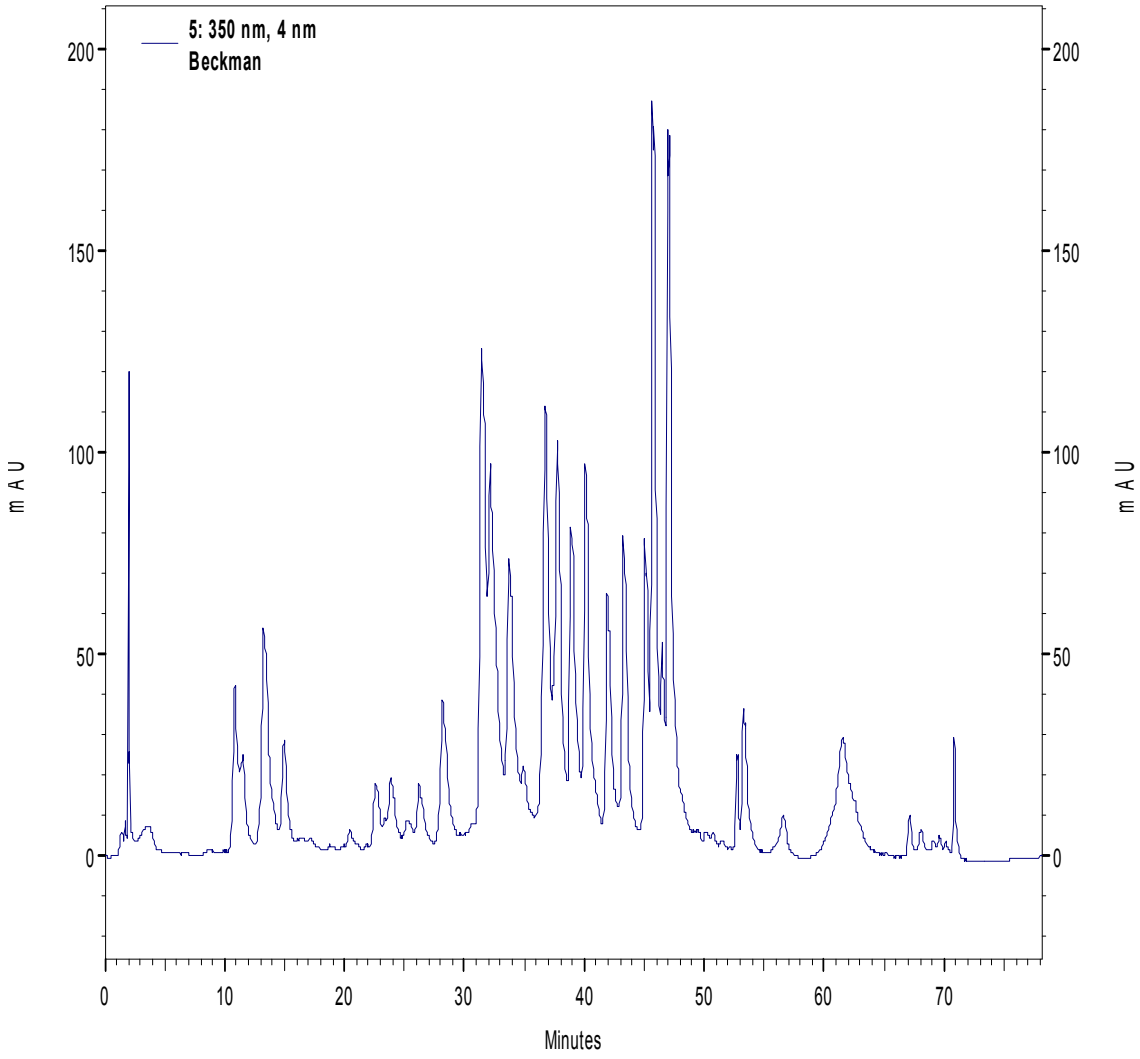

Most peaks are assumed to be caused by free amine molecules from *E. coli* extracts exposed to 5 minutes of hydrogen peroxide adjusted with TNBSA. Peak at ~11-12 minutes is assumed to be the peak eluted by TNBSA alone.

Figure 47. Day 3 TNBSA + *E. coli* treated with 5 min. of hydrogen peroxide chromatogram.

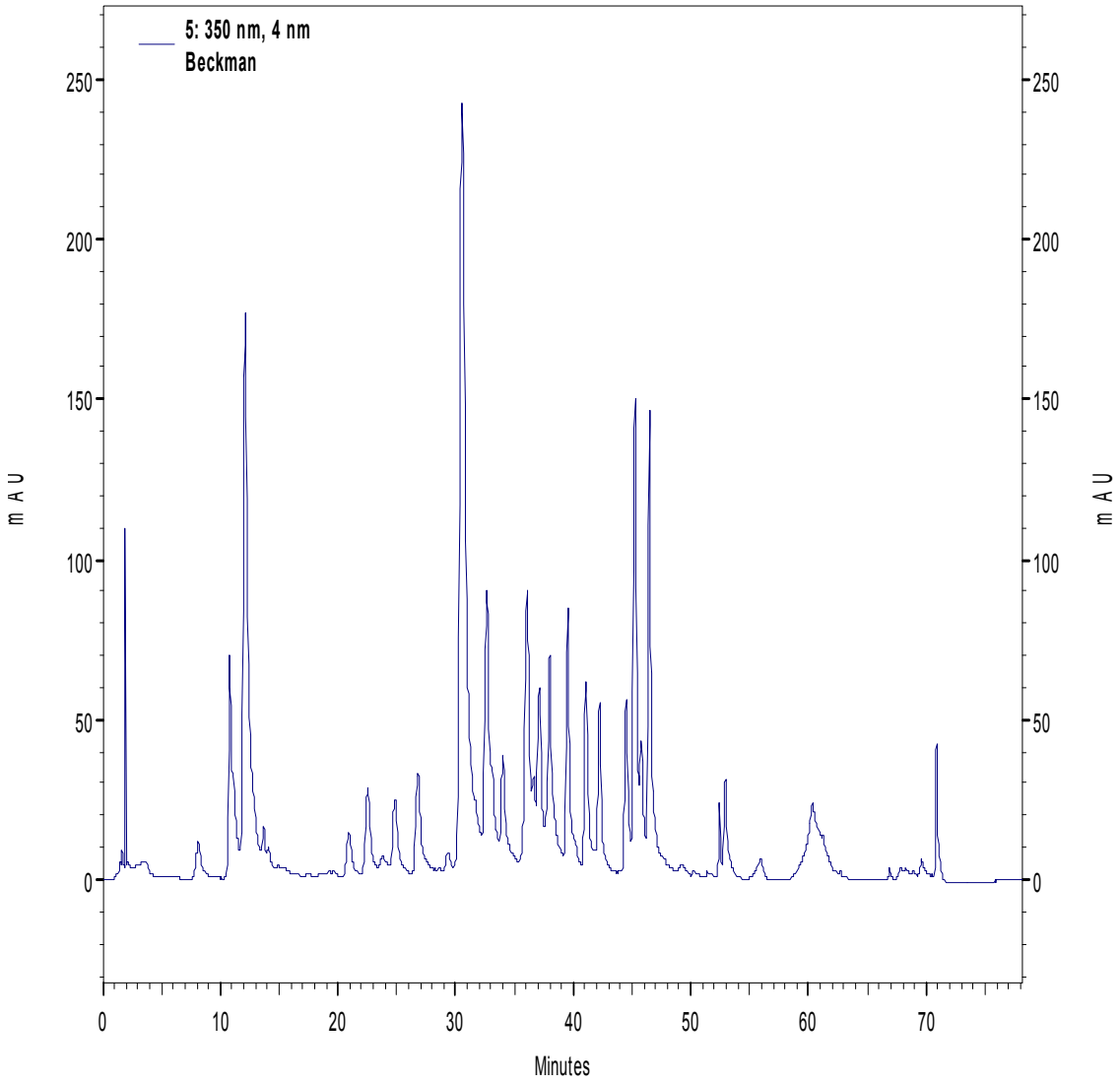

Most peaks are assumed to be caused by free amine molecules from *E. coli* extracts exposed to 5 minutes of hydrogen peroxide adjusted with TNBSA. Peak at ~11-12 minutes is assumed to be the peak eluted by TNBSA alone.

Figure 48. Day 4 TNBSA + *E. coli* treated with 5 min. of hydrogen peroxide chromatogram.

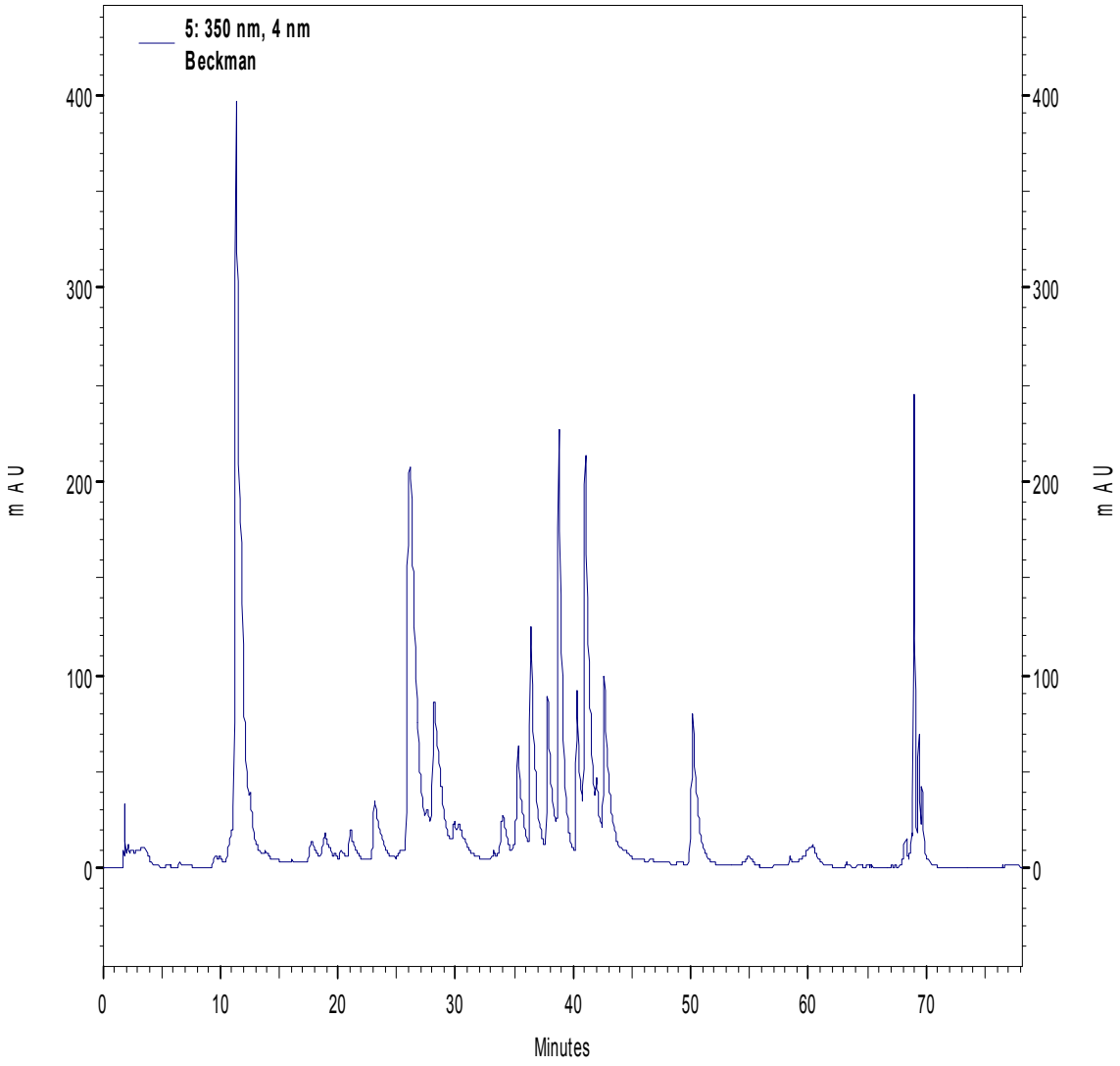

Most peaks are assumed to be caused by free amine molecules from *E. coli* extracts exposed to 5 minutes of hydrogen peroxide adjusted with TNBSA. Peak at ~11-12 minutes is assumed to be the peak eluted by TNBSA alone.

Figure 49. Day 1, sample 1 50:50 10 mM serine: 10 mM cysteine mix with TNBSA chromatogram.

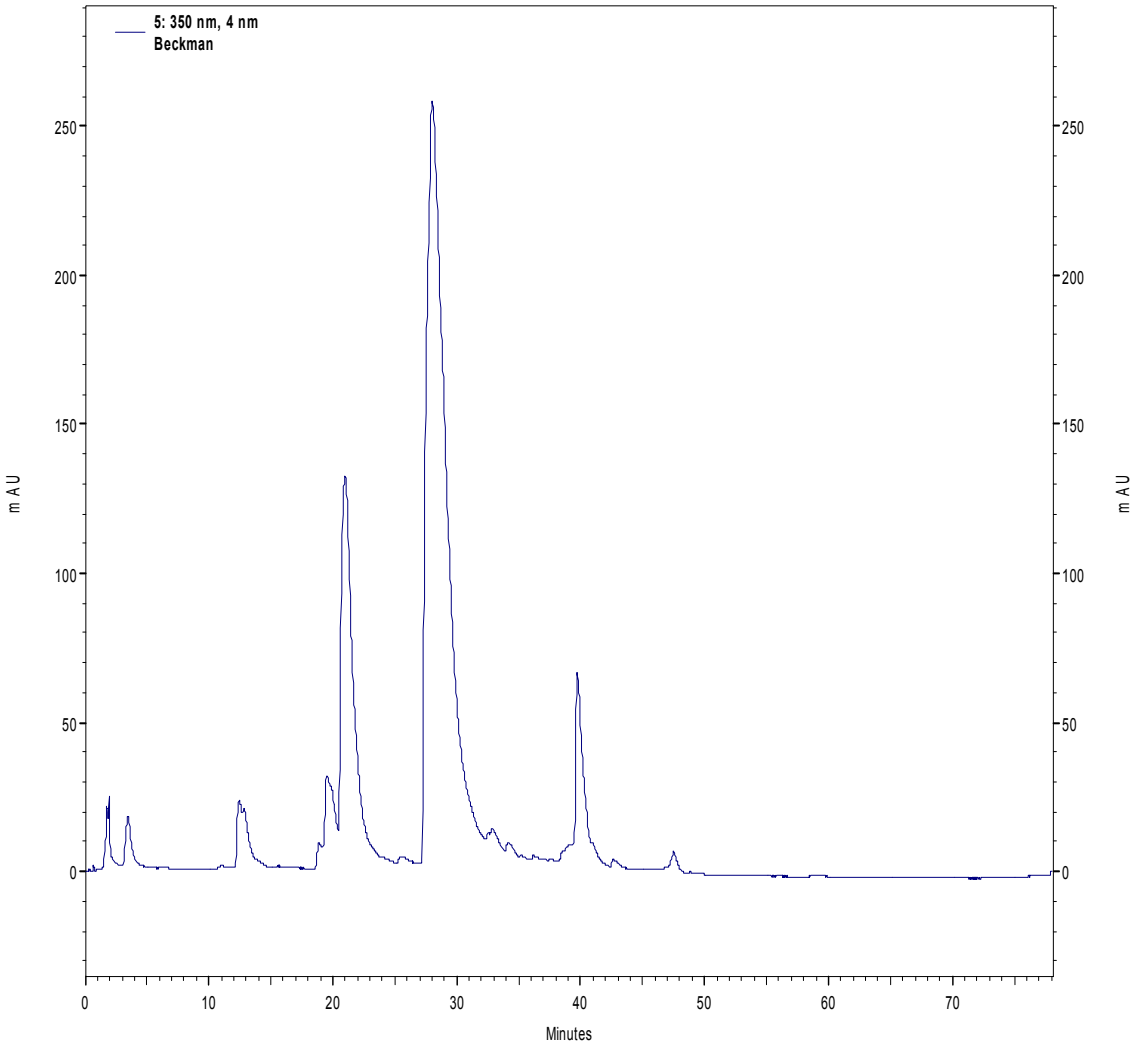

Peak at ~19 minutes is assumed to be caused by the amino acid serine adjusted with TNBSA. Peak at ~29 minutes is assumed to be caused by the amino acid cysteine adjusted with TNBSA. Peak at ~11-12 minutes is assumed to be the peak eluted by TNBSA alone. Other peaks are caused by unknown molecules.

Figure 50. Day 1, sample 2 50:50 10 mM serine: 10 mM cysteine mix with TNBSA chromatogram.

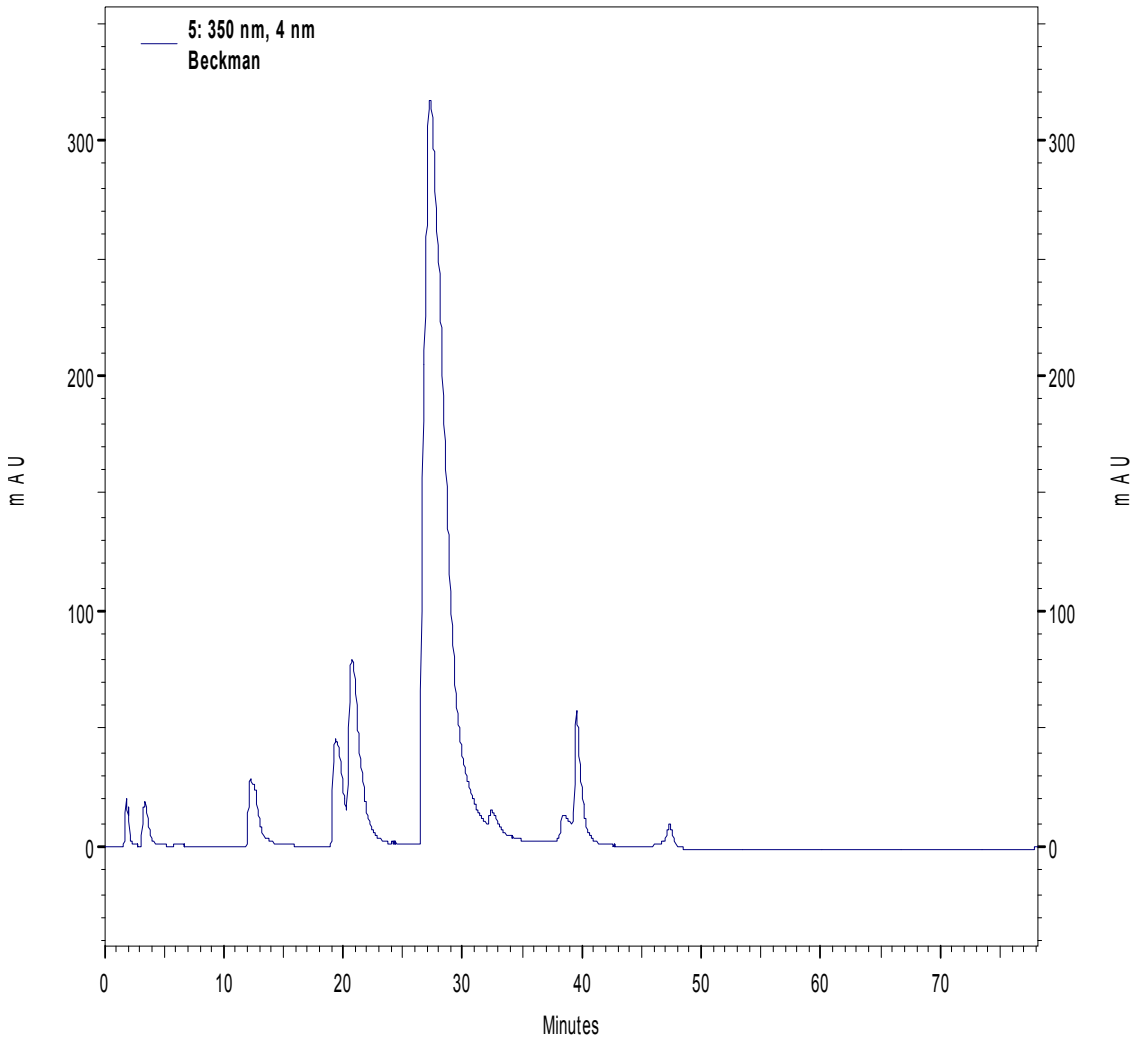

Peak at ~19 minutes is assumed to be caused by the amino acid serine adjusted with TNBSA. Peak at ~29 minutes is assumed to be caused by the amino acid cysteine adjusted with TNBSA. Peak at ~11-12 minutes is assumed to be the peak eluted by TNBSA alone. Other peaks are caused by unknown molecules.

Figure 51. Day 1, sample 3 50:50 10 mM serine: 10 mM cysteine mix with TNBSA chromatogram.

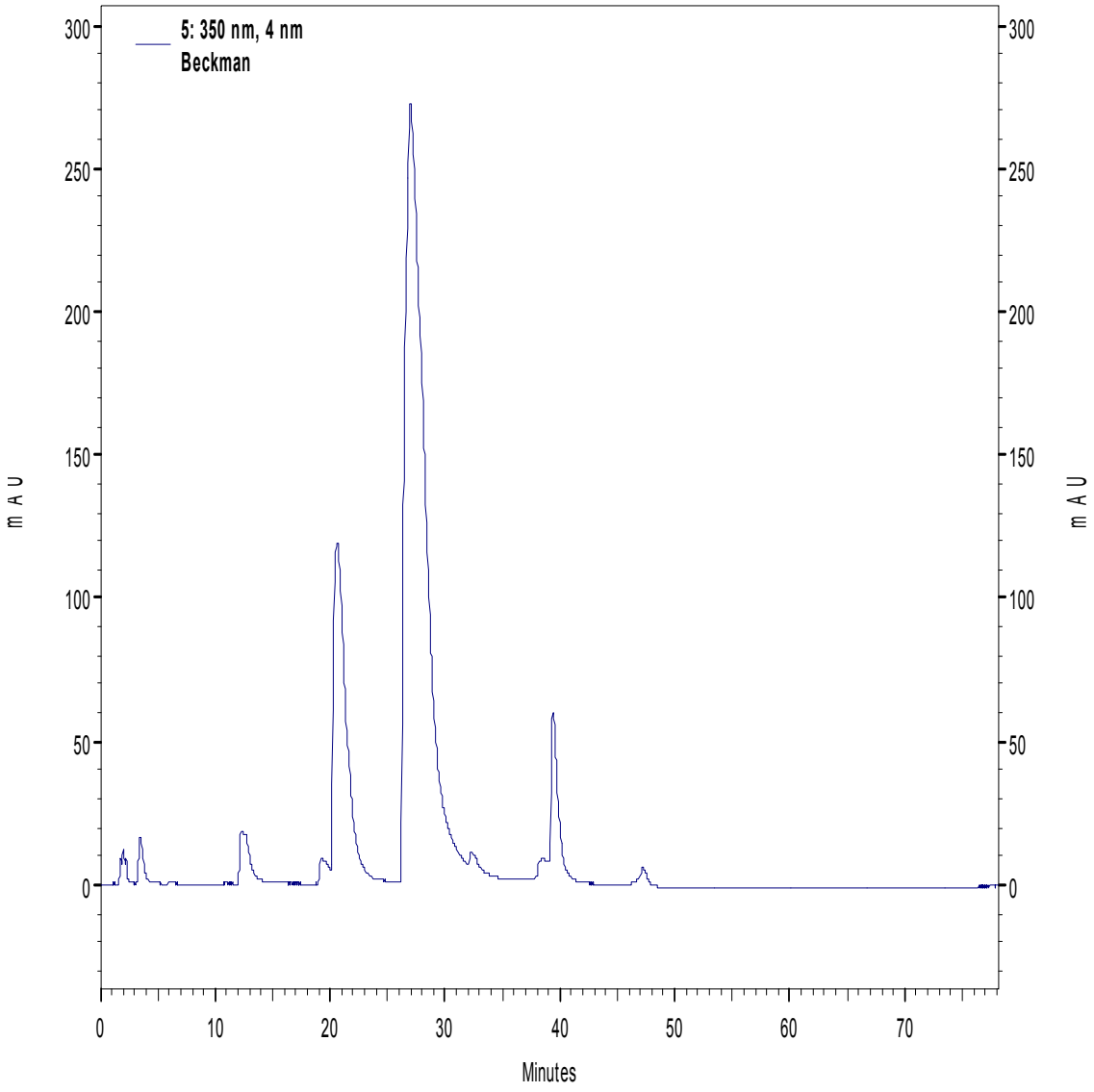

Peak at ~19 minutes is assumed to be caused by the amino acid serine adjusted with TNBSA. Peak at ~29 minutes is assumed to be caused by the amino acid cysteine adjusted with TNBSA. Peak at ~11-12 minutes is assumed to be the peak eluted by TNBSA alone. Other peaks are caused by unknown molecules.

Figure 52. Day 2, sample 1 50:50 10 mM serine: 10 mM cysteine mix with TNBSA chromatogram.

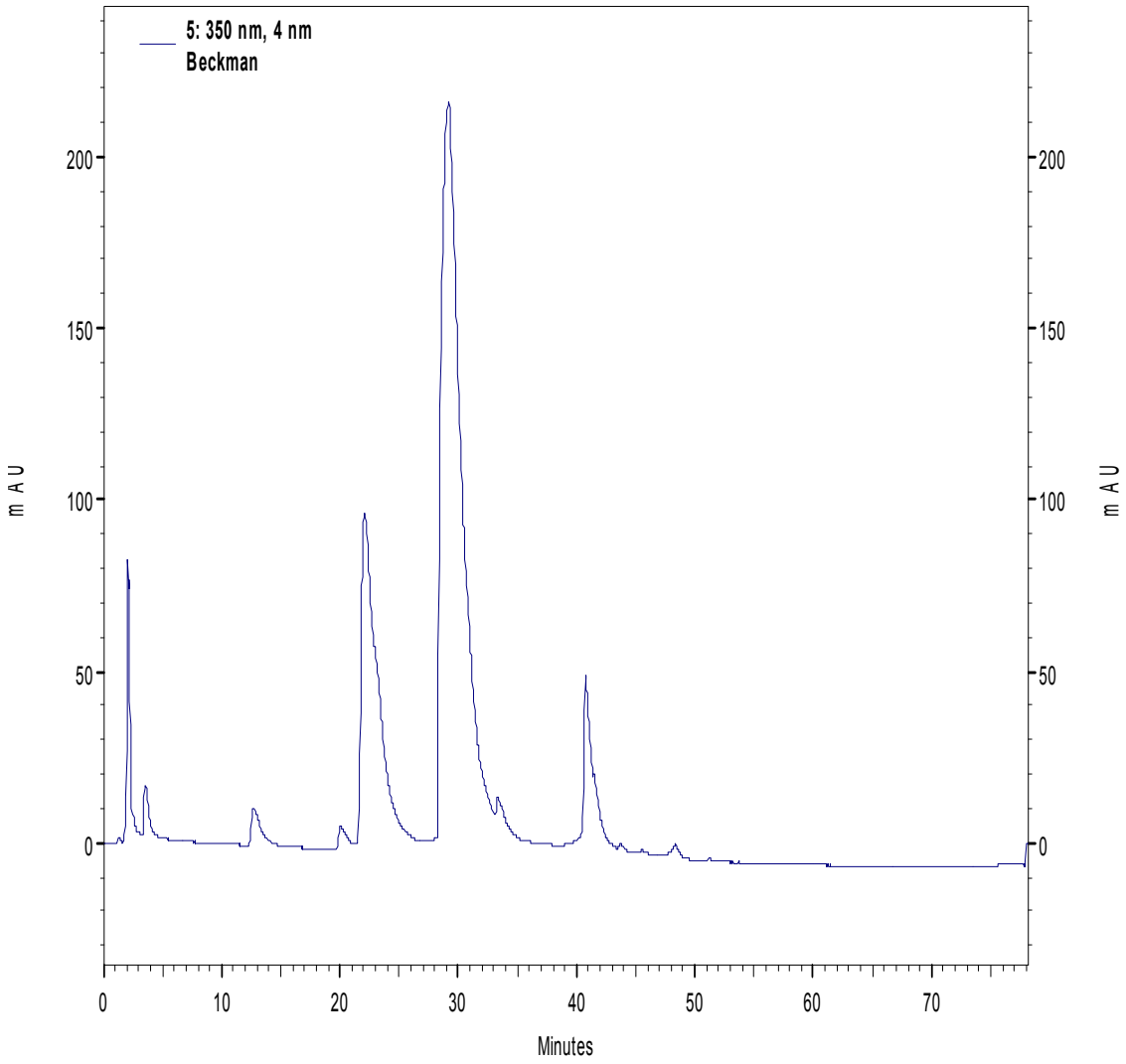

Peak at ~19 minutes is assumed to be caused by the amino acid serine adjusted with TNBSA. Peak at ~29 minutes is assumed to be caused by the amino acid cysteine adjusted with TNBSA. Peak at ~11-12 minutes is assumed to be the peak eluted by TNBSA alone. Other peaks are caused by unknown molecules.

Figure 53. Day 2, sample 2 50:50 10 mM serine: 10 mM cysteine mix with TNBSA chromatogram.

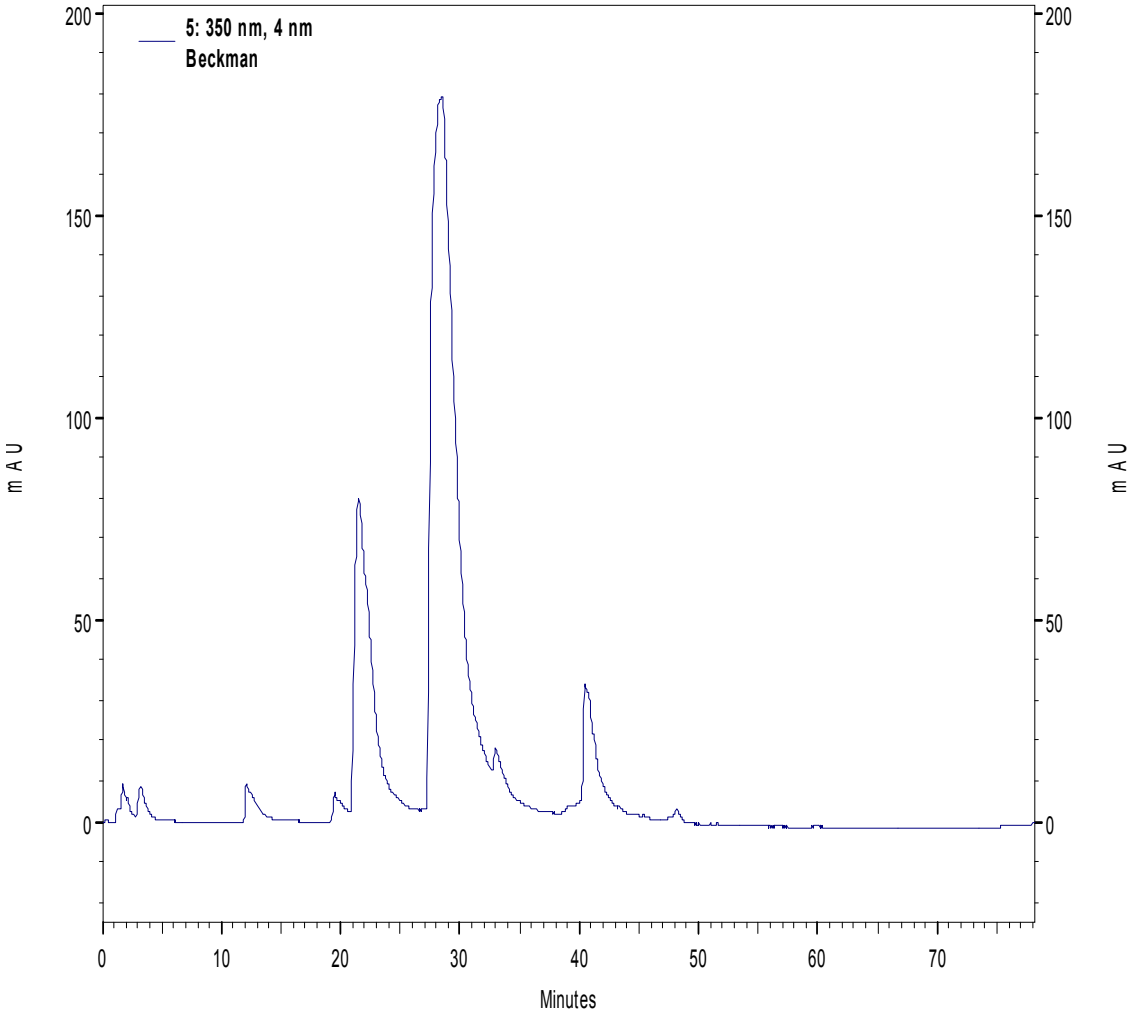

Peak at ~19 minutes is assumed to be caused by the amino acid serine adjusted with TNBSA. Peak at ~29 minutes is assumed to be caused by the amino acid cysteine adjusted with TNBSA. Peak at ~11-12 minutes is assumed to be the peak eluted by TNBSA alone. Other peaks are caused by unknown molecules.

Figure 54. Day 2, sample 3 50:50 10 mM serine: 10 mM cysteine mix with TNBSA chromatogram.

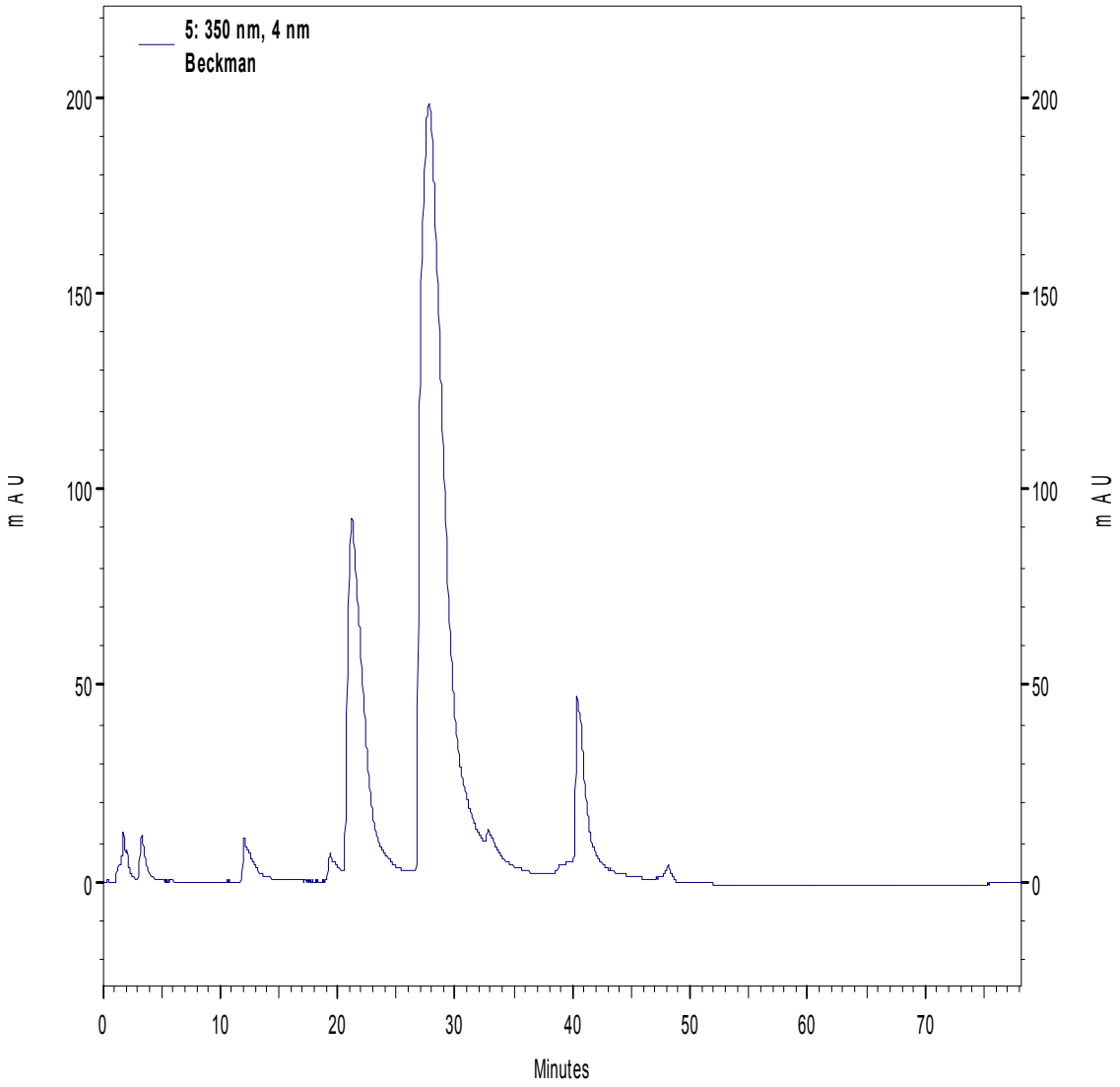

Peak at ~19 minutes is assumed to be caused by the amino acid serine adjusted with TNBSA. Peak at ~29 minutes is assumed to be caused by the amino acid cysteine adjusted with TNBSA. Peak at ~11-12 minutes is assumed to be the peak eluted by TNBSA alone. Other peaks are caused by unknown molecules.

Figure 55. Day 3, sample 1 50:50 10 mM serine: 10 mM cysteine mix with TNBSA chromatogram.

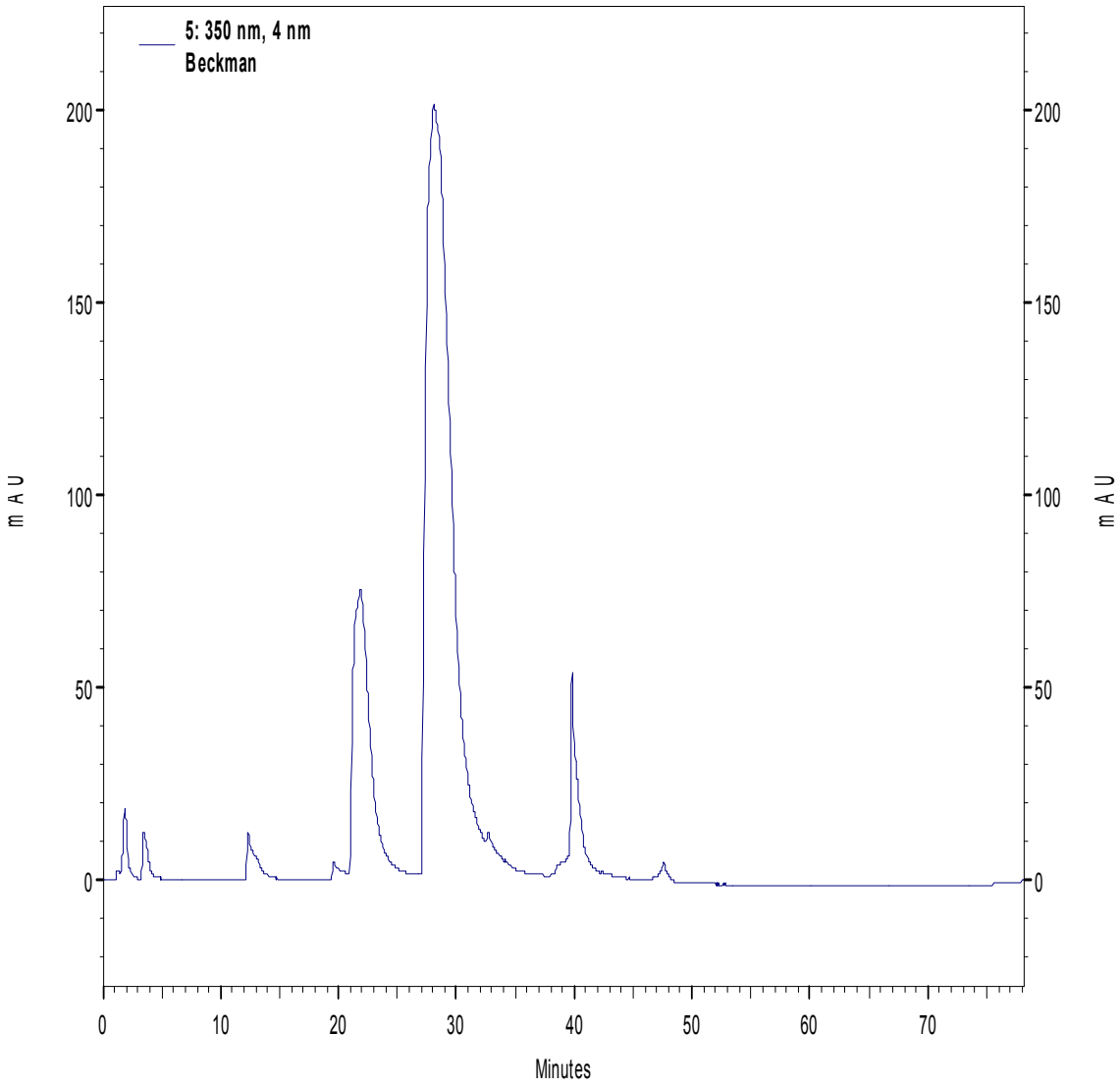

Peak at ~19 minutes is assumed to be caused by the amino acid serine adjusted with TNBSA. Peak at ~29 minutes is assumed to be caused by the amino acid cysteine adjusted with TNBSA. Peak at ~11-12 minutes is assumed to be the peak eluted by TNBSA alone. Other peaks are caused by unknown molecules.

Figure 56. Day 3, sample 2 50:50 10 mM serine: 10 mM cysteine mix with TNBSA chromatogram.

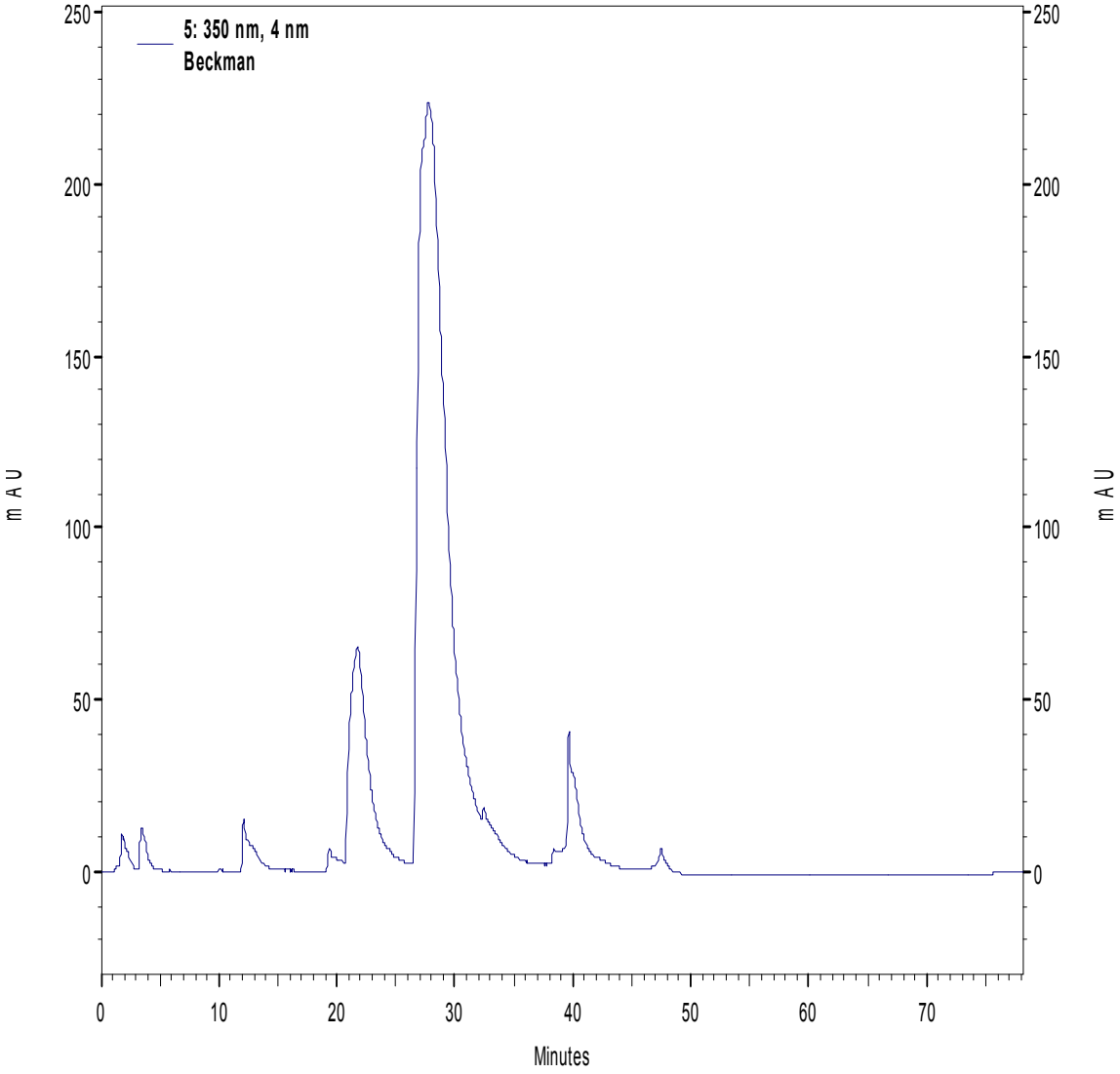

Peak at ~19 minutes is assumed to be caused by the amino acid serine adjusted with TNBSA. Peak at ~29 minutes is assumed to be caused by the amino acid cysteine adjusted with TNBSA. Peak at ~11-12 minutes is assumed to be the peak eluted by TNBSA alone. Other peaks are caused by unknown molecules.

Figure 57. Day 3, sample 3 50:50 10 mM serine: 10 mM cysteine mix with TNBSA chromatogram.

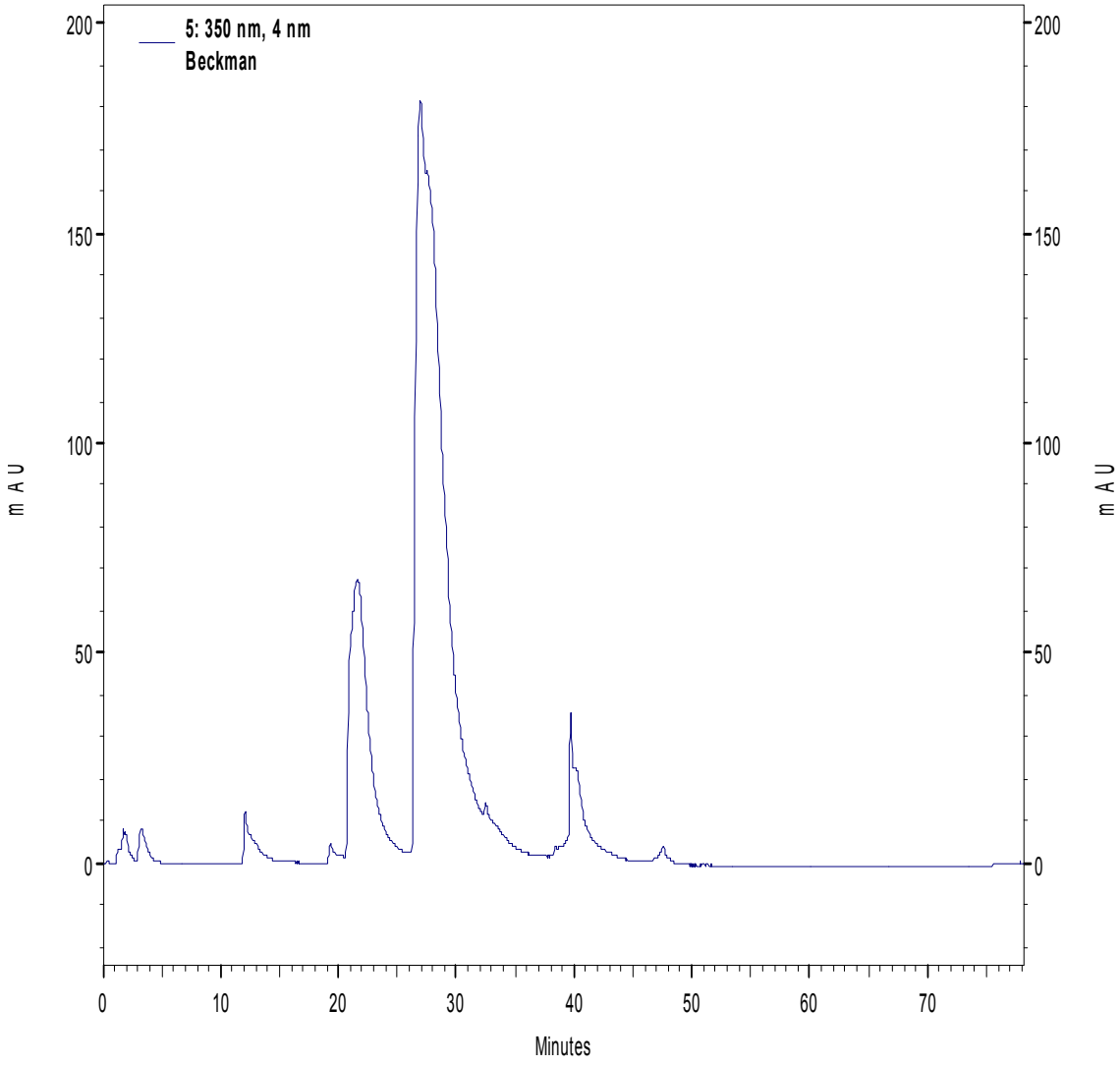

Peak at ~19 minutes is assumed to be caused by the amino acid serine adjusted with TNBSA. Peak at ~29 minutes is assumed to be caused by the amino acid cysteine adjusted with TNBSA. Peak at ~11-12 minutes is assumed to be the peak eluted by TNBSA alone. Other peaks are caused by unknown molecules.

Figure 58. Sample 1 50:50 5 mM serine: 5 mM cysteine mix with TNBSA chromatogram.

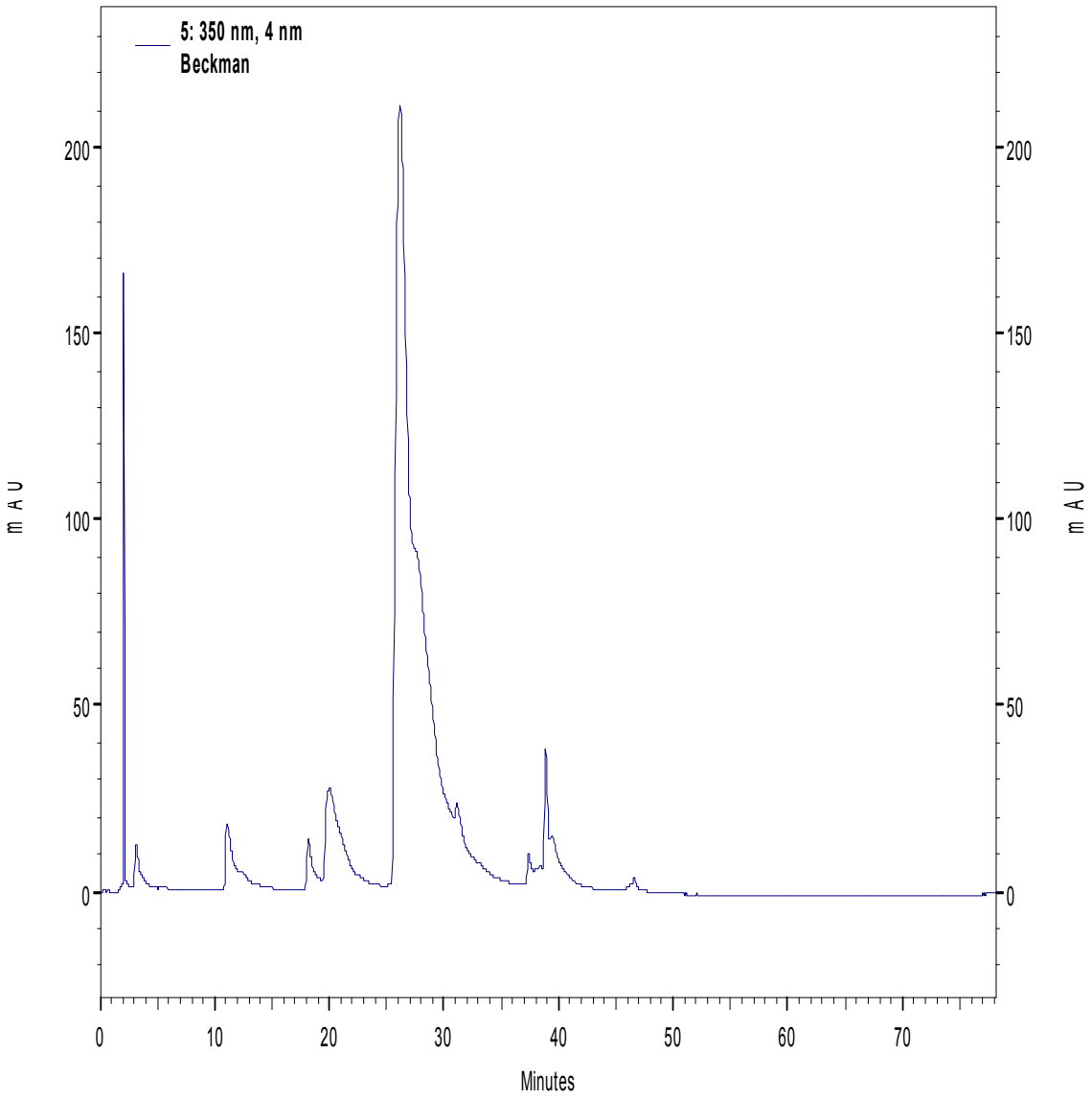

Peak at ~19 minutes is assumed to be caused by the amino acid serine adjusted with TNBSA. Peak at ~29 minutes is assumed to be caused by the amino acid cysteine adjusted with TNBSA. Peak at ~11-12 minutes is assumed to be the peak eluted by TNBSA alone. Other peaks are caused by unknown molecules.

Figure 59. Sample 2 50:50 5 mM serine: 5 mM cysteine mix with TNBSA chromatogram.

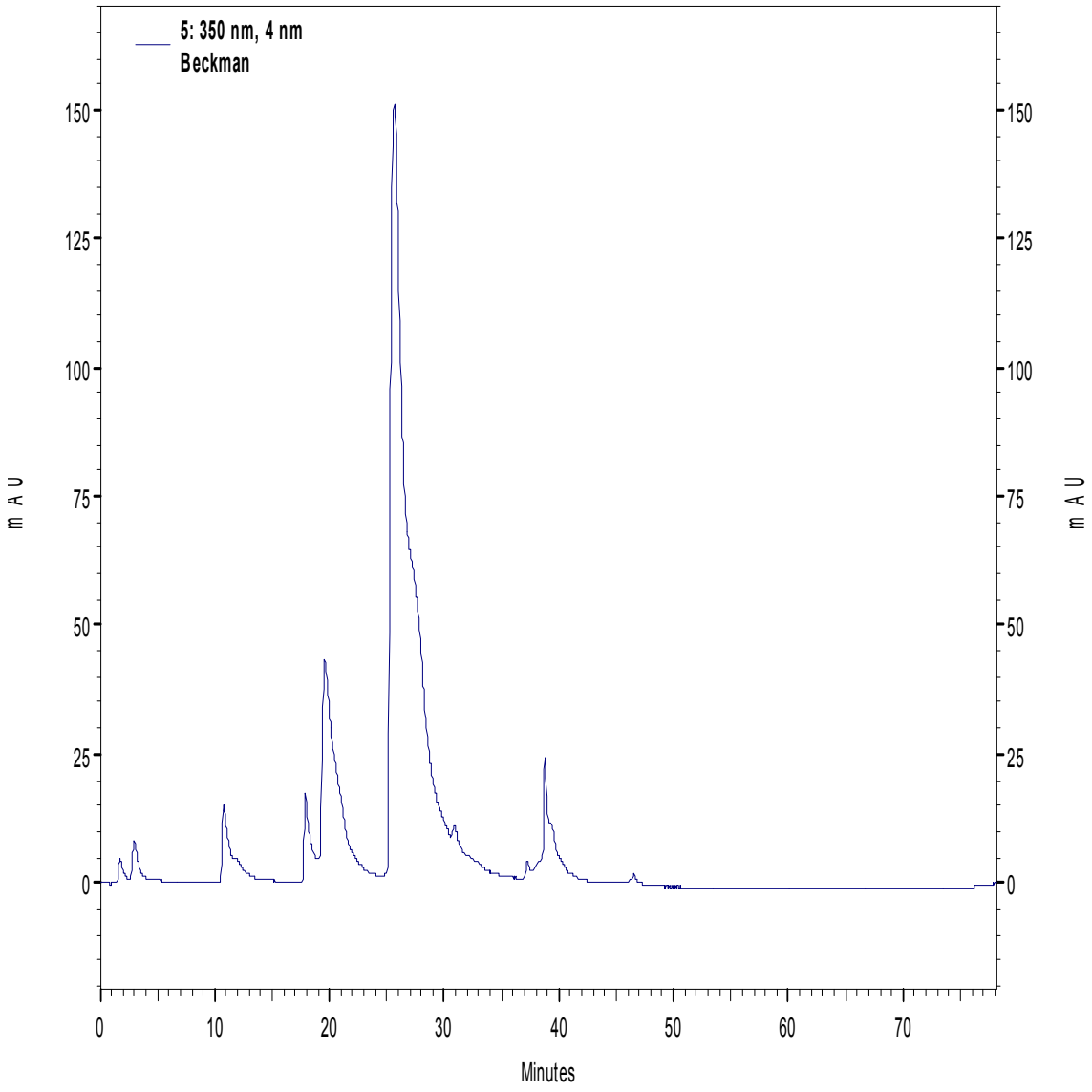

Peak at ~19 minutes is assumed to be caused by the amino acid serine adjusted with TNBSA. Peak at ~29 minutes is assumed to be caused by the amino acid cysteine adjusted with TNBSA. Peak at ~11-12 minutes is assumed to be the peak eluted by TNBSA alone. Other peaks are caused by unknown molecules.

Figure 60. Sample 3 50:50 5 mM serine: 5 mM cysteine mix with TNBSA chromatogram.

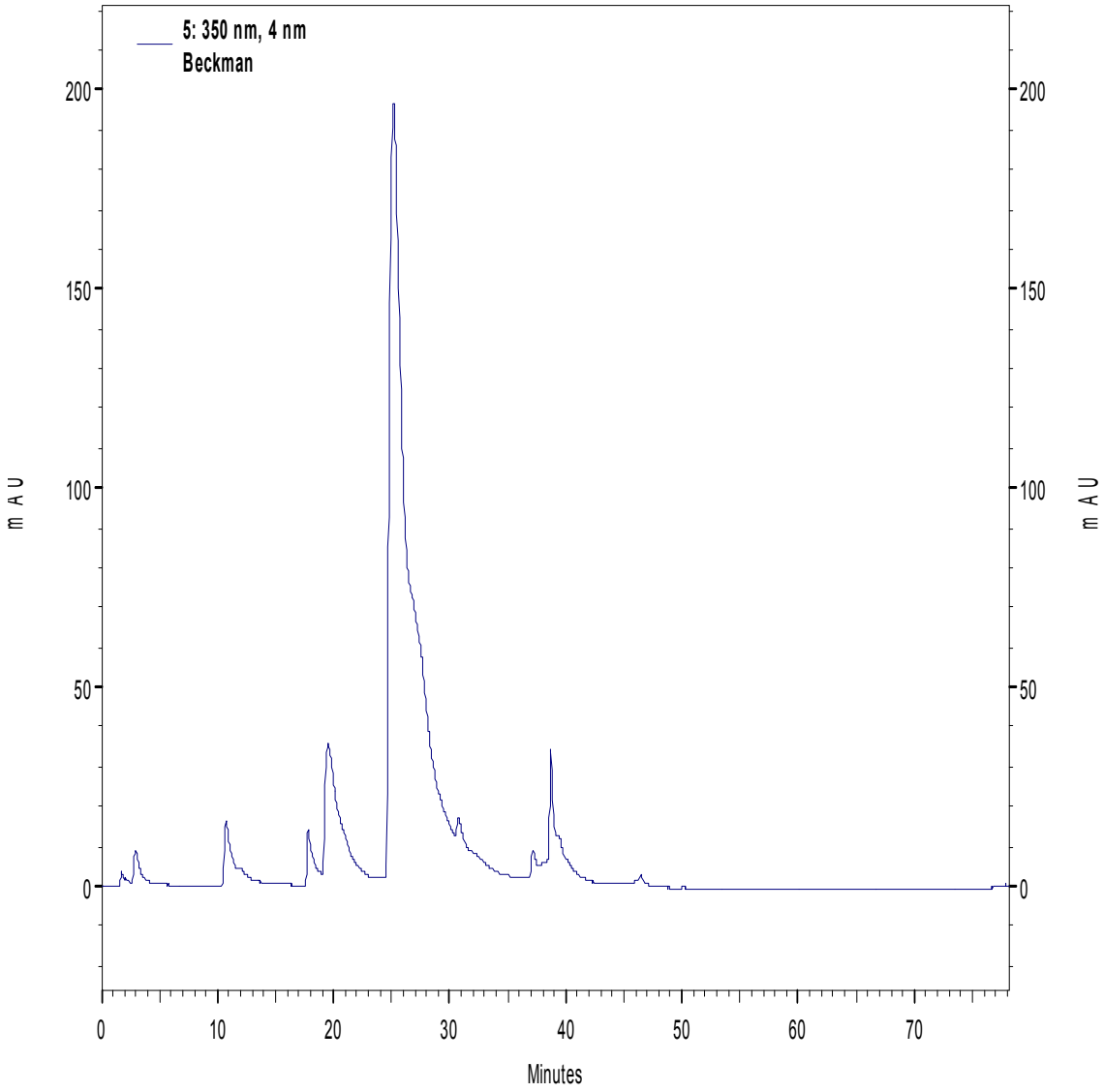

Peak at ~19 minutes is assumed to be caused by the amino acid serine adjusted with TNBSA. Peak at ~29 minutes is assumed to be caused by the amino acid cysteine adjusted with TNBSA. Peak at ~11-12 minutes is assumed to be the peak eluted by TNBSA alone. Other peaks are caused by unknown molecules.

Figure 61. 100% 10 mM serine with TNBSA chromatogram.

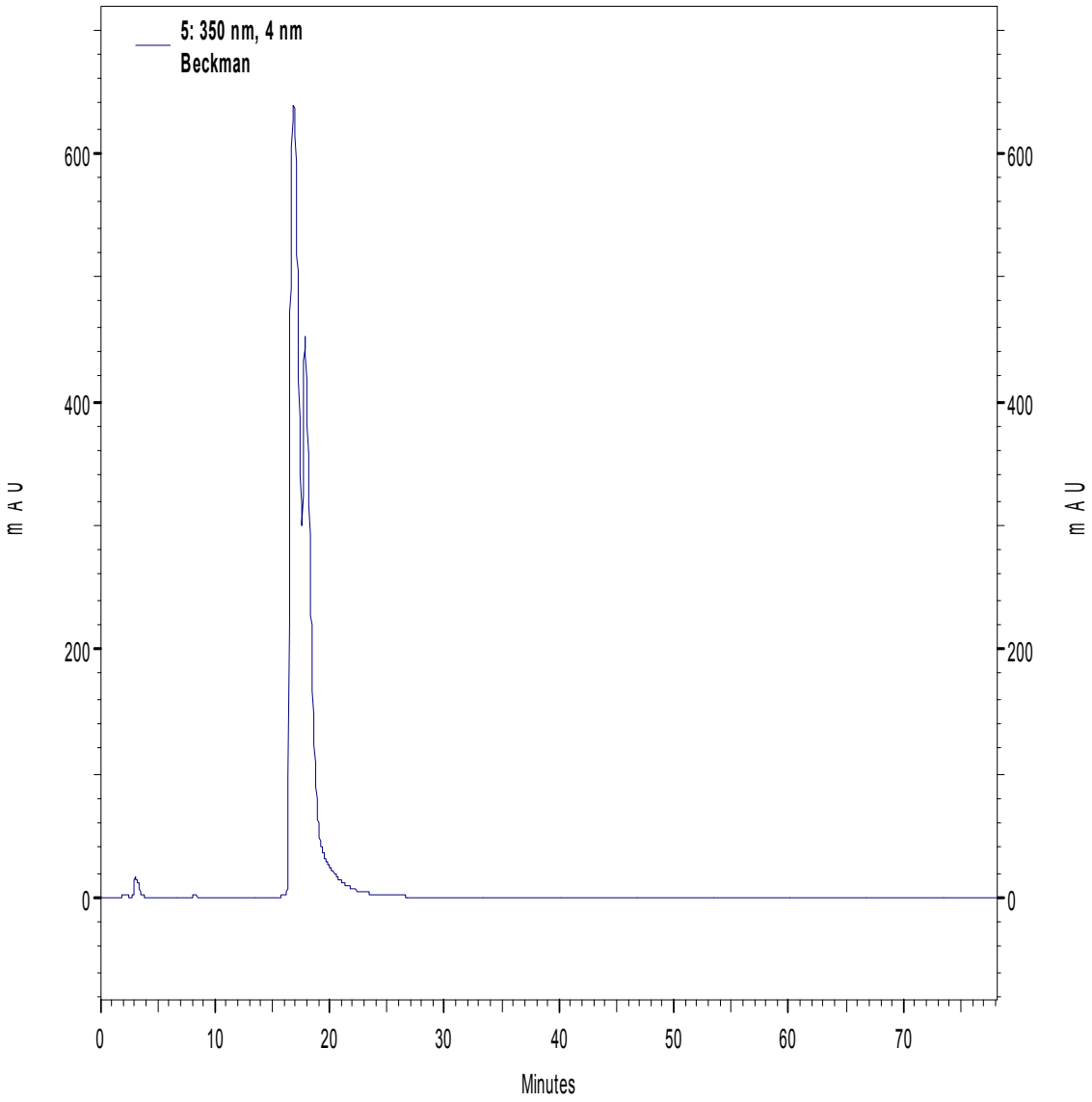

Peak at ~19 minutes is assumed to be caused by the amino acid serine adjusted with TNBSA. Peak at ~11-12 minutes is assumed to be the peak eluted by TNBSA alone.

Figure 62. 100% 10 mM cysteine with TNBSA chromatogram.

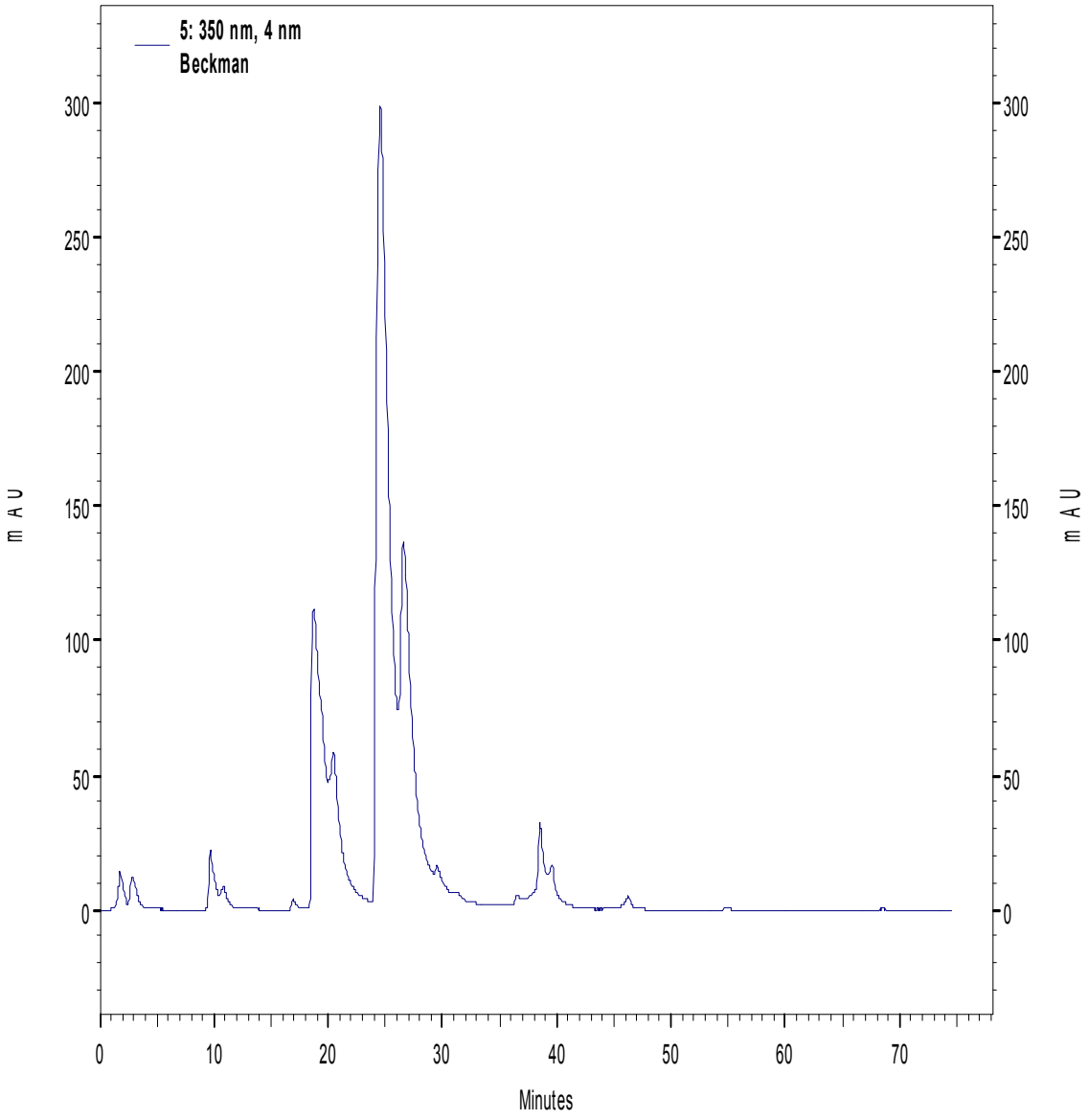

Peak at ~29 minutes is assumed to be caused by the amino acid cysteine adjusted with TNBSA. Peak at ~11-12 minutes is assumed to be the peak eluted by TNBSA alone. Other peaks are caused by unknown molecules.

Figure 63. 50:50 10 mM serine: 10 mM cysteine with DTNB chromatogram.

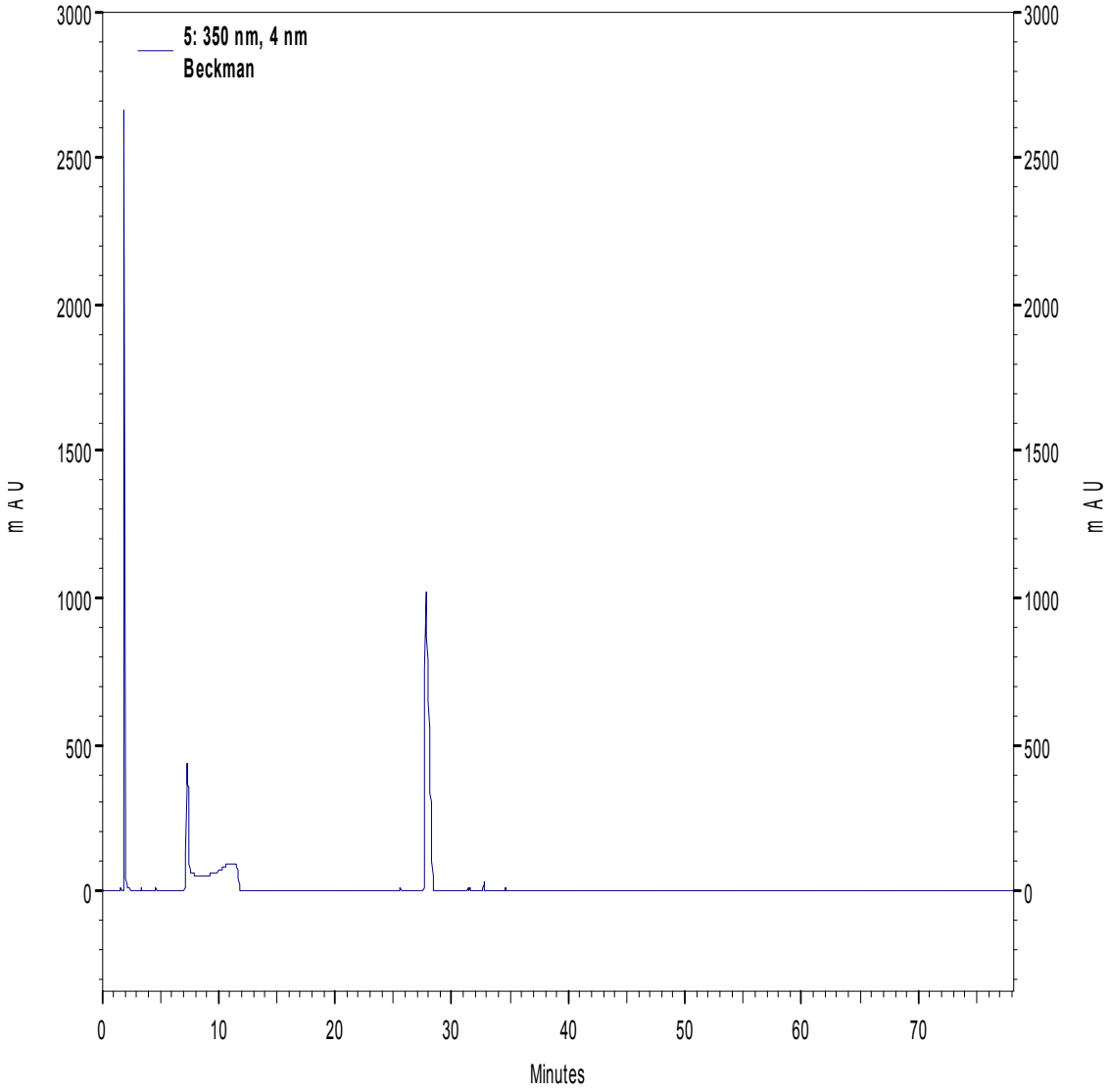

Peak at ~6 minutes is assumed to be caused by the amino acid cysteine adjusted with DTNB. Peak at ~29 minutes is assumed to be the peak eluted by DTNB alone. Serine should not and was assumed not to react with DTNB.

Table 15. DTNB area percent data for the cysteine peak and the highest average (appearing in 3 or more runs in both control and experiment) area percent peak (found at roughly 14.5 minutes).

Run	Day 1 Control	Day 1 Exp.	Day 2 Control	Day 2 Exp.	Day 3 Control	Day 3 Exp.	Day 4 Control	Day 4 Exp.
Cys Peak (~6.0 minutes)	22.83%	20.81%	29.81%	8.90%	36.14%	17.69%	0.21%	32.20%
Peak @ ~14.5 minutes	5.64%	0.72%	8.72%	5.95%	9.11%	6.12%	0.17%	1.26%

Table 16. TNBSA area percent data for the cysteine peak, the serine peak, and the highest average (appearing in 3 or more runs in both control and experiment) area percent peak (found at roughly 12.1 minutes).

Run	Day 1 Control	Day 1 Exp.	Day 2 Control	Day 2 Exp.	Day 3 Control	Day 3 Exp.	Day 4 Control	Day 4 Exp.
Cys Peak (~29.0 minutes)	3.54%	ND	2.95%	4.37%	5.92%	10.71%	0.82%	0.55%
Ser Peak (~22.70 minutes)	1.86%	ND	1.80%	2.50%	3.80%	2.52%	3.06%	1.62%
Peak @ ~12.1 minutes	1.62%	0.13%	19.93%	14.58%	1.08%	12.40%	ND	39.65%

ND is not detected.

Table 17. 10 mM serine and 10 mM cysteine 50:50 by volume major peaks average and standard deviation values for retention times, lambda max, and percent of the total area under the peaks designated to each individual peak.

Retention Time (Min.)		Percent Area		λ max		Number of Runs peak appears in (out of 9)
Average	Standard Deviation	Average	Standard Deviation	Average	Standard Deviation	
12.34388	0.306138	1.640551	0.158427	350	4.869732	8
19.41886	0.106101	1.69107	1.663832	347.7143	1.112697	7
21.38156	0.505417	18.09027	3.774712	348	0	9
27.89456	0.652366	67.26743	4.023634	351	0	9
32.70744	0.340041	3.127736	1.042076	357.5556	20.01944	9
39.11171	0.48401	1.842503	1.661113	347.2857	1.603567	7
39.99078	0.477268	6.229857	1.46933	348.4444	1.333333	9
47.69067	0.393041	0.794793	0.165838	369.5556	81.55537	9

Table 18. Comparisons of area percents of 5 mM serine: 5 mM cysteine (1/2 concentration) 50:50 by volume with TNBSA runs against same day (Day 1) 10 mM serine: 10mM cysteine (full concentration) 50: 50 by volume with TNBSA runs.

Peak Retention Time (Min)	½ Conc. Sample 1	½ Conc. Sample 2	½ Conc. Sample 3	Full conc. Sample 1, Day 1	Full conc. Sample 2, Day 1	Full conc. Sample 3, Day 1	P-value*
10.85533	3.153	2.33434	2.77532	1.91106	4.55484	1.40201	0.90211
17.967	1.412	2.55866	1.61614	3.60905			N/A
19.7 (Ser)	7.188	15.6378	10.1526	19.5011	10.2728	18.9038	0.24822
25.66133 (Cys)	72.03	67.9640	70.8430	62.5590	74.2859	68.4421	0.63412
30.91667	4.731	3.40439	5.55614				N/A
33.46667	2.359	1.54696	0.81871	1.76365	2.77624	2.17485	0.28137
37.25	0.961	0.53488	1.11097	1.26791	1.62272	1.10343	0.11561
38.97767	7.338	5.66217	6.43412	6.07375	4.85600	5.47641	0.16693
46.539	0.833	0.35672	0.69292	0.90384	1.13352	0.71483	0.19424

*- P-values were derived from unpaired t-tests from the three ½ concentration samples compared to the full concentration samples. Blue p-values are over 0.1, and are considered insignificant. The red 30.92 peak and corresponding area percents are highlighted because this peak was not found in any full concentration HPLC chromatograms. A blank space is no peak.
Samples read at the wavelength 350 nm.

Table 19. Comparisons of area percents of 5 mM serine: 5 mM cysteine (1/2 concentration) 50:50 by volume with TNBSA runs against same day (Day 2) 10 mM serine: 10mM cysteine (full concentration) 50: 50 by volume with TNBSA runs.

Peak Retention Time (Min)	½ Conc. Sample 1	½ Conc. Sample 2	½ Conc. Sample 3	Full conc. Sample 1, Day 2	Full conc. Sample 2, Day 2	Full conc. Sample 3, Day 2	P-value*
10.85533	3.1534	2.33434	2.77532	1.75105	1.50091	1.61711	0.01025
17.967	1.4121	2.55866	1.61614		0.96910	0.89147	0.13401
19.7 (Ser)	7.1880	15.6378	10.1526	22.9225	19.876	20.4796	0.01879
25.66133 (Cys)	72.025	67.9640	70.8430	62.8442	64.2627	64.7803	0.00917
30.91667	4.7308	3.40439	5.55614				N/A
33.46667	2.3589	1.54696	0.81871	3.24667	4.83766	3.56418	0.02484
37.25	0.9610	0.53488	1.11097		0.46062		N/A
38.97767	7.3378	5.66217	6.43412	8.50338	7.39845	8.10090	0.05900
46.539	0.8329	0.35672	0.69292	0.73227	0.69457	0.56654	0.81750

*- P-values were derived from unpaired t-tests from the three ½ concentration samples compared to the full concentration samples. Blue p-values are over 0.1, and are considered insignificant. The red 30.92 peak and corresponding area percents are highlighted because this peak was not found in any full concentration HPLC chromatograms. A blank space is no peak.
Samples read at the wavelength 350 nm.

Table 20. Comparisons of area percents of 5 mM serine: 5 mM cysteine (1/2 concentration) 50:50 by volume with TNBSA runs against same day (Day 3) 10 mM serine: 10mM cysteine (full concentration) 50: 50 by volume with TNBSA runs.

Peak Retention Time (Min)	½ Conc. Sample 1	½ Conc. Sample 2	½ Conc. Sample 3	Full conc. Sample 1, Day 3	Full conc. Sample 2, Day 3	Full conc. Sample 3, Day 3	P-value*
10.85533	3.15338	2.33434	2.77532	1.55412	1.68515	1.70300	0.01012
17.967	1.41209	2.55866	1.61614	0.60447	0.71987	0.48870	0.02489
19.7 (Ser)	7.18803	15.6378	10.1526	18.6755	13.8958	18.2854	0.11005
25.66133 (Cys)	72.0252	67.9640	70.8430	71.7365	68.1183	68.3779	0.63259
30.91667	4.73075	3.40439	5.55614				N/A
33.46667	2.35887	1.54696	0.81871	1.94559	3.99960	3.84119	0.10131
37.25	0.96095	0.53488	1.11097	0.74003	5.34047	2.36234	0.22531
38.97767	7.33782	5.66217	6.43412	6.07484	5.34047	4.24452	0.15515
46.539	0.83290	0.35672	0.69292	0.81032	0.90031	0.69696	0.31662

*- P-values were derived from unpaired t-tests from the three ½ concentration samples compared to the full concentration samples. Blue p-values are over 0.1, and are considered insignificant. The red 30.92 peak and corresponding area percents are highlighted because this peak was not found in any full concentration HPLC chromatograms. A blank space is no peak.
Samples read at the wavelength 350 nm.

Table 21. Comparisons of area percents of 5 mM serine: 5 mM cysteine (1/2 concentration) 50:50 by volume with TNBSA runs against different days (All sample 1's.) 10 mM serine: 10mM cysteine (full concentration) 50: 50 by volume with TNBSA runs.

Peak Retention Time (Min)	½ Conc. Sample 1	½ Conc. Sample 2	½ Conc. Sample 3	Full conc. Sample 1, Day 1	Full conc. Sample 1, Day 2	Full conc. Sample 1, Day 3	P-value*
10.85533	3.1534	2.33434	2.77532	1.91106	1.75105	1.55412	0.01705
17.967	1.4121	2.55866	1.61614	3.60905		0.60447	0.85270
19.7 (Ser)	7.1880	15.6378	10.1526	19.5011	22.9225	18.6755	0.02850
25.66133 (Cys)	72.025	67.9640	70.8430	62.5590	62.8442	71.7365	0.23232
30.91667	4.7308	3.40439	5.55614				N/A
33.46667	2.3589	1.54696	0.81871	1.76365	3.24667	1.94559	0.31302
37.25	0.9610	0.53488	1.11097	1.26791		0.74003	0.68043
38.97767	7.3378	5.66217	6.43412	6.07375	8.50338	6.07484	0.68915
46.539	0.8329	0.35672	0.69292	0.90384	0.73227	0.81032	0.27774

*- P-values were derived from unpaired t-tests from the three ½ concentration samples compared to the full concentration samples. Blue p-values are over 0.1, and are considered insignificant. The red 30.92 peak and corresponding area percents are highlighted because this peak was not found in any full concentration HPLC chromatograms. A blank space is no peak.
Samples were read at the wavelength 350 nm.

Table 22. Comparisons of area percents of 5 mM serine: 5 mM cysteine (1/2 concentration) 50:50 by volume with TNBSA runs against different days (All sample 2's.) 10 mM serine: 10mM cysteine (full concentration) 50: 50 by volume with TNBSA runs.

Peak Retention Time (Min)	½ Conc. Sample 1	½ Conc. Sample 2	½ Conc. Sample 3	Full conc. Sample 2, Day 1	Full conc. Sample 2, Day 2	Full conc. Sample 2, Day 3	P-value*
10.85533	3.1534	2.33434	2.77532	4.55484	1.50091	1.68515	0.87238
17.967	1.4121	2.55866	1.61614		0.96910	0.71987	0.11651
19.7 (Ser)	7.1880	15.6378	10.1526	10.2728	19.876	13.8958	0.3795
25.66133 (Cys)	72.025	67.9640	70.8430	74.2859	64.2627	68.1183	0.68292
30.91667	4.7308	3.40439	5.55614				
33.46667	2.3589	1.54696	0.81871	2.77624	4.83766	3.99960	0.03696
37.25	0.9610	0.53488	1.11097	1.62272	0.46062	5.34047	0.33948
38.97767	7.3378	5.66217	6.43412	4.85600	7.39845	5.34047	0.54062
46.539	0.8329	0.35672	0.69292	1.1335	0.69457	0.90031	0.21169

*- P-values were derived from unpaired t-tests from the three ½ concentration samples compared to the full concentration samples. Blue p-values are over 0.1, and are considered insignificant. The red 30.92 peak and corresponding area percents are highlighted because this peak was not found in any full concentration HPLC chromatograms. A blank space is no peak.
Samples read at the wavelength 350 nm.

Table 23. Comparisons of area percents of 5 mM serine: 5 mM cysteine (1/2 concentration) 50:50 by volume with TNBSA runs against different days (All sample 3's.) 10 mM serine: 10mM cysteine (full concentration) 50: 50 by volume with TNBSA runs.

Peak Retention Time (Min)	½ Conc. Sample 1	½ Conc. Sample 2	½ Conc. Sample 3	Full conc. Sample 3, Day 1	Full conc. Sample 3, Day 2	Full conc. Sample 3, Day 3	P-value*
10.85533	3.1534	2.33434	2.77532	1.40201	1.61711	1.70300	0.00956
17.967	1.4121	2.55866	1.61614		0.89147	0.48870	0.09231
19.7 (Ser)	7.1880	15.6378	10.1526	18.9038	20.4796	18.2854	0.03243
25.66133 (Cys)	72.025	67.9640	70.8430	68.4421	64.7803	68.3779	0.14602
30.91667	4.7308	3.40439	5.55614				
33.46667	2.3589	1.54696	0.81871	2.17485	3.56418	3.84119	0.07623
37.25	0.9610	0.53488	1.11097	1.10343		2.36234	0.19481
38.97767	7.3378	5.66217	6.43412	5.47641	8.10090	4.24452	0.68612
46.539	0.8329	0.35672	0.69292	0.71483	0.56654	0.69696	0.84062

*- P-values were derived from unpaired t-tests from the three ½ concentration samples compared to the full concentration samples. Blue p-values are over 0.1, and are considered insignificant. The red 30.92 peak and corresponding area percents are highlighted because this peak was not found in any full concentration HPLC chromatograms. A blank space is no peak.
Samples read at the wavelength 350 nm.

Table 24. Comparisons of DTNB and TNBSA UV-Vis data and ratios between control and experimental runs.

SAMPLE	DTNB, read at 412 nm	TNBSA, read at 335 nm	RATIO OF DTNB: TNBSA
Day 1, Control	1.8423	2.795	0.659392
Day 1, Experiment	1.968	2.34	0.841026
Day 2, Control	1.91	9.87	0.193516
Day 2, Experiment	1.58	8.232	0.191934
Day 3, Control	1.638	6.22	0.263344
Day 3, Experiment	1.494	4.294	0.347927
Day 4, Control	1.284	6.257	0.20521
Day 4, Experiment	1.365	5.089	0.268226

Works Cited

1. **Col, J.** (1996) Bacteria. *Enchanted Learning.* [Online] [Cited: November 10, 2008.] http://www.enchantedlearning.com/subjects/bacterium/.
2. **Liu, X., Ng, C., French, T.** (2000) *Global Adaptations Resulting from High Population Densities in Escherichia coli Cultures.* American Society for Microbiology, **Aug.,** 4158-4164.
3. **Boor, K. J.** (2006) *Bacterial Stress Responses: What Doesn't Kill Them Can Make Them Stronger.* PLoS Biology, **4**, e(23).
4. **Voet, D., Voet, J. G.** (2004) *Biochemistry: 3rd Addition Volume 1.* John Wiley & Sons, Inc. 0-471-25090-2.
5. **Ferreira, A., O'Bryne, C. P., Boor, K. J.** (2001) *Role of çB in Heat, Ethanol, Acid, and Oxidative Stress Resistance and during Carbon Starvation in Listeria monocytogenes*. American Soceity of Microbiology, **67,** PMCID: PMC93189.
6. **Hegde, A., Bhat, G.K., Mallya, S.** (2009) *Effect of stress on production of heat labile enterotoxin by Escherichia coli.* Indian J. Med. Microbiol., **27**, 325-328.
7. **Lerner A., Castro-Sowinski, S., Lerner, H., Okon, Y., Burdman, S.** (2009) *Glycogen phosphorylase is involved in stress endurance and biofilm formation in Azospirillum brasilense Sp7.* FEMS Microbiol. Lett., Epub ahead of print.
8. **Chung, C. N., Niemala, S.L., Miller, R.H.** (1988) *One-step preparation of competent Escherichia coli: transformation and storage of bacterial cells in the same solution.* PNAS , **86,** 2172-2175.

9. **Sutcliffe, J.G.** (1978) *Nucleotide sequence of the ampicillin resistance gene of Escherichia coli plasmid pBR322.* Proc. Natl. Acad. Sci. U. S. A., **75**, 3737-3741.
10. **Uhlich, G.A.** (2009) *KatP contributes to OxyR-regulated hydrogen peroxide resistance in Escherichia coli serotype O157:H7.* Microbiology, Epub ahead of print.
11. **Jung, I.L**., **Kim, I.G.** (2003). *Transcription of ahpC, katG, and katE genes in Escherichia coli is regulated by polyamines: polyamine-deficient mutant sensitive to H2O2-induced oxidative damage.* Biochem. Biophys. Res. Commun. , 915-922.
12. **Alba, B. M., Gross, C. A.** (2004) *Regulation of the Escherichia coli σE-dependent envelope stress response.* Molecular Microbiology, **52**, 613-619.
13. **Cuny, C., Lesbats, M., Dukan, S.** (2007) *Induction of a Global Stress Response during the First Step of Escherichia coli Plate Growth*. Applied and Environmental Microbiology, **73,** 885-889.
14. **Imlay, J. A.** (2003) *Pathways of Oxidative Damage*. Auu. Rev. Microbiol., **57**, 395-418.
15. **Landmesser, U., Drexler, H.** (2003) *Oxidative stress, the renin-angiotensin system, and atherosclerosis.* European Heart Journal Supplements, **5**, A3-A7.
16. **Christen, Y.** (2000) *Oxidative Stress and Alzheimer's Disease*. American Journal of Clinical Nutrition, **71,** 621s-629s.
17. **Merry, B.J.** (2002) *Role of Oxidative Stress in Ageing*. Endocrine Abstracts. **4**, S11.
18. **Craig, M., Slauch, J. M.** (2009) *Phagocytic Superoxide Specifically Damages an Extracytoplasmic Target to Inhibit or Kill Salmonella*. PLoS One, **4**.

19. **Imlay, J.** (2008) *Cellular Defenses against Superoxide and Hydrogen Peroxide.* Annual Review of Biochemistry, **77,** 756-766.

20. **Liu, H., Colavatti, R., Rovira, I., Finkel T.** (2005) *Redox-Dependent Transcriptional Regulation.* American Heart Association, Inc., 967-974.

21. **Chan, E., Weiss, B.** (1987) *Endonuclease IV of Eschericia coli is induced by paraquat.* Proc. Natl. Acad. Sci., **84**, 3189-3193.

22. Amabile Cuevas, C. F., Demple, B. (1991) *Molecular Charachterization of the soxRS genes of Eschericia coli: two genes control a superoxide stress regulon.* Nucleic Acids Res., **19**, 4479-4484.

23. **Wefers, H., Sies, H.** (1983) *Oxidation of glutathione by the superoxide radical to the disulfide and the sulfonate yielding singlet oxygen.* J. Biochem., **137,** 29-36.

24. Imlay, J.A., Linn, S. (1988) *DNA damage and oxygen radical toxicity.* Science, **240**, 640-642.

25. **Zheng, M., Aslund, F., Storz, G.** (1998) *Activation of the OxyR transcription factor by reversible disulfide bond formation.* Science, **279**, 1718-1721.

26. **Altuvia, S. [et al.]** (1998) *The Escherichia coli OxyS regulatory RNA represses fhlA translation by blocking ribosome binding,* The EMBO Journal. **17,** 6069-6075.

27. **Davidson, M.** (2004) *Molecular Expressions: The Amino Acid Collection - Glutothione* [Online] // Molecular Expressions. - Florida State University. (Cited: February 27, 2007). http://micro.magnet.fsu.edu/aminoacids/pages/glutathione.html.

28. **Farr, S. B., Kogoma T.** (1991) *Oxidative Stress Responses in Escherichia coli and Salmonella typhimurium.* Microbiological Reviews, **55**, 561-585.

29. **Lin, J. [et al.]** (1995) *Comparative analysis of extreme acid survival in Salmonella typhimurium, Shigella flexneri, and Escherichia coli*. Journal of Bacteriology, Vol. **177,** 4097-4104.

30. **Giannella, R. A., Broitman, S. A., Zamcheck, N.** (1973) *Influence of gastric acidity on bacterial and p,arasitic enteric infections. A perspective*. Annual International Medicane, **78**, 271-276.

31. **Castanie-Cornet, M., Penfound, T. A., Smith, D., Elliot, J. F., Foster, J. W.** (1999) *Control of Acid Resistance in Escherichia coli*. Journal of Bacteriology. **181**, 3525-3535.

32. **Gong, S., Hope, R., Foster, J. W.** (2003) *YjdE (AdiC) Is the Arginine:Agmatine Antiporter Essential for Arginine-Dependent Acid Resistance in Escherichia coli*. Journal of Bacteriology, **185**, 4402-4409.

33. **Rowbury, R.J.** (1997) *Regulatory components, including integration host factor, CysB and H-NS, that influence pH responses in Escherichia coli.* Letters in Applied Microbiology, **24,** 319-328.

34. **Iyer, R., Williams, C., Miller C.** (2003) *Arginine-Agmatine Antiporter in Extreme Acid Resistance in Escherichia coli.* Journal of Bacteriology, **185**, 6556-6561.

35. **Neely, M. N., Dell, C. L., Olson, E. R.** (1994) *Roles of LysP and CadC in Mediating the Lysine Requirement.* Journal of Bacteriology. **176**, 3278-3285.

36. **Hersh, B. M. [et al.]** (1996) *A Glutamate-Dependent Acid Resistance Gene in Escherichia coli.* Journal of Bacteriology, **178,** 3978-3981.

37. **Smith, D. K., Kassam T., Singh, B., Elliott, J. F.** (1992) *Escherichia coli has two homologous glutamate decarboxylase genes that map to distinct loci.* Journal of Bacteriology, **174**, 5820-5826.

38. **Ma, Z., Masuda, N., Foster, J. W.** (2004) *Characterization of EvgAS-YdeO-GadE Branched Regulatory Circuit Governing Glutamate-Dependent Acid Resistance in Escherichia coli.* Journal of Bacteriology, **186**, 7378-7389.

39. **Copper Sulfate** (1994) [Online] // Extoxnet. - Cornell University. (Cited: February 5, 2009). - http://pmep.cce.cornell.edu/profiles/extoxnet/carbaryl-dicrotophos/copper-sulfate-ext.html.

40. **Mondovi', B., Bannister, J.V.** (1987) *The Active Site of Copper Proteins* // Life Chemistry Reports incorporating International Journal of Chronobiology / book editors Bannister, J.V., Michelson, A.M., Harwood Academic Publishers.

41. **Goldstein, S., Meyerstein, D., Gidon, C.** (1993). *The Fenton reagents.* Free Radical Biology and Medicine, **15**, 435-445.

42. **Hoshino, N., Kimura, T., Yamaji, A., Ando, T.** (1999) *Damage to the cytoplasmic membrane of Escherichia coli by catechin-copper (II) complexes.* Free Radical Biology and Medicine, **27**, 1245-1250.

43. **Bontidean, L. [et al.]** (2002) *Bacterial Metal-Responsive Elements and Their Use in Biosensers of Heavy Metals* // Heavy Metals in the Environment / book auth. S. Bibudhendra, CRC Press.

44. **Sarkar, B.** (2002) *Heavy Metals in the Environment.* CRC Press.

45. **Ghosh, M., Rosen, B. P.** (2002) *Microbial Resistance Mechanisms for Heavy Metals and Metalloids* // Heavy Metals in the Environment / book auth. S. Bibudhendra, CRC Press.

46. Stoyanov, J. V., Hobman J. L., Brown, N. L. (2001) *CueR (YbbI) of Escherichia coli is a MerR family regulator controlling expression of the copper exporter CopA.* Molecular Microbiology, **39**, 502-512.

47. **Stoyanov, J. V., Brown, N. L.** (2003) *The Escherichia coli Copper-responsive copA Promoter Is Activated by Gold.* J. Biol. Chem. **278**, 1407-1410.

48. **Munson, G. P., Lam, D. L., Outten, W., O'Halloran, T. V.** (2000) *Identification of a Copper-Responsive Two-Component System on the Chromosome of Escherichia coli K-12.* Journal of Bacteriology, **182**, 5864-5871.

49. **Holleman, A. F.** (2001). *Inorganic Chemistry.* San Diego: Academic Press.

50. **Masterton, W. L., Hurley, C. N.** (1997) *Chemistry: Principles and Reactions*. Saunders College Publishing.

51. **Leive, L.** (1965) *A nonspecific increase in permeability in Escherichia Coli produced by EDTA.* Microbiology, **53**, 745-750.

52. **Leive, L.** (1965) *Actinomycin sensitivity in Escherichia coli produced by EDTA.* Biochemical and Biophysical Research Communications, **18**, 13-17.

53. **Ko, K.Y., Mendoncam, A.F., Ismail, H., Ahn, D.U.** (2009) *Ethylenediaminetetraacetate and lysozyme improves antimicrobial activities of ovotransferrin against Escherichia coli O157:H7.* Poult Sci., **88**, 406-414.

54. **Knasmueller, S., Szakmary, A., Wottawa, A.** (1989) I*nvestigations on the use of EDTA-permeabilized E. coli cells in liquid suspension and animal-mediated genotoxicity assays.* Mutat. Res., **216**, 189-196.

55. **Shellman, V. L., Pettijohn, D. E.** (1991) *Introduction of Proteins into Living Bacterial Cells: Distribution of Labeled HU Protein in Escherechia coli*. Journal of Bacteriology, **173**, 3047-3059.

56. **Asad, N. R., Leitao, A. C.** (1991) *Effects of Metal Ion Chelators on DNA Strand Breaks and Inactivation Produced by Hydrogen Peroxide in Escherichia coli: Detection of Iron-Independent Lesions.* Journal of Bacteriology, **173**, 2562-2568.

57. **Maurer, L. M. [et al.]** (2004) *pH Regulates Genes for Flagellar Motility, Catabolism, and Oxidative Stress in Escherichia coli K-12*. Journal of Bacteriology, **187**, 304-319.

58. **Kannan, G. [et al.]** (2007) *Rapid acid treatment of Escherichia coli: transcriptomic response and recovery.* BMC Microbiology, **8**.

59. **Moreno, M., Foster, J.W.** (1999) *Inducible acid tolerance mechanisms in enteric bacteria.* Novartis Found Symp., **221**, 55-69.

60. **Hantke, K.** (2001) *Iron and metal regulation in bacteria.* Current Opinion in Microbiology, **4,** 172-177.

61. **Wolf, S. G. [et al.]** (1999) *DNA protection by stress-induced biocrystallization.* Nature, **400,** 83-85.

62. **Choi, S. H., Baumler, D. J., Kaspar, C. W.** (2000) *Contribution of dps to Acid Stress Tolerance and Oxidative Stress Tolerance in Escherichia coli O157:H7.* Applied and Environmental Microbiology, **66**, 3911-3916.

63. **Schnetz, K.** (2008) *Fine-tuned growth phase control of dps, encoding a DNA protection protein, by FIS and H-NS.* Molecular Microbiology, **68**, 1345-1347.

64. **Bearson, B. L., Lee, I. S., Casey, T. A.** (2009) *Escherichia coli O157 : H7 glutamate- and arginine-dependent acid-resistance systems protect against oxidative stress during extreme acid challenge.* Microbiology, **155**, 805-812.

65. **Battistoni, A. [et al.]** (2000) *Increased Expression of Periplasmic Cu,Zn Superoxide Dismutase Enhances Survival of Escherichia coli Invasive Strains within Nonphagocytic Cells.* Infection and Immunitiy, **68**, 30-37.

66. **Aruoma, O., Halliwell, B., Dizdaroglu, E., Gaweski M.** (1991) *Copper-Ion Dependent Damage to the bases in DNA in the presence of hydrogen-peroxide.* Biochemical Journal, **273**, 601-604.

67. **Elzanoska, H., Wolcott, R. G., Hannum, D. M., Hurst, J. K.** (1995) *Bactericidal Properties of Hydrogen Peroxide and Copper and Iron-Containing Complex Ions in Relation to Leukocyte Function.* Free Radical Biology & Medicine, **18**, 437-449.

68. **Halliwell, B., Glutteridge, J.M.C.** (1998) *Free Radicals in Biology and Medicine, 2nd Edition.* Clarendon Press.

69. **Fenton, H.** (1894) *Oxidation of tartaric acid in presence of iron.* J. Chem. Soc., **65,** 899-911.

70. **Cadenas, E.** (1989) *Biochemistry of oxygen toxicity.* Annual Rev. Biochemistry, **58**, 79-110.

71. **Chan, P. C., Kesner, L.** (1980) *Copper (II) complex-catalyzed oxidation of NADH by hydrogen peroxide.* Biological Trace Element Research, **2**, 159-174.

72. **Benov, L. T., Fridovich, I.** (1994) *Escherichia coli Expresses a Copper- and Zinc-containing Superoxide Dismutase.* The Journal of Biological Chemistry, **269**, 25310-25314.

73. **Mueller, J., Janz S.** (1993) *Modulation of the H_2O_2-induced SOS response in Escherichia coli PQ300 by amino acids, metal chelators, antioxidants, and scavengers of reactive oxygen species.* Environ. Mol. Mutagen, **22**, 157-163.

74. **Garrett, S. J.** (1998) *CEM 333 EDTA Formation Constants* [Online] // Instrumental Analysis (CEM 333) Resource Page. - Michagan State University. (Cited: March 15, 2009). - http://www.cem.msu.edu/~cem333/EDTATable.html.

75. **Martell, A.M., Smith, R.M.** (2001) *CNIST Critically Selected Stability Constants of Metal Complexes Database.* Plenum Press.

76. **Alakomi, H. L. [et al.]** (2000) *Lactic Acid Permeabilizes Gram-Negative Bacteria by Disrupting the Outer Membrane.* Applied and Environmental Microbiology, **66**, 2001-2005.

77. **Rensing, C., Grass, G.** (2003) *Escherichia coli mechanisms of copper homeostasis in a changing environment.* FEMS Microbiology Rev., **27**, 197-213.

78. **Marquis, R.E., Keller D.M.** (1975) *Enzymatic adaptation by bacteria under pressure.* Journal of Bacteriology, **122**, 575-584.

79. **Ishii, A. [et al.]** (2004) *Analysis of hydrostatic pressure effects on transcriptionin Escherichia coli by DNA microarray procedure.* Extremophiles, **9**, 65-73.

80. **Strøm, A.R., Kaasen, I.** (1993) *Trehalose metabolism in Escherichia coli: stress protection and stress regulation of gene expression.* Mol. Microbiology, **8**, 205-210.

81. **Zundel, M.A., Basturea, G.N., Deutscher, M.P.** (2009) *Initiation of ribosome degradation during starvation in Escherichia coli.* RNA, **March**, 1-7.

82. **Gunasekera, T.S., Csonka, L.N., Paliy, O.** (2008) *Genome-wide transcriptional responses of Escherichia coli K-12 to continuous osmotic and heat stresses.* Journal of Bacteriology, **190**, 3712-3720.

83. **Hong, J., Ahn, J., Kim, B. C., Gu, M. B.** (2009) *Construction of a functional network for common DNA damage responses in Escherichia coli.* Genomics, doi:10.1016/j.ygeno.2009.01.010.

84. **Jacobson, R.H., Zhang, X.J., DuBose, R.F., Matthews B.W.** (1994) *Three-dimensional structure of beta-galactosidase from E. coli*. Nature, **369**, 761-766.

85. **Matthews, B.W.** (2005) *The structure of E. coli's beta-galactosidase*. Comptes Rendus Biologies, **328**, 549-556.

86. **Cesca, B. [et al.]** (1984) *Beta-D-galactosidase of Lactobacillus species*. Folia microbiologica, **29**, 288-294.

87. **Suzuki, K., Tanaka, H.** (1975) *Lactosylceramide beta-galactosidase in human sphingolipidoses. Evidence for two genetically distinct enzymes.* JBC, **250**, 2324-2332.

88. **Wallenfels, K., Weil, R.** (1972) *Beta-Galactosidase* // The Enzymes: 3rd Edition vol. 7 / book auth. P. D. Boyer, Academic Press.

89. **Sinnott, M.L., Withers, S. G.** (1978) *The necessity of magnesium cation for acid assistance aglycone departure in catalysis by Escherichia coli (lacZ) beta-galactosidase.* Biochem. J., **175**, 539-546.

90. **Edwards, R.A., Cupples, C.G., Huber, R.E.** (1990) *Site specific mutants of beta-galactosidase show that Tyr-503 is unimportant in Mg2+ binding but that Glu-461 is very important and may be a ligand to Mg2+.* Biochem. Biophys. Res. Commun., **171**, 33-37.

91. **Cupples, C. G., Miller, J. H., Huber, R. E.** (1990) *Determination of the roles of Glu-461 in beta-galactosidase (Escherichia coli) using site-specific mutagenesis.* The Journal of Biological Chemistry, **265**, 5512-5518.

92. **Douglas, H. [et al.]** (2001) *A Structural View of the Action of Escherichia coli (lacZ) β-Galactosidase*. Biochemsitry, **40**, 14781-14794.

93. **Campbell, J. H., Lengyel, J. A., Langridge, J.** (1973) *Evolution of a Second Gene for β-Galactosidase in Escherichia coli.* Proc. Nat. Acad. Sci. USA, **70**, 1841-1845.

94. **McClean, P.** (1997) *The lac Operon - an Inducible system* [Online] // Prokaryotic Gene Expression. (Cited on: March 13, 2009). http://www.ndsu.nodak.edu/instruct/mcclean/plsc431/prokaryo/prokaryo2.htm.

95. **Yanisch-Perron, C. [et al.]** (1985) *Improved M13 phage cloning vectors and host strains: nucleotide sequences of the M13mp18 and pUC19 vectors.* Gene, **33**, 103-109.

96. **Taylor, R. [et al.]** (1993) *E. coli host strains significantly affect the quality of small scale plasmid DNA preparations used for sequencing.* Nucleic Acids Res., **21,** 1677-1678.

97. **Turner, P.** (2005). *Microbiology.* New York: Taylor & Francis Group.

98. **Azwiefel, G., Jim Hu, S.** (2008) *DH5-Alpha - EcoliWiki* [Online] // E coli Hub. - Media Wiki. (Cited on: November 20, 2008). http://ecoliwiki.net/colipedia/index.php/DH5_alpha.

99. **Juers, D.H. [et al.]** (2000) *High resolution refinement of beta-galactosidase in a new crystal form reveals multiple metal binding sites and provides a crystal basis for alpha-complementation.* Protein Science, **9**, 1685-1699.

100. **Amplicon Express.** (2009). *Amplicon Express - Your BAC library and pooling specialists*. Amplicon Express. [Online] (Cited on: August 7, 2009) http://www.genomex.com/aexVectors.php.

101. **Promega** (2007) *pGEM-T and pGEM-T Easy Vector Systems.* Promega Corp. Part# TM042.

102. **Gunsekera, T. S., Csonka, L. N., Paliy, O.** (2008) *Genome-Wide Transcriptional Responses of Escherichia coli K-12 to Continuous Osmotic and Heat Stresses.* Journal of Bacteriology, **190**, 3712-3720.

103. **Crawley, M. J.** (2007) *The R Book,* Wiley.

104. **Bidlingmeyer, B. A.** (1992) *Practical HPLC methodology and applications*, John Wiley & Sons.

105. **GlobalSpec., Inc.** (1999-2009) *HPLC Detectors Specifications.* [Online] GlobalSpec, The Engineering Search Engine. [Cited: August 22, 2009] http://laboratory-equipment.globalspec.com/Specifications/Labware_Test_Measurement/Chromatography_Instruments/HPLC_Detectors.

106. **Clark, J.** (2007) *High Performance Liquid Chromotagraphy-HPLC.* [Online] Chemguide. [Cited: February 15, 2009.] http://www.chemguide.co.uk/analysis/chromatography/hplc.html.

107. **Scott, R.P.W.** (2008) *Diode Array.* [Online] Library4science, LLC. [Cited: March 25, 2009.] http://www.chromatography-online.org/topics/diode/array.html.

108. **Hermanson, G.T**. (2008) *Bioconjugate Techniques,* Academic Press (Product # 20036).

109. **Riddles, P.W., Blakeley, R. L., Zerner, B.** (1979) *Ellman's reagent: 5,5'-dithiobis(2-nitrobenzoic acid)—a reexamination.* Elsevier, Inc., **94**, 75-81.

110. **Chena, W, Zhaoa, Y, Seefeldta, T, Guan, X.** (2008) *Determination of thiols and disulfides via HPLC quantification of 5-thio-2-nitrobenzoic acid.* Journal of Pharmacuetical and Biomedical Analysis, **48**, 1375-1380.

111. **Juenke, J. M., Brown, P. I., McMillin, G. A., Urry, F. M.** (2003) *Procedure for the Monitoring of Gabapentin with 2,4,6-Trinitrobenzene Sulfonic Acid Derivatization Followed by HPLC with Ultraviolet Detection.* Clinical Chemistry, **49**, 1198-1201.

112. **Cayot, P., Tainturier, G.** (1997) *The Quantification of Protein Amino Groups by the Trinitrobenzenesulfonic Acid Method: A Reexamination.* Analytical Biochemsitry, **249**, 184-200.